Spatio – temporal Patterns and Controls on Cold-water Coral Reef Development: The Moira Mounds, Porcupine Seabight, Offshore Ireland

Aaron Lim, B.Sc. (Hons)

Ph.D. Thesis

National University of Ireland, Cork.

Geology, School of Biological, Earth and Environmental Sciences

January, 2017

Head of School: Prof. Sarah Culloty

Supervisor of research: Prof. Andy Wheeler

Advisor: Dr. Ed Jarvis

Contents

List of figures

List of tables

List of abbreviations

*.shp	Shapefile
°C	degrees Celsius (temperature)
BMP	Belgica Mound Province
$CaCO_3$	Calcium Carbonate
CTD	Conductivity-Temperature-Depth
CWC	Cold Water Coral
H_2O_2	Hydrogen Peroxide
MBES	Multibeam Echosounder
MOW	Mediterranean Outflow Water
ROV	Remotely Operated Vehicle
SAC	Special Area of Conservation
SSS	Side Scan Sonar
UCC	University College Cork
XYZ	Latitude, Longitude, Depth

Declaration

The research presented here is the authors own work and has not been submitted for another degree at University College Cork or elsewhere.

Signed 

Aaron Lim, author.

Signed 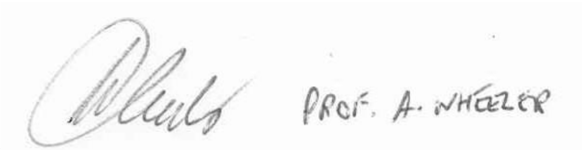

Prof. Andrew Wheeler, supervisor of research.

Acknowledgements

Upon coming this far, I realise that, above all else, this degree has been a measure of perseverance, creativity, love for solving problems and answering questions on a certain topic. Along the way, I've noticed many changes in myself, the way I think, my lifestyle, my aspirations and my priorities. As such, there are many people I would like to acknowledge who helped me to complete this body of work and embrace these changes.

Firstly, I would like to thank my parents, Majella and Adrian, grandparents, Robert and Rita, and family (sisters, niece, nephews, cousin, brother-in-law, aunt and uncle) for trusting and supporting my decisions to follow where my mind wanted to go. I would also like to thank them for allowing me to keep rocks on the window sill and paying a keen interest in what I've been doing for the past few years.

There are many people with whom I've "served time" in the office that have bounced ideas back and forward, gone for pints with after work, competed in the "Office Olympics", and generally made the days more enjoyable. Thank you to Will, Dave, Marian, Aidan, Caroline and Joanne. A special thanks to my long-time office mates, Brenton and Mohit (Gandu-Chu-Tiya, mo-man, mo-minion), for serious craic every day and, in particular, Mark "the operator" Coughlan, who taught me about "the birds and the bees" in the office, on research cruises and gave genuine support throughout.

There have been numerous, long research cruises on which data for this project were collected. Many of these people have selflessly given their own time to help achieve this. For that, I would like to thank Chris McGonigle, Kevin Power, Raissa Hogan, Niamh Connolly, Edel O' Donnell, Eileen Mc Carthy, Findabhair Ní

Fhaolain and Zsuzanna Tóth for their time, knowledge, enthusiasm and hard work. A huge thank you to the MI, the crew of the RV Celtic Explorer and Holland 1 ROV.

I would like to thank the staff in the School of BEES who have all contributed to my experience as a Ph.D. student namely Dr. John Reavy, Dr. Pat Meere, Mary Lehane, Dr. Richard Unitt, Dr. Bettie Higgs, Dr. Giulio Solferino and Dr. Maria McNamara. A special thank you to Dr. Ed Jarvis, the research advisor for this project, for extremely useful advice on a range of topics from ripples to history of the department (and everything in between!) and really, really good times.

I would like to acknowledge the Irish Research Council for funding this project for 1 year, without which the project may have had a very different outcome. I would like to thank Dr. Agostina “yellow stuff” Vertino for setting up and organising lab work in Milano-Bicocca and for her hospitality when needed at the early stages of the project.

As is apparent from this body of work, I’ve a keen interest in seabed mapping and, in particular, the multibeam echosounder. I would like to thank Dr. Boris Dorschel for first introducing me to the multibeam echosounder in July, 2011. A special thank you to Aodhan Fitzgerald and Dr. Fabio Sachetti for further developing this interest and sending me to Norway to learn about multibeam operation from Kongsberg.

A personal thank you to Zoë, you have supported me through the harder parts of the Ph.D., listened to my daily rants (and crap stories), shown light at the end of the tunnel and really helped me out when needed. I’m forever grateful.

I’ve got to travel to over 10 different countries and see things that most will not get the chance to with this Ph.D. Its completion represents the end of a chapter in my life which started in 2008 where a, former lecturer and now, good friend, mentor and supervisor, Prof. Andy Wheeler, fascinated me by earth surface processes and inspired me to pursue a career in marine geoscience. Andy took a chance, taking me on a life-changing research cruise in 2011 and has gone above and beyond the role of research supervisor many times, when he didn’t need to. I’ve learned so much from you Andy, thank you so much for everything.

Thank you all,

Aaron

Abstract

Cold-water corals (CWC) are sessile, filter-feeding organisms that trap sediment generating positive topographic features on the seabed called CWC reefs. These reefs are common along the North East Atlantic Ocean, particularly along the Irish continental margin from 700- 1000 m deep where suitable substrates are available in the form of glacial erratics and productive surface water-fed bottom currents are available along the margin. Over the past decade, numerous research efforts have generated a significant body of knowledge on cold-water coral reef and mound development and their environmental thresholds. However, these research efforts are largely limited in resolution and the range of study sites and datasets analysed. Here, a local-regional assessment of a chain of CWC reefs and their local environment is carried out. Then, within the context of its surrounding local-regional environment, one of these reefs (Piddington Mound) is imaged and analysed at the highest-known resolution. In light of these research findings, a best practice approach for reef characterisation is put forward. Adopting this approach, the reef is further studied at an equal resolution 4 years later.

The chosen studied site is the previously ungroundtruthed, downslope Moira Mounds area. The Moira Mounds have been the subject of previous research efforts where they have been divided into 4 areas based on their geographic distribution; the northern area, the up-slope area, the midslope area and the downslope area. The mounds in northern area and upslope area have been recorded as inactive. Similarly, significant imaging and mapping efforts have shown that the midslope area is mostly inactive. In 2011, the VENTuRE cruise, on board the RV Celtic Explorer with the Holland 1 ROV imaged the Moira Mounds in the downslope area. This preliminary assessment revealed that these mounds changed in size, stage of growth

and vitality over a 10 km study site. As such, 3 more research cruises (Eurofleets_Moira_Mounds, WICPro and QuERCi) developed a data repository of the downslope Moira Mounds which are analysed and presented herein. This data includes oblique and downward-facing high-definition ROV video data, CTD data, box cores and ROV-borne multibeam.

The ROV footage was analysed to generate a seabed facies distribution map. The observed facies incorporated the on-mound areas (colonies, thickets, mounds) and off-mound areas (sediment-type, ripple-type and ripple direction). Current proxies were applied to the sediment samples and bedform observations. The results were spatially analysed within a GIS revealing that the Moira Mounds are hosted within a dynamic environment. In the south of the downslope area, mounds are small with low quantities of live coral where currents appear weak. Conversely, in the north of the downslope area, mounds are large with high quantities of live coral where currents appear relatively strong. The net effect of the bottom current is evidenced by both ripple-type variation and sediment-derived current proxies from south to north across the area.

Downward-facing video footage was mosaicked into a full-reef georeferenced raster layer. The entire reef was manually classified using a quadrat-based approach. Spatial statistics shows that the facies across the reef are clustered into rings, based concentrically around the mound summit. Micro-bathymetry, derived from the ROV-mounted multibeam echosounder showed the local sedimentary environment and mound morphology. Some parallels are drawn between facies observations at the Piddington Mound and the Wilson Rings model. However, a more refined model based on currents and environmental forcing is put forward. This shows that the distribution of facies across the mound are related to, typical coral lifecycle processes (growth and decay), mound morphology (clasts rolling down the steepened mound slope) and changes in current speeds.

Subsequently, the exact proportion of facies quantities are known across the Piddington Mound. As such, the minimum number of images required to accurately characterise the mound surface are determined by use of a robust sample size estimation technique. Further, a series of typical survey designs are assessed using the determined sample size. Despite being the most commonly used survey design for ROV-based video inspections in cold-water coral reef habitats, single-pass video surveys produce the least representative results while the least used survey design (gridded line surveys) produce the most accurate results. This established video survey technique is applied to video data collected from the mound four years later showing that the mound surface changed by 19%, suggesting that in 20 years, almost the entire mound surface can change.

As the first detailed investigation of the downslope Moira Mounds and the highest resolution image survey of an entire cold-water coral reef, this thesis reveals that the Moira Mounds exist in a strong, bedload-dominated current where changes in substrate-type and current speed are reflected in mound morphology, stage of growth and status (live or dead). It shows that the Moira Mounds appear to have a typical ring-like growth pattern. The application and suitability of downward-facing video mosaicking in this dynamic habitat and its subsequent analyses are demonstrated. As such, the heterogeneity of the downslope Moira Mounds are outlined at a local-regional scale and at a reef-scale with a suitable qualitative and quantitative methodology described.

1 Introduction

The work presented here provides a detailed multidisciplinary investigation of the hydrodynamics, sedimentology, environmental influences and habitat variability of a chain of small-sized cold-water coral (CWC) reefs in the eastern Porcupine Seabight, known as the *Moira Mounds*. These CWC reefs exhibit spatial variation in size (height and diameter), status (predominantly live or dead coral frameworks), sediment type, current speed and surface-facies at both the reef- and reef chain-scales. Through thorough analyses of box cores, bathymetry, backscatter, video and CTD's (conductivity, temperature and depth), this spatial variation is quantified and linked to the processes driving CWC reef development. In a wider context, the novel nature of the resolution and techniques utilised herein, allows for a series of recommendations for studying similar-sized CWC reefs to be made.

1.1 Cold-water corals

Cold-water corals have been known about since the mid-eighteenth century by fishermen and scientists when they were recovered in dredge nets from cold, deep, dark parts of the ocean. The first well-known documentation of cold-water corals are a series of notes in a book dating back to 1755 called *The Natural History of Norway* by the Right Reverend Erich Pontoppidan. Here, his description of the coral is akin to an entirely white flower in full bloom. It wasn't until the 1970's and, in particular, the past 15 years that advances in technology have revealed their true, wide-ranging biogeographic extent; from polar to tropical latitudes, shallow to deep waters and concentrated on the continental shelves and slopes. Sadly, by the time of their discovery, many of these cold-water coral habitats have shown damage from anthropogenic activities such as trawling and litter. Today, coral ecosystems are typically associated with shallow, tropical seas. However, of the 5100 known coral species, over half exist in cold, deep water settings.

Cold-water corals can be defined as "animals in the cnidarian classes Anthozoa and Hydrozoa that produce either calcium carbonate (aragonite or calcitic) secretions, resulting in a continuous skeleton or as numerous microscopic, individualised sclerites, or that have a black, horn-like, proteinaceous axis" (Cairns, 2007). The most common and well-studied cold-water coral is *Lophelia pertusa*, a framework-forming Scleractinian coral (Freiwald and Wilson, 1998; Rogers, 1999). *L. Pertusa* is azooxanthellate which means it does not require a symbiotic relationship with the sunlight-dependant, zooxanthellate algae. Its independency of zooxanthellate algae means that *L. Pertusa* is not depth-restricted to the light-penetrating water depths like its shallow, tropical-water counterpart the zooxanthellate corals (e.g. *Acropora* and *Porites*). Zibrowius (1980) provide a systematic taxonomic classification of *L. Pertusa*:

Phylum: Cnidaria

Class: Anthozoa

Subclass: Hexacorllia

Order: Scleractinia

Family: Caryophyllidae (Gray, 1846)

Subfamily: Desmophyllinae (Vaughan and Wells, 1943)

Genus: *Lophelia* (Milne, Edwards and Haime, 1849)

Species: *Lophelia pertusa* (Linneus, 1758)

L. Pertusa is known for its bush-like colony development, which can grow to several metres across. As the coral framework develops, branches of these colonies can anastomose, which can strengthen the framework. *L. Pertusa* is typically white but, orange, yellow and light red variations also occur relating to the mucoid tissue-covering (the coenosarc) on the outside of the coral skeleton. The skeleton itself is grown through the accretion of aragonite crystals and biomineralisation of the coenosarc (Freiwald and Wilson, 1998; Mortensen and Rapp, 1998). Predominantly, reproduction of the coral occurs through intra-tenticular budding where an existing polyp "mouth" stretches to form a second (Freiwald and Wilson, 1998). The full polyp divides into two, until eventually, it forms tentacles and can function independently.

A suitable substrate for initial coral settlement is considered to be a main pre-requisite for CWC development (Dorschel et al., 2005a; Foubert et al., 2011a; Squires, 1964b; Wilson, 1979b). This is necessary for two reasons; so the coral larvae can settle and grow by secreting a basal holdfast to the substrate and for support when subjected to high current speeds (Roberts et al., 2009a). *Lophelia* needs a hard substrate on which to settle upon (pebbles, shells, dead corals, etc.) (Haas et al., 2009). In the CWC-abundant north east Atlantic, hard substrates for coral settlement are widely available in the form of rock-outcrops, glacial erratics & gravels (Dorschel et al., 2009b). Once settled, coral colonies may grow to areas of soft sediment by recolonising coral rubble from previous colonies that have become physically broken (Roberts et al., 2003; Wilson, 1979). Conversely, isolated coral thickets have been observed on a mobile sediment substrate in the Darwin Mounds (Northern Rockall Trough) and the Moira Mounds (Porcupine

Seabight) (Mienis et al., 2009a). De Mol *et al.* (2007) use seismic lines over Therese Mound in the Belgica Mound Province (BMP), Porcupine Seabight, offshore Ireland to outline the substratum and underlying geology of these mounds.

Lophelia appears to be quite tolerant of a wide range of salinities. While best described to exist in 'typical marine salinities' (Dorschel et al., 2009b), it is known to exist in varying salinity ranges 35-37 g/kg (Haas et al., 2009) or 31.7-38.8 g/kg (Fink et al., 2012). Further discrepancy exists between the temperature range at which CWC exist. While it appears to be accepted that the lower temperature limit for CWC (*Lophelia*) is 4 °C, the upper temperature limit varies between authors; 12 °C (Roberts et al., 2003), 13 °C (Haas et al., 2009) to 13.8 °C (Fink et al., 2012). Fink et al. (2012) measure a dissolved oxygen range for the existence of CWC in the eastern Mediterranean during the Holocene of 2.6 - 7.2 ml l^{-1}. Temperature and salinity vary depending on water mass properties. In the Porcupine Seabight, the CWC-influencing water mass is Mediterranean Outflow Water (MOW) which is characterised by a salinity maximum between 600 m and 1100 m (Dullo et al., 2008b; White, 2007; White and Dorschel, 2010b).

As CWC are sessile and filter-feeding organisms, enhanced bottom currents are vital for coral growth by supplying food (Davies et al., 2009a; Duineveld et al., 2007b; Mueller et al., 2014a; Purser et al., 2010a; van Oevelen et al., 2016). These enhanced currents concentrate Particulate Organic Matter (POM), flush it through coral colonies, supply sediment for stability and carry detrital material away from coral polyps (Frederiksen et al., 1992). These enhanced currents are the result of topographic-hydrodynamic interactions on elevated areas of seabed (Roberts et al., 2003). All mound provinces along the European continental margin exist in areas where enhanced currents interact with topography and rate of food encounter is increased (Mienis et al., 2009a). Evidence for strong bottom currents can be found within mound provinces along the north east Atlantic margin by the presence of contourite channels, sediment waves, scoured-moats, sand sheets and ripples (Dorschel et al., 2007a; Dorschel et al., 2005a; Dorschel et al., 2009b; Hebbeln et al., 2016a; Kozachenko, 2005a).

Like all organisms, CWC rely on food for growth. Food is initially supplied through enhanced surface productivity (Davies et al., 2009a; Duineveld et al., 2007b). This effect can be seen during the Pleistocene whereby surface productivity played a major role in controlling the onset and cessation of coral growth in the North East Atlantic (Fink et al., 2012). Mortensen et al. (2001) show that CWC thrive on a varied diet. Building on this, a case study by Duineveld et al. (2004) exhibit CWC on the Galicia bank thriving on a mixed diet of zooplankton and algae. Roberts et al. (2003) suggest that CWC only rely on a food chain supported by surface productivity. This is based on submersible and aquaria observations which show CWC catching live prey (calanoid copepods). More recently, seasonal variation in particle flow to CWC's has attributed to the varying activity of internal waves (Mienis et al., 2009a). At this point, it is worth noting that the environmental conditions noted so far are broad-scale factors (<1 km). Dolan et al. (2008) argue that local-scale (10 cm to 1 km) factors (patterns of distribution, environmental gradients and topographic variables) are also important to understand spatial ecology and habitat structures (meso- and micro-scale) of CWC habitats.

Hydrostatic pressure (depth) appears to have little or no control on CWC scleractinians. For example, in optimal environmental conditions, *Lophelia* and *Desmophyllum* have been found in water at depths of 39 m, 8 m and 2 m (Roberts et al., 2009a). Thus, it is not the depth at which the organism occurs but rather the depth at which their preferential temperature occurs at. In the Porcupine Seabight, this depth range is 500m to 1100m (White and Dorschel, 2010b; White et al., 2005). The depth at which various physio-chemical parameters exist also has an effect on CWC distribution. The Calcium Compensation Depth (CCD) and the Aragonite Compensation Depth (ACD) both control the depth at which CWC can exist. Calcium Carbonate ($CaCO3$) exists as two different polymorphs; calcite and aragonite. While these minerals have the same chemical composition, they have a different crystal habit. These minerals vary in habit, colour, hardness and stability. Aragonite is physically hard but chemically unstable while calcite is physically soft but chemically stable. Six of the main framework-forming CWC (*Lophelia*, *Madrepora*, *Goniocorella*, *Oculina*, *Enallopsammia* and *Solenosmilia*) build their skeletons from Aragonite (Roberts et al., 2009a). However, there are CWC who make their skeletons from calcite. The increasing pressure with depth causes minerals to dissolve at certain depths. At the CCD, calcite will dissolve (dissolution). Similarly, as aragonite is chemically less stable, it will dissolve at a shallower depth than calcite. Thus, it is not possible for different species of CWC to exist at depths below the CCD or ACD.

Continued CWC development can result in positive topographic features called CWC reefs or CWC carbonate mounds (Roberts et al., 2009a). Sediment supply seems to be a significant factor for CWC reef development (Foubert et al., 2011a; IODP 307 Expedition scientists, 2005; Wheeler et al., 2005a) because, infilling the coral framework, it provides stability against strong bottom currents (Dorschel et al., 2009a) and protects the base of the coral colony from bioerosion (Beuck et al., 2010; Freiwald and Schönfeld, 1996). This sedimentation process has been observed, amongst others, in submarine dives at the Miami Terrace where corals are forming muddy mounds (Correa et al., 2012a; Neumann and Ball, 1970b). Allogenic sediment can make up a dominant component of mound sediment. For instance, >50% of the Challenger Mound in the Porcupine Seabight consists of terrigenous sediment (Pirlet et al., 2011a; Thierens et al., 2013c) and 50 - 90% of the Darwin Mounds, northern Rockall Trough (Scottish - Atlantic margin), are composed of contourite sands (Huvenne et al., 2009a; Victorero et al., 2016). The importance of terrigenous sediment in CWC reefs and carbonate mounds as a driver for mound growth has previously been discussed (Pirlet et al., 2011a). Sediment-driven vertical reef growth affords the corals access to faster-flowing water with a greater POM to lithic ratio promoting further reef development (Roberts et al., 2003; Roberts et al., 2008b; Wheeler et al., 2005a). This topic and reef sedimentology is described in much greater detail further on.

1.1.1 Cold-water coral reefs

When the framework-building cold-water corals (e.g. *L. pertusa* and *M. Oculata*) and the local hydrodynamic regime interact, a positive feedback mechanism, resulting in the formation of complex morphological structures on the seabed is developed (De Mol et al., 2007a; Roberts et al., 2009a; Wheeler et al., 2000; Wheeler et al., 2005a; Wheeler et al., 2008a). These positive bathymetric biogenic features on the seabed are called CWC reefs, also referred to as mounds or banks (De Mol et al., 2007a; Dorschel, 2003; Squires, 1964b; Wilson, 1979a). Elegantly described by Roberts et al. (2009a), a CWC carbonate mound can be formed through successive periods of CWC reef development, and can generate bathymetric features up to 350 m from base to summit (Henriet et al., 2014 and references therein). The focus of this body of work is on the CWC reef stage of development.

1.1.2 Initial cold water coral reef growth

If environmental conditions are favourable, then coral larvae will settle. However, only those settled upon a suitable substrate will continue to grow. As these corals grow, colonies may intermingle increasing coral density. This leads to the development of coral thickets. These thickets provide support and protection, attracting other organisms to this new habitat. Geologically, the subject of reef initiation has been relatively poorly documented and examined with few papers directly addressing this e.g. Squires (1964b), Wilson (1979a) and Douarin et al. (2013). Despite some work concerning reef initiation and development in more recent studies (Dorschel et al., 2005b; Foubert et al., 2011a; Frank et al., 2005; Wheeler et al., 2011a) these research are primarily concerned with the environment of reef initiation and development rather than the initiation process *itself*. See Table 1 for examples.

Wilson (1979a) and Squires (1964) both outline 4 stages in the initiation of coral banks; Colony, Thicket, Coppice and Bank. Wilson (1979a) describe a CWC bank development model based on analyses of a specimen found off-Shetland and submersible dives. Conversely, Squires (1964b) develop a similar model based on outcrop fossil thickets in Wairarapa, New Zealand. Much more recently and long overdue, Douarin et al. (2014) build on these CWC reef development models utilising CT scans, U-series dating and MSCL (multi-sensor core logger) data from vibrocores at the Mingulay Reef complex offshore Scotland to identify distinctive layers. These layers are used to identify dominating reef processes to model cold-water coral reef build-up. Presented here are the findings of Wilson (1979), Squires (1964) and Douarin *et al*. (2013) supplemented by other work.

Dominant growth direction (De Mol *et al*. 2007)	**Wilson (1964)/Squires (1979a)**	**Dorschel *et al.* (2005)**	**Foubert *et al.* (2011)**	**Douarin *et al.* (2013)**
N/A	N/A	Trigger	Erosion > Deposition	N/A
Horizontal	Colony		Erosion = Deposition	Reef initiation
	Thicket	Booster		Framework expansion
	Coppice			Framework collapse
Vertical	Bank	Bank		Coral rubble
N/A	N/A	Burial	Deposition > Erosion	Geological structure

Table 1 Relative stages of CWC reef development adapted from various authors.

1.1.3 Colony

Cold water corals generally settle on local seabed structures that provide a hard substrate in an elevated position, higher in the water column. This gives the coral access to faster flowing water with a relatively high nutrient flux and sediment supply for growth and stability (De Mol et al., 2007a) while keeping the coral anchored at the same time. Wilson (1979a) uses museum specimens to derive ideas on the initial outward growth process of coral colonies. This shows lateral growth from the initial point of settlement to a small pebble 4 cm away. Further lateral growth lead to the successive attachment of the colony to two more pebbles. The final attachment, before the sample had been collected, was on a fourth pebble on which five branches of the colony converged. At this point the colony had reached

26 cm above the original attachment point. Unlike tropical corals, ahermatypic coral colony-form is dendriform (Wilson, 1979b). Initially, colonies can be mm's in size but can grow to diameters >1 m where they can be isolated from other colonies or occur in patches (thickets) (Squires, 1964b). Stratigraphically, the formation of a coral framework initiates frictional drag resulting in deposition of a sediment-rich layer (Douarin et al., 2013).

1.1.4 Thicket

A coral thicket can be simply described as an aggregation of closely associated coral colonies. Based on the Wilson Rings Theory (Wilson, 1979b), the transition of the colony stage to the thicket stage is the weakening and subsequent breakage of lower coral branches through bioerosion. Consequently, the broken coral fragments now serve as suitable substrate on which new colonies settle. At this stage, coral fragments are relatively well-preserved resulting from framework shelter and subsequent rapid burial (Douarin et al., 2013). The thicket can now be characterised by a definable extent of coral laterally and vertically (Squires, 1964b). The increased density of the coral framework allows the thicket to build sediment as shown by the presence of ripples (e.g. Wheeler et al., 2005a). The thicket tends to grow toward the prevailing current (Dorschel et al., 2007a). It now offers shelter, support and protection, a suitable habitat for a highly diverse fauna including sponges, echinoderms and fish, previously not associated with the initial colony (Dorschel et al., 2005a; Squires, 1964b). This increased biological activity in turn promotes reef sedimentation within the thicket microenvironment by production of bioclasts and micrite or by reef aggregation (Roberts et al., 2009a). Vibrocore observations show that the thicket stage of development can be characterised by a coral-rich layer (Douarin et al., 2013). It is worth noting that depending on environmental conditions, at this stage, colonial CWC's can form various types of habitats: thickets (e.g. Porcupine Seabight, West Ireland) or Hanging Gardens (e.g. steep cliff overhangs in the Sicilian channel) depending on the substratum they colonise (Beuck et al., 2010).

1.1.5 Coppice

At the first instance, a coral thicket becomes a coral coppice when a significant amount of debris accumulates around the base of a thicket (Squires, 1964b). In the Wilson Rings theory, this stage can be defined when coral debris is generated by those colonies settled upon the debris from the first colony (Wilson, 1979b). Douarin et al. (2014) mention a similar stage of development in a reef build-up model (Figure 1). This stage is classed by collapse of the framework as a function of its own weight and degree of (bio)erosion at the soft tissue-barren base. Furthermore, they state that this suggests that coral frameworks have a definitive life-span controlled by its weight and bioerosion.

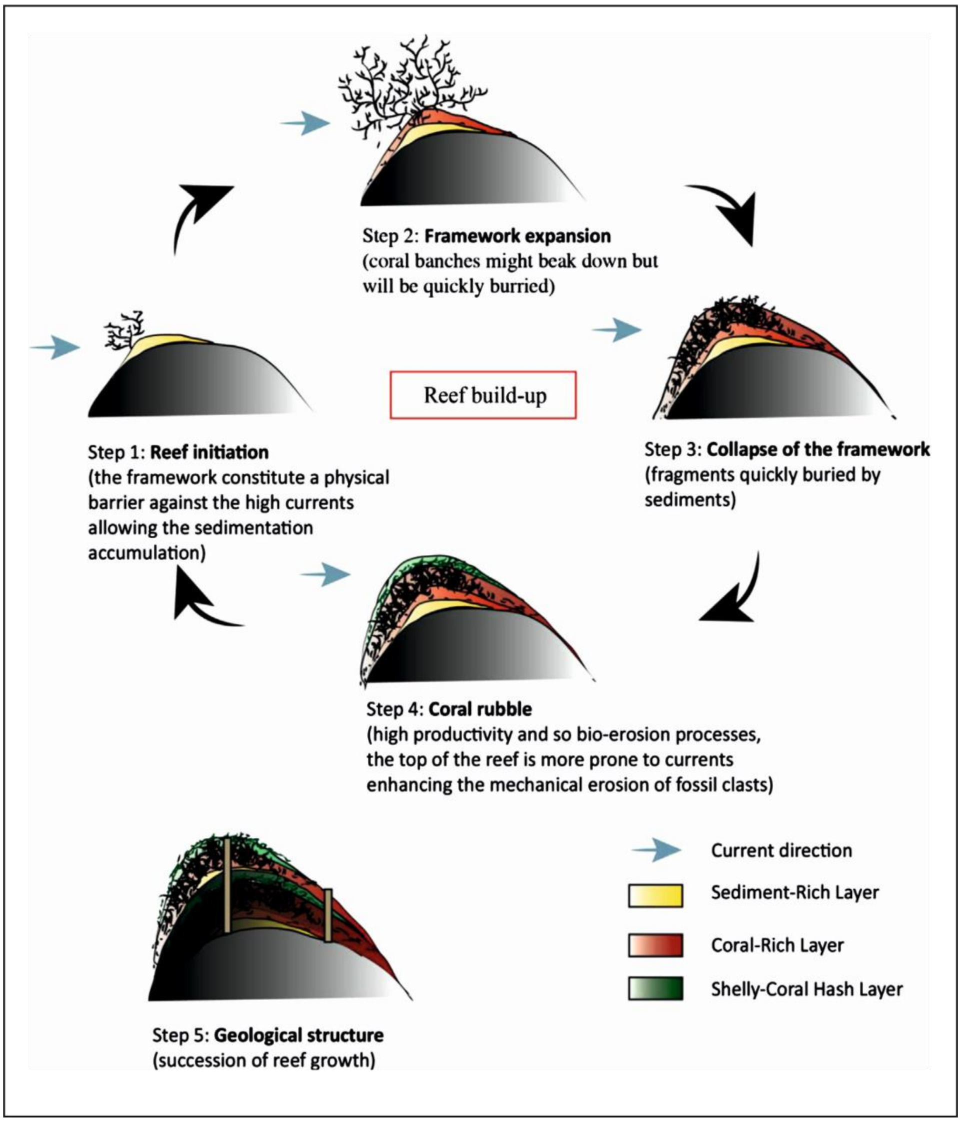

Figure 1 Reef build-up model proposed by Douarin et al. (2013)

1.1.6 Bank

The bank stage of coral development is most elegantly described by Squires (1964); 'Large in size with impressive faunal entities', the coral bank is formed through the continuous addition of coral debris from the living cap of coral. Squires (1964) further divides the near-surface and surface into 3 layers: 1) Living cap of coral; 2) open mat of coral skeletal debris and; 3) Solid mass of skeletal debris and impacted mud which provides a suitable niche for boring organisms in turn destroying and compacting the coral. Roberts et al. (2009) accurately describe this stage of development as a cold-water coral reef; a coral bank within its first generation. Herein, this stage of development is referred to as “reef”, in line with the definition by Roberts et al. (2009a).

1.1.7 Vertical reef growth

The positive topography developed by CWC's is owed predominantly to the framework-forming Scleractinian CWC's namely *Lophelia* and *Madrepora* *(Vertino et al., 2010b; Wheeler et al., 2007b).* Scleractinia grow vertically through the water column above the benthic boundary layer into faster flowing water with increased nutrient flux and a greater Particulate Organic Matter (POM):lithic suspension ratio (Dorschel et al., 2007a; Foubert et al., 2011a; Wheeler et al., 2005a; Wheeler et al., 2007b). Access to this faster flowing water stimulates further coral growth, sediment accretion and hence, further mound elevation (Foubert et al., 2011a). Thus, coral growth within a well-balanced current regime starts a positive feedback mechanism (Foubert et al., 2011a). While initial coral bank development during a period of low- or non-deposition results in a broad mound base, later phases of coral bank development results in growth in a vertical direction (De Mol et al., 2007a) (see Fig. 1.2a). This vertical growth is governed by reef sedimentation.

1.1.8 Reef sedimentology

There are two main sources of reef sediment: autochthonous (formed *in situ*) and allochthonous (transported/inherited). Autochthonous reef sediments are bioclastic (coral rubble, coral colonies, shell fragments etc.) resulting from bioerosion/biocorrosion, collapse under its own weight, increased current speeds or diagenetic cements (Beuck et al., 2010; Douarin et al., 2013; Roberts et al., 2009a). Allochthonous reef sediments can be biogenic (foraminifers, pteropods etc.) or siliceous (mud to fine sand grade material) in origin (Roberts et al., 2009a). Thus, reef sediment is typically bimodel. The proportion of these sediments vary due to a number of processes including climatic (glacial-interglacial), sediment source, biological activity and currents. As a result, coral mounds develop distinctive layers reflecting the dominant mechanism of deposition (Douarin et al., 2013).

Cold-water coral reefs trap and accrete sediment through a process called sediment baffling. Sediment baffling is an important reef-building process as it allows deposition in an otherwise non-depositional environment (e.g. Figure 2) (De Mol et al., 2007a; Roberts et al., 2009a). This is the result of coral framework-hydrodynamic interactions; colonial coral frameworks increase seabed roughness, causing friction between the coral and current. This retards current flow allowing sediment baffling/deposition to take place.

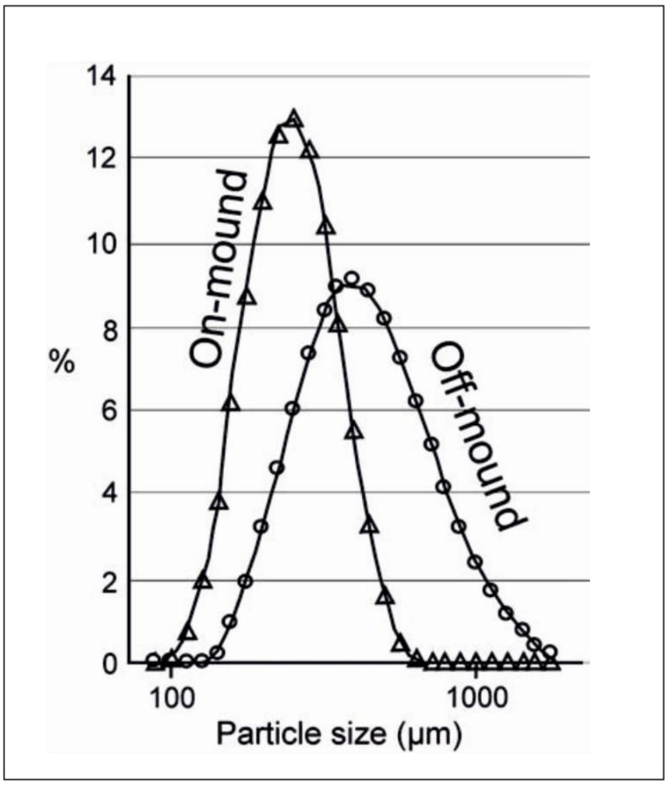

Figure 2 Grain-size distribution curve.

Comparison of typical on- and off-mound grain-size distribution at the Moira Mounds, Belgica Mound Province, eastern Porcupine Seabight, offshore Ireland (source Wheeler et al., 2011a)

The baffling of sediment by coral frameworks supports the framework and strengthens construction. When sediment supply is high, sediment can fill an entire framework leaving behind a smoothed flank and gentle slope (De Mol et al., 2007a). Conversely, if sediment supply is low or if current strength increases (keeping particles in suspension) frameworks may stay exposed or grow in-pace with sedimentation. The effect of sediment baffling within the coral framework can be seen upon examination of ripple-type and morphology over the transition of off-mound to on-mound areas (Kozachenko, 2005a).

Wheeler *et al.* (2011) use ROV video data to examine ripple-type from off- to on-mound at the Moira Mounds, Belgica Mound Province, Porcupine Seabight, offshore Ireland. Analysis of the off-mound area reveal the presence of sinuously crested ripples suggesting active bedload sediment transport. On-mound, these ripples become straight crested due to the decreasing energy/current speeds associated with the frictional drag capacity of coral frameworks (Wheeler et al., 2011a).

De Mol *et al*. (2007) generate sediment isopach maps derived from seismic lines to examine sediment thickness through time. Coral mound interior appears to vary between study sites (Correa et al., 2012a; Douarin et al., 2013; Masson et al., 2003a). Cores have also been analysed to reveal distinctive layering. For example, Douarin *et al*. (2013) use piston cores through the Mingulay Reef Complex to examine reef development. Correa *et al*. (2012) use geophysical data to show cold-water coral ridges at the base of the Miami Terrace, South Florida that are entirely biogenic in origin and are not coral topped sediment waves. This contrasts with sediment waves overgrown with cold-water corals (coral-topped) in the Belgica Mound Province, Porcupine Seabight, offshore Ireland (Foubert et al., 2011a).

As corals rely on currents for food and sediment, cold-water coral reef and mound morphology is thought to be controlled by current regime (Correa et al., 2012b; De Mol et al., 2007a; Huvenne et al., 2009a; Masson et al., 2003a; Wheeler et al., 2011a). Immediate evidence for this can be seen using high-resolution multibeam and backscatter data; elongate sediment tails orientated parallel to prevailing current direction as can be seen in the Belgica Mound Province (Wheeler et al., 2007b) and in particular, the Moira Mounds (Wheeler et al., 2011a). Similarly, this trait can also be found in the Darwin Mounds, Rockall Trough, north east Atlantic (Huvenne et al., 2009a). Typically, mound morphology is circular to ovoid with downstream elongation. However, this is not always the case, Correa *et al*. (2012)

examine an area of the Great Bahama Bank, Straits of Florida using high-resolution, AUV-mounted multibeam bathymetry and acoustic doppler current profiler (ADCP) showing an apparent lack of correlation between current direction and mound morphology as well as current strength and mound size.

Wheeler *et al*. (2007) describe two types of mound morphologies: inherited and developed. Developed mound morphologies refer to mounds whose gross morphology can be completely attributed to hydrodynamics/current regime i.e. grow independent of substrate or colonisation site structure. Developed mound morphologies maintain an equilibrium with prevailing current regime (Wheeler et al., 2007b; Wheeler et al., 2008b). Inherited mound morphologies, as the name suggests, have a morphology directly related to the underlying substrate/colonisation site. This is common for *Lophelia* reefs as they generally settle in elevated areas with a suitable substrate (Roberts et al., 2009a). Thus, these mounds have a strong substrate control (Wheeler et al., 2007b). The ridge-shaped Sula Reef Complex on the Norwegian shelf (Freiwald et al., 2002), one of the largest cold-water coral reefs in the north east Atlantic, is an example of a mound showing inherited morphology (Wheeler et al., 2007b).

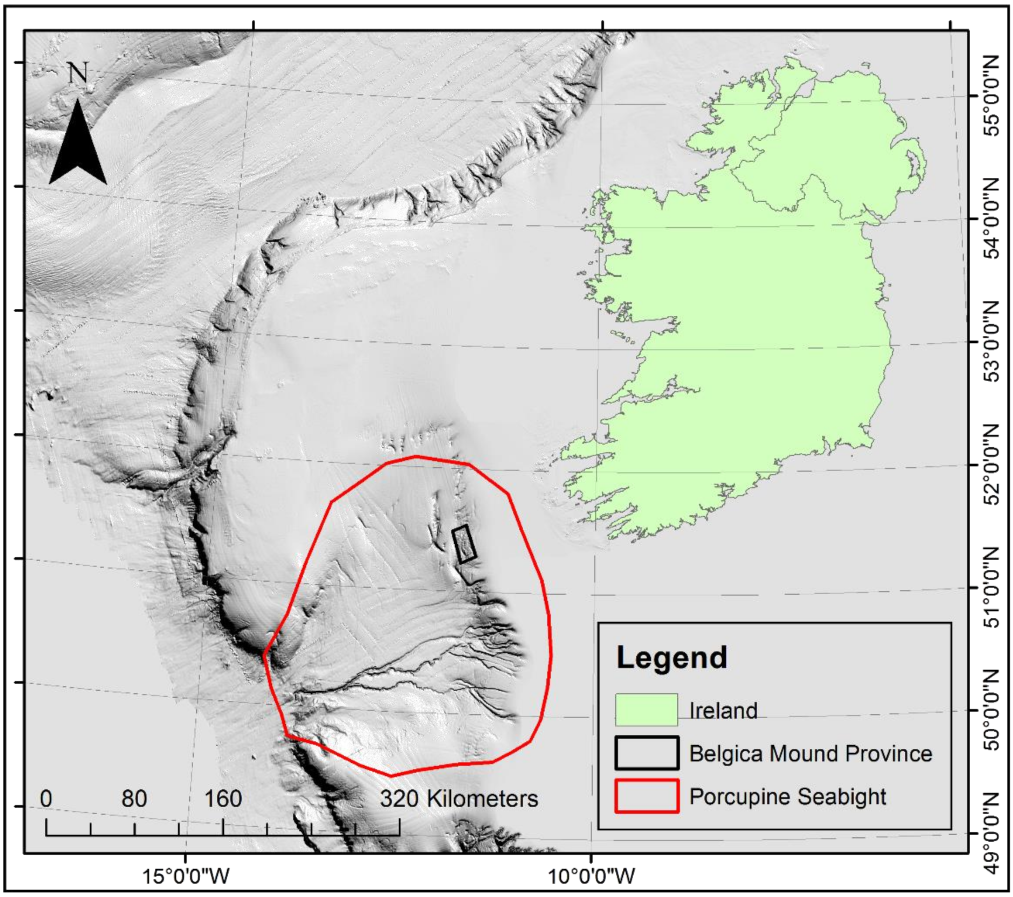

Figure 3 Porcupine Seabight location map.

Showing Ireland, the Porcupine Seabight and the Beligica Mound Province Special Area of Conservation.

1.2 The study area

The Belgica Mound Province (BMP) (Figure 3) is located on the eastern margin of the Porcupine Seabight: a north-south, large embayment on the Irish continental margin, north east Atlantic (Beyer et al., 2003b; Dorschel et al., 2007a; Henriet et al., 1998; Huvenne et al., 2002b; van Rooij et al., 2003b). Some of the BMP is within a Special Area of Conservation (SAC) designated under the EU Habitats Directive. The first major mapping effort of the BMP was carried out in 2003 using a hull-mounted multibeam echosounder, revealing a distinct undulating bathymetry: a profusion of CWC carbonate mounds (Beyer et al., 2003b). The BMP is characterised by its abundance of coral mound features which occur in the form of coral carbonate mounds and cold-water coral reefs (Foubert et al., 2005a; Wheeler et al., 2005a). Carbonate mounds occur in 2 distinct chains orientated parallel to the continental shelf; the eastern chain is largely moribund (with a mainly dead coral cover; Foubert et al., 2005) while the western chain is mostly active with a profusion of live coral (De Mol et al., 2007a; Dorschel et al., 2007a; Eisele et al., 2008b). Carbonate mound morphologies range from conical to elongate ridge-like forms and are typically 1 km across and 100 m tall (Wheeler et al., 2005a). Contourite drifts have accumulated between the giant carbonate mounds and buried their upslope flanks (Beyer et al., 2003b; Van Rooij et al., 2003a). To the east, these CWC carbonate mounds are enclosed by the continental shelf and to the west, enclosed by a blind channel, the Arwen Channel, which runs through the BMP (Murphy and Wheeler, 2017; Van Rooij, 2004b), formerly connected to the shelf break. Some of the most pioneering research on CWC carbonate mounds has been carried out within the BMP including the well-studied Galway Mound, Thérèse Mound and Challenger Mound (De Mol et al., 2007b; Dorschel et al., 2007a; Eisele et al., 2008a; Huvenne et al., 2009c; Kano et al., 2007; Thierens et al., 2010a; Titschack et al., 2009b).

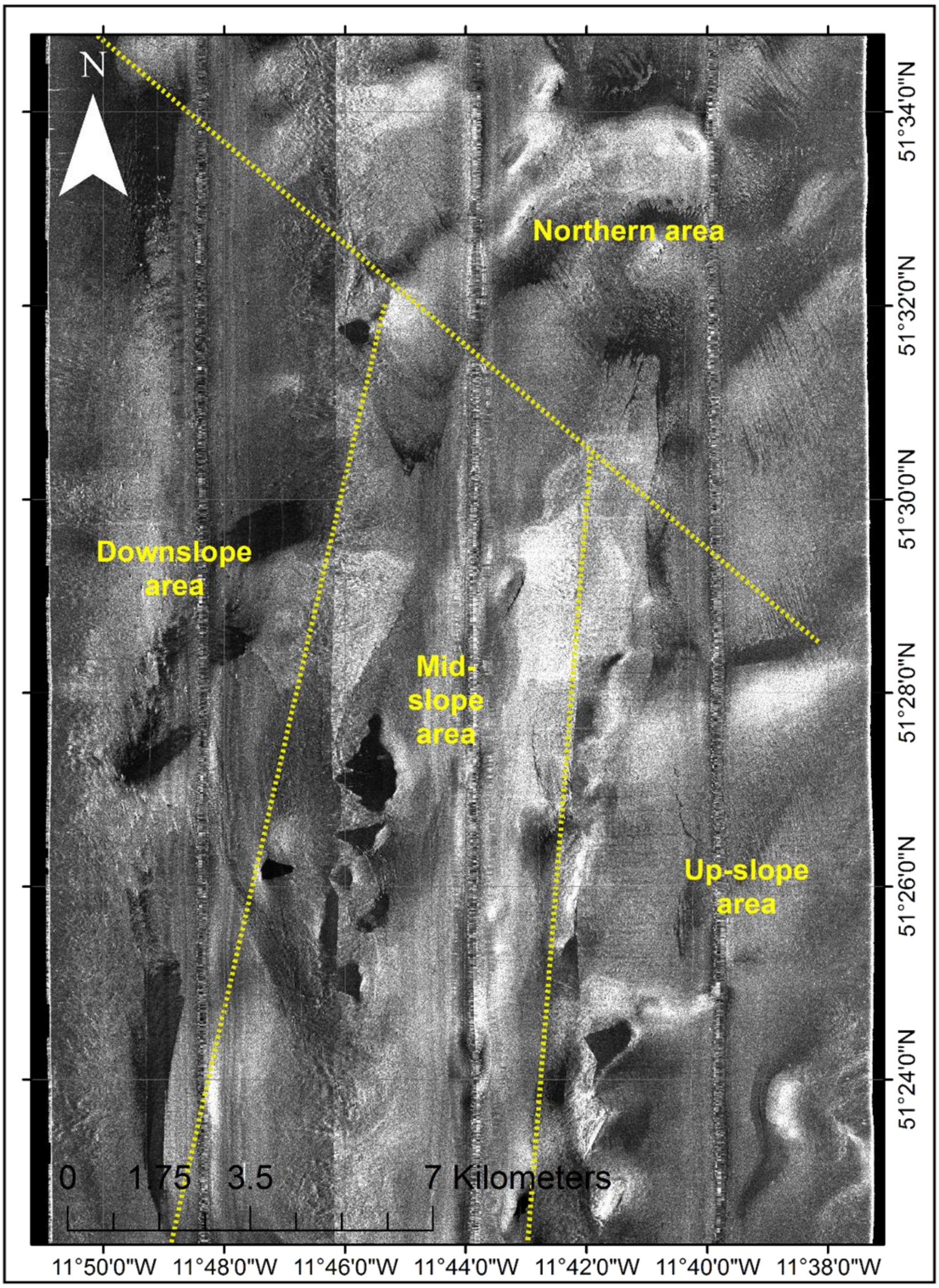

Figure 4 Belgica Mound Province Special Area of Conservation.

Map showing side scan sonar imagery of the Belgica Mound Province and geographic division of the Moira Mounds (after Wheeler et al., 2011).

The Moira Mounds are small-type CWC reefs (approx. 30 m across and 10 m tall) found throughout the BMP (Wheeler et al., 2005a). They were first mentioned by

Wheeler et al. (2005a) and (Kozachenko, 2005a) after being imaged by TOBI (towed ocean bottom instrument) side scan sonar and later ground-truthed by ROV-mounted video. This revealed them as circular to ovoid features of relatively higher backscatter than the surrounding seabed. While no definitive dating has confirmed their age, it is speculated that they are Holocene features based on their size, seismic profiles and the surrounding seabed substrate (Foubert et al., 2011a; Huvenne et al., 2005a; Kozachenko, 2005a). The Moira Mounds in the BMP can be further subdivided into 4 areas or chains of mounds based on the distribution of approx. 256 Moira Mounds; the "up-slope area", the "mid-slope area", the "down-slope area" and the "northern area" (Figure 4) (Wheeler et al., 2011a). While the number of Moira Mounds in the northern and the up-slope areas are relatively sparse, the main focus of research has been carried out on the mid- and down-slope areas. The mid-slope area occurs between the chain of CWC carbonate mound structures. The Moira Mounds here are thought to represent mound formation under "stressed" conditions due to high sediment flux (Foubert et al., 2011a). The down-slope area is unique as it occurs within the Arwen Channel. This body of research examines the lesser-studied, westernmost extent of, predominantly active, Moira Mounds which occur in and around the Arwen Channel.

1.3 Aims and objectives of research

The broad aim of this body of research is to understand the spatio-temporal development of the Moira Mounds at the reef-chain-scale and the individual reef-scale. As such, the research is divided into a series of focussed research areas explained below. Each individual research area has been written as a paper and is either "*under review*", "*submitted*" or ready to be submitted to an international, peer-reviewed scientific journal and is presented in this thesis as a chapter (chapters 2, 3 and 4). The research programme aims to build on each chapter progressively.

Chapter 2 (Hydrodynamic and sedimentological influences on cold-water coral reef development) examines the downslope Moira Mounds on a local-regional scale (10 m – 1km). It utilises multibeam bathymetry, TOBI backscatter, CTD's, ROV-mounted video and box cores through the downslope Moira Mounds **to understand the reef-influencing currents**. It creates a seabed zonation, incorporating Moira Mounds in different stages of development, a current speed gradient, differing substrate-types and physio-chemical parameters of the benthic water mass to **specify the environmental parameters on reef development** and **assess the effect of hydrodynamics on reef development**. To put these findings into a wider context, the environmental parameters and hydrodynamics are **compared with other CWC reef habitats**. As such, this chapter answers 3 main research questions:

1) What is the nature of the current affecting the downslope Moira Mounds?
2) What is the effect of hydrodynamics on reef development?
3) In light of this research, how do the downslope Moira Mounds compare with other reef habitats?

Building on the findings of local-regional-scale downslope Moira Mound reef processes and development in chapter 2, chapter 3 (Cold-water coral reef spatial zonation, organisation and environmental controls: the case of the Piddington Mound, Porcupine Seabight, NE Atlantic) utilises a thoroughly collected and accurately positioned video data set **to generate the first cold water coral reef-scale video mosaic**. A supervised classification, using CWC-reef typical classifiers is carried out on this video mosaic and its subsequent spatial analyses reveal how the surface of the Piddington Mound is organised thereby allowing **to understand reef-scale spatial organisation**. Two potential scenarios are put forward **to assess**

the influences on this spatial organisation. To broaden the scope of these research findings, other mounds in the downslope area are examined **to assess how representative the Piddington Mound is**. As such, this chapter answers 3 main research questions:

1) Does the Piddington Mound exhibit a spatial organisation?
2) What are the influences on this organisation?
3) How representative is the Piddington Mound?

In line with financial constraints, weather- and sea-state dependency of research cruises, chapter 4 (Determining seabed video-survey density and data temporal validity (shelf life) for best practice cold-water coral reef characterisation), **highlights the need for adequate spatial coverage in dynamic marine environments**, such as CWC habitats. It builds on existing video mosaic coverage of the Piddington Mound area **to calculate the minimum number of images required to accurately characterise the surface of a CWC reef**. Several ROV-based survey designs are tested (e.g. single-pass video transects, gridded surveys and contour-following transects) **to assess the best way to collect imagery at the Piddington Mound**. Repeat video imaging of the Piddington Mound 4 years later allows this chapter to repeat the analysis at a 4-year resolution. This **highlights the temporal variability on the Piddington Mound** and in light of previous work (e.g. chapter 3) **makes inferences on the processes that led to mound surface change over 4-years**. This variability implicates the temporal consistency (shelf life) of image samples from CWC reefs and as such, a series of **recommendations for best practice video surveying and sampling are outlined**. As such, this chapter answers 4 main research questions:

1) What is the minimum amount of seabed imagery needed to accurately characterise the Piddington Mound?

2) What is the most representative way by which to collect this seabed imagery?
3) What is the temporal variability of the Piddington Mound over 4 years?
4) What are the implications for temporally and spatially separated samples?

1.4 Chapter references

Beuck, L., Freiwald, A., Taviani, M., 2010. Spatiotemporal bioerosion patterns in deep-water scleractinians from off Santa Maria di Leuca (Apulia, Ionian Sea). Deep-Sea Research II 57, 458-470.

Beyer, A., Schenke, H.W., Klenke, M., Niederjasper, F., 2003. High resolution bathymetry of the eastern slope of the Porcupine Seabight. Mar. Geol. 198, 27-54.

Cairns, S.D., 2007. Deep-water corals: an overview with special reference to diversity and distribution of deep-water scleractinian corals. Bulletin of marine Science 81, 311-322.

Correa, T.B.S., Eberli, G.P., Grasmueck, M., Reed, J.K., Correa, A.M.S., 2012a. Genesis and morphology of cold-water coral ridges in a unidirectional current regime. Mar. Geol. 326–328, 14-27.

Correa, T.B.S., Grasmueck, M., Eberli, G.P., Reed, J.K., Verwer, K., Purkis, S.A.M., 2012b. Variability of cold-water coral mounds in a high sediment input and tidal current regime, Straits of Florida. Sedimentology 59, 1278-1304.

Davies, A.J., Duineveld, G.C., Lavaleye, M.S., Bergman, M.J., van Haren, H., Roberts, J.M., 2009. Downwelling and deep-water bottom currents as food supply mechanisms to the cold-water coral Lophelia pertusa (Scleractinia) at the Mingulay Reef complex. Limnology and Oceanography 54, 620.

De Mol, B., Kozachenko, M., Wheeler, A., Alvares, H., Henriet, J.-P., Olu-Le Roy, K., 2007a. Thérèse Mound: a case study of coral bank development in the Belgica Mound Province, Porcupine Seabight. Int J Earth Sci (Geol Rundsch) 96, 103-120.

De Mol, B., Kozachenko, M., Wheeler, A.J., Alvares, H., Henriet, J.-P., Olu-Le Roy, K., 2007b. Thérèse Mound: a case study of coral bank development in the Belgica Mound Province, Porcupine Seabight. International Journal of Earth Sciences 96, 103-120.

Dolan, M.F.J., Grehan, A.J., Guinan, J.C., Brown, C., 2008. Modelling the local distribution of cold-water corals in relation to bathymetric variables: Adding spatial context to deep-sea video data. Deep-Sea Research I 55, 1564-1579.

Dorschel, B., 2003. Late Quaternary Development of a deep-water Carbonate Mound in the northeast Atlantic, RCOM-Bremen. University of Bremen, bremen, p. 90.

Dorschel, B., Hebbeln, D., Foubert, A., White, M., Wheeler, A.J., 2007. Hydrodynamics and cold-water coral facies distribution related to recent sedimentary processes at Galway Mound west of Ireland. Marine Geology 244, 184-195.

Dorschel, B., Hebbeln, D., Rüggeberg, A., Dullo, W.-C., Freiwald, A., 2005a. Growth and erosion of a cold-water coral covered carbonate mound in the Northeast Atlantic during the late Pleistocene and Holocene. EPSL 233, 33-44.

Dorschel, B., Hebbeln, D., Rüggeberg, A., Dullo, W.-C., Freiwald, A., 2005b. Growth and erosion of a cold-water coral covered carbonate mound in the Northeast Atlantic during the Late Pleistocene and Holocene. Earth and Planetary Science Letters 233, 33-44.

Dorschel, B., Wheeler, A.J., Huvenne, V.A.I., de Haas, H., 2009a. Cold-water coral mounds in an erosive environmental setting: TOBI side-scan sonar data and ROV video footage from the northwest Porcupine Bank, NE Atlantic. Mar. Geol. 264, 218-229.

Dorschel, B., Wheeler, A.J., Huvenne, V.A.I., de Haas, H., 2009b. Cold-water coral mounds in an erosive environmental setting: TOBI side-scan sonar data and ROV video footage from the northwest Porcupine Bank, NE Atlantic. Marine Geology 264, 218-229.

Douarin, M., Sinclair, D.J., Elliot, M., Henry, L.-A., Long, D., Mitchison, F., Roberts, J.M., 2014. Changes in fossil assemblage in sediment cores from Mingulay Reef Complex (NE Atlantic): Implications for coral reef build-up. Deep Sea Research Part II: Topical Studies in Oceanography 99, 286-296.

Duineveld, G., Lavaleye, M., Berghuis, E., 2004. Particle flux and food supply to a seamount cold-water coral community (Galicia Bank, NW Spain). Marine Ecology Progress Series 277, 13-23.

Duineveld, G.C.A., Lavaleye, M.S.S., Bergman, M.J.N., de Stigter, H.C., Mienis, F., 2007. Trophic structure of a cold-water coral mound community (Rockall Bank, NE Atlantic) in relation to the near-bottom particle supply and current regime. Bulletin of Marine Science 81, 449-467.

Dullo, W.-C., Flögel, S., Rüggeberg, A., 2008. Cold-water coral growth in relation to the hydrography of the Celtic and Nordic European continental margin. Marine Ecology Progress Series 371, 165-176.

Eisele, M., Hebbeln, D., Wienberg, C., 2008a. Growth history of a cold-water coral covered carbonate mound - Galway Mound, Porcupine Seabight, NE-Atlantic. Mar. Geol. 253, 160-169.

Eisele, M., Hebbeln, D., Wienberg, C., 2008b. Growth history of a cold-water coral covered carbonate mound — Galway Mound, Porcupine Seabight, NE-Atlantic. Marine Geology 253, 160-169.

Fink, H.G., Wienberg, C., Hebbeln, D., McGregor, H.V., Schmiedl, G., Taviani, M., Freiwald, A., 2012. Oxygen control on Holocene cold-water coral development in the eastern Mediterranean Sea. Deep Sea Research Part I: Oceanographic Research Papers 62, 89-96.

Foubert, A., Beck, T., Wheeler, A., Opderbecke, J., Grehan, A., Klages, M., Thiede, J., Henriet, J.-P., 2005. New view of the Belgica Mounds, Porcupine Seabight, NE Atlantic: preliminary results from the Polarstern ARK-XIX/3a ROV cruise, in: Freiwald, A., Roberts, J.M. (Eds.), Cold-Water Corals and Ecosystems. Springer Berlin Heidelberg, pp. 403-415.

Foubert, A., Huvenne, V.A.I., Wheeler, A., Kozachenko, M., Opderbecke, J., Henriet, J.P., 2011. The Moira Mounds, small cold-water coral mounds in the Porcupine Seabight, NE Atlantic: Part B—Evaluating the impact of sediment dynamics through high-resolution ROV-borne bathymetric mapping. Marine Geology 282, 65-78.

Frank, N., Lutringer, A., Paterne, M., Blamart, D., Henriet, J.-P., van Rooij, D., van Weering, T.C.E., 2005. Deep-water corals of the northeastern Atlantic margin: carbonate mound evolution and upper intermediate water ventilation during the Holocene, in: Freiwald, A., Roberts, J.M. (Eds.), Cold-water Corals and Ecosystems. Springer, Berlin, Heidelberg, New York, pp. 113-133.

Frederiksen, R., Jensen, A., Westerberg, H., 1992. The distribution of the scleractinian coral *Lophelia pertusa* around the Faroe Islands and the relation to internal tidal mixing. Sarsia 77, 157-171.

Freiwald, A., Hühnerbach, V., Lindberg, B., Wilson, J., Campbell, J., 2002. The Sula Reef Complex, Norwegian shelf. Facies 47, 179-200.

Freiwald, A., Schönfeld, J., 1996. Substrate pitting and boring pattern of *Hyrrokkin sarcophaga* Cedhagen, 1994 (Foraminifera) in a modern deep-water coral reef mound. Mar. Micropaleontol. 28, 199-207.

Freiwald, A., Wilson, J.B., 1998. Taphonomy of modern, deep, cold-temperate water coral reefs. Historical Biology 13, 37-52.

Haas, H., Mienis, F., Frank, N., Richter, T., Steinacher, R., Stigter, H., Land, C., Weering, T.E., 2009. Morphology and sedimentology of (clustered) cold-water coral mounds at the south Rockall Trough margins, NE Atlantic Ocean. Facies 55, 1-26.

Hebbeln, D., Van Rooij, D., Wienberg, C., 2016. Good neighbours shaped by vigorous currents: Cold-water coral mounds and contourites in the North Atlantic. Mar. Geol. 378, 171-185.

Henriet, J.-P., De Mol, B., Pillen, S., Vanneste, M., Van Rooij, D., Versteeg, W., Croker, P.F., Shannon, P.M., Unnithan, V., Bouriak, S., Chachkine, P., BELGICA 97 Shipboard scientific crew, 1998. Gas hydrate crystals may help build reefs. Nature 391, 648-649.

Henriet, J.P., Hamoumi, N., Da Silva, A.C., Foubert, A., Lauridsen, B.W., Rüggeberg, A., Van Rooij, D., 2014. Carbonate mounds: From paradox to World Heritage. Marine Geology 352, 89-110.

Huvenne, V.A.I., Beyer, A., de Haas, H., Dekindt, K., Henriet, J.-P., Kozachenko, M., Olu-Le Roy, K., Wheeler, A.J., participants, T.P.c., participants, C.c., 2005. The seabed appearance of different coral bank provinces in the Porcupine Seabight, NE Atlantic: results from sidescan sonar and ROV seabed mapping, in: Freiwald, A., Roberts, J.M. (Eds.), Cold-water Corals and Ecosystems. Springer-Verlag, Berlin Heidelberg, pp. 535-569.

Huvenne, V.A.I., Blondel, P., Henriet, J.P., 2002. Textural analyses of sidescan sonar imagery from two mound provinces in the Porcupine Seabight. Marine Geology 189, 323-341.

Huvenne, V.A.I., Masson, D.G., Wheeler, A.J., 2009a. Sediment dynamics of a sandy contourite: the sedimentary context of the Darwin cold-water coral mounds, Northern Rockall Trough. Int J Earth Sci (Geol Rundsch) 98, 865-884.

Huvenne, V.A.I., Van Rooij, D., De Mol, B., Thierens, M., O'Donnell, R., Foubert, A.T.G., 2009b. Sediment dynamics and palaeo-environmental context at key stages in the Challenger cold-water coral mound formation: Clues from sediment deposits at the mound base. Deep Sea Res. Part I 56, 2263-2280.

IODP 307 Expedition scientists, 2005. Modern carbonate mounds: Porcupine drilling. IODP Prel. Rept., 307, p. 58.

Kano, A., Ferdelman, T.G., Williams, T., Henriet, J.-P., Ishikawa, T., Kawagoe, N., Takashima, C., Kakizaki, Y., Abe, K., Sakai, S., Browning, E.L., Li, X., Andres, M.S., Bjerager, M., Cragg, B.A., De Mol, B., Dorschel, B., Foubert, A.T.G., Frank, T.D., Fuwa, Y., Gaillot, P., Gharib, J.J., Gregg, J.M., Huvenne, V.A.I., Léonide, P., Mangelsdorf, K., Monteys, X., Novosel, I., O'Donnell, R., Rüggeberg, A., Samarkin, V.A., Sasaki, K., Spivack, A.J., Tanaka, A., Titschack, J., van Rooij, D., Wheeler, A.J., 2007. Age constraints on the origin and growth history of a deep-water coral mound in the northeast Atlantic drilled during Integrated Ocean Drilling Program Expedition 307. Geology 35, 1051-1054.

Kozachenko, M., 2005. Present and Past Environments of the Belgica Mounds (deep-water coral carbonate mounds) Eastern Porcupine Seabight, North East Atlantic (unpublished PhD Thesis), Department of Geography and Geology. University College Cork, Cork, p. 221.

Masson, D.G., Bett, B.J., Billett, D.S.M., Jacobs, C.L., Wheeler, A.J., Wynn, R.B., 2003. The origin of deep-water, coral-topped mounds in the northern Rockall Trough, Northeast Atlantic. Marine Geology 194, 159-180.

Mienis, F., de Stigter, H.C., de Haas, H., van Weering, T.C.E., 2009. Near-bed particle deposition and resuspension in a cold-water coral mound area at the Southwest Rockall Trough margin, NE Atlantic. Deep Sea Res. Part I 56, 1026-1038.

Mortensen, P.B., Hovland, M.T., Fosså, J.H., Furevik, D.M., 2001. Distribution, abundance and size of *Lophelia pertusa* coral reefs in mid-Norway in relation to seabed characteristics. Journal of the Marine Biological Association of the UK Volume 81, Issue 04, Aug 2001, 581-597.

Mortensen, P.B., Rapp, H.T., 1998. Oxygen and carbon isotope ratios related to grows line pattern in skeletons of *Lophelia pertusa* (L) (Anthozoa,Scleractinia): Implications for determination of linear extension rates. Sarsia 83, 433-446.

Mueller, C., Larsson, A.I., Veuger, B., Middelburg, J., van Oevelen, D., 2014. Opportunistic feeding on various organic food sources by the cold-water coral Lophelia pertusa. Biogeosciences 11, 123-133.

Murphy, P., Wheeler, A.J., in press. A GIS-based application of drainage basin analysis and geomorphometry in the submarine environment: The Gollum Canyon System, North-east Atlantic, in: Bartlett, D., Celliers, L. (Eds.), Geoinformatics for Marine and Coastal Management. CRC Press, Taylor & Francis Group, Boca Raton, USA.

Neumann, A.C., Ball, M.M., 1970. Submersible Observations in the Straits of Florida: Geology and Bottom Currents. Geological Society of America Bulletin 81, 2861-2874.

Pirlet, H., Colin, C., Thierens, M., Latruwe, K., Van Rooij, D., Foubert, A., Frank, N., Blamart, D., Huvenne, V.A., Swennen, R., 2011. The importance of the terrigenous fraction within a cold-water coral mound: A case study. Mar. Geol. 282, 13-25.

Purser, A., Larsson, A.I., Thomsen, L., van Oevelen, D., 2010. The influence of flow velocity and food concentration on *Lophelia pertusa* (Scleractinia) zooplankton capture rates. Journal of Experimental Marine Biology and Ecology 395, 55-62.

Roberts, J.M., Long, D., Wilson, J.B., Mortensen, P.B., Gage, J.D., 2003. The cold-water coral Lophelia pertusa (Scleractinia) and enigmatic seabed mounds along the north-east Atlantic margin: are they related? Marine Pollution Bulletin 46, 7-20.

Roberts, J.M., Long, L.-A.H.D., Hartley, J.P., 2008. Cold-water coral reef frameworks, megafaunal communities and evidence for coral carbonate mounds on the Hatton Bank, north east Atlantic. Facies 54, 297-316.

Roberts, J.M., Wheeler, A., Freiwald, A., Cairns, S., 2009. Cold-Water Corals: The Biology and Geology of Deep-Sea Coral Habitats. Cambridge University Press.

Rogers, A.D., 1999. The biology of *Lophelia pertusa* (Linnaeus 1758) and other deep-water reef-forming corals and impacts from human activities. International Review of Hydrobiology 84, 315-406.

Squires, D.F., 1964. Fossil coral thickets in Wairarapa, New Zealand. Journal Paleontol. 38, 904-915.

Thierens, M., Browning, E.L., Prilet, H., Loutre, M.-F., Dorschel, B., Huvenne, V.A.I., Titschack, J., Colin, C., Foubert, A.T.G., Wheeler, A.J., 2013. Cold-water coral carbonate mounds as unique palaeo-archives: the Plio-Pleistocene Challenger Mound record (NE Atlantic). Quaternary Science Reviews 73, 14-30.

Thierens, M., Titschack, J., Dorschel, B., Huvenne, V.A.I., Wheeler, A.J., Stuut, J.-B.W., O'Donnell, R., 2010. The 2.6 Ma depositional sequence from the Challenger cold-water coral carbonate mound (IODP Exp. 307): sediment contributors and hydrodynamic palaeo-environments. Mar. Geol. 271, 260-277.

Titschack, J., Thierens, M., Dorschel, B., Schulbert, C., Freiwald, A., Kano, A., Takashima, C., Kawagoe, N., Li, X., 2009. Carbonate budget of a cold-water coral mound (Challenger Mound, IODP Exp. 307). Mar. Geol. 259, 36-46.

van Oevelen, D., Mueller, C.E., Lundälv, T., Middelburg, J.J., 2016. Food selectivity and processing by the cold-water coral Lophelia pertusa. Biogeosciences 13, 5789.

Van Rooij, D., 2004. An integrated study of Quaternary sedimentary processes on the eastern slope of the Porcupine Seabight, SW of Ireland, Renard Centre of Marine Geology. University Gent, Belgium, p. 355.

Van Rooij, D., De Mol, B., Huvenne, V., Ivanov, M., Henriet, J.P., 2003a. Seismic evidence of current-controlled sedimentation in the Belgica mound province, upper Porcupine slope, southwest of Ireland. Marine Geology 195, 31-53.

van Rooij, D., De Mol, B., Huvenne, V.A.I., Ivanov, M.K., Henriet, J.-P., 2003b. Seismic evidences of current-controlled sedimentation in the Belgica mound province, upper Porcupine slope, southwest of Ireland. Mar. Geol. 195, 31-53.

Vertino, A., Savini, A., Rosso, A., Di Geronimo, I., Mastrototaro, F., Sanfilippo, R., Gay, G., Etiope, G., 2010. Benthic habitat characterization and distribution from two representative sites of the deep-water SML Coral Province (Mediterranean). Deep Sea Research Part II: Topical Studies in Oceanography 57, 380-396.

Victorero, L., Blamart, D., Pons-Branchu, E., Mavrogordato, M.N., Huvenne, V.A.I., 2016. Reconstruction of the formation history of the Darwin Mounds, N Rockall Trough: How the dynamics of a sandy contourite affected cold-water coral growth. Mar. Geol. 378, 186-195.

Wheeler, Kozachenko, M., Henry, L.A., Foubert, A., de Haas, H., Huvenne, V.A.I., Masson, D.G., Olu, K., 2011. The Moira Mounds, small cold-water coral banks in the Porcupine Seabight, NE Atlantic: Part A—an early stage growth phase for future coral carbonate mounds? Marine Geology 282, 53-64.

Wheeler, A., Bett, B., Billett, D., Masson, D., 2000. High resolution side-scan sonar mapping of deep-water coral mounds: surface morphology and processes affecting growth. Eos, Transactions, American Geophysical Union 81, F638.

Wheeler, A., Kozachenko, M., Beyer, A., Foubert, A., Huvenne, V.I., Klages, M., Masson, D., Olu-Le Roy, K., Thiede, J., 2005. Sedimentary processes and carbonate mounds in the Belgica Mound province, Porcupine Seabight, NE Atlantic, in: Freiwald, A., Roberts, J.M. (Eds.), Cold-Water Corals and Ecosystems. Springer Berlin Heidelberg, pp. 571-603.

Wheeler, A.J., Beyer, A., Freiwald, A., Haas, H., Huvenne, V.A.I., Kozachenko, M., Olu-Le Roy, K., Opderbecke, J., 2007. Morphology and environment of cold-water coral carbonate mounds on the NW European margin. Int J Earth Sci (Geol Rundsch) 96, 37-56.

Wheeler, A.J., Kozachenko, M., Masson, D.G., Huvenne, V.A.I., 2008a. Influence of benthic sediment transport on cold-water coral bank morphology and growth: the example of the Darwin Mounds, north-east Atlantic. Sedimentology 55, 1875-1887.

Wheeler, A.J., Kozachenko, M., Masson, D.G., Huvenne, V.A.I., 2008b. Influence of benthic sediment transport on cold-water coral bank morphology and growth: the example of the Darwin Mounds, north-east Atlantic. Sedimentology 55, 1875-1887.

White, M., 2007. Benthic dynamics at the carbonate mound regions of the Porcupine Sea Bight continental margin. International Journal of Earth Sciences 96, 1-9.

White, M., Dorschel, B., 2010. The importance of the permanent thermocline to the cold water coral carbonate mound distribution in the NE Atlantic. EPSL 296, 395-402.

White, M., Mohn, C., de Stigter, H.C., Mottram, G., 2005. Deep-water coral development as a function of hydrodynamics and surface productivity around the submarine banks of the Rockall Trough, NE Atlantic, in: Freiwald, A., Roberts, J.M. (Eds.), Cold-water Corals and Ecosystems. Springer, Berlin, Heidelberg, New York, pp. 503-514.

Wilson, J.B., 1979a. "Patch" development of the deep-water coral *Lophelia pertusa* (L.) on the Rockall bank. Journal of the Marine Biological Association of the United Kingdom 59, 165-177.

Wilson, J.B., 1979b. ‘Patch’ development of the deep-water coral Lophelia Pertusa (L.) on Rockall Bank. Journal of the Marine Biological Association of the United Kingdom 59, 165-177.

Zibrowius, H., 1980. Les Scléractiniaires de la Méditerranée et de l'Atlantique nord-oriental. Mémoires de l'Institut océanographique, Monaco.

2 Hydrodynamic and sedimentological influences on cold-water coral reef development

(Current status: ready for submission)

Aaron Lim* [a)], Andrew J. Wheeler [a) b)], Veerle A.I. Huvenne [c)], Agostina Vertino [d, e)], Silvia Spezzaferri [f)], Henk de Haas [g)]

This chapter acts as a suitable introduction to, and baseline study of, the downslope Moira Mounds area through a multidisciplinary investigation of the contemporary environmental conditions, hydrodynamic regime and sedimentological processes. The scale of the study (1 m to 10 km) bridges the identified local-processes to known regional-processes and is therefore adequate to contextualise and inform the studies presented in chapters 3 and 4 that are of a high spatial resolution at a scale of 25 cm to 60 m. Previous work divides the Moira Mounds into 4 sizable areas (> 10 km) (Wheeler et al., 2011) and uses sedimentary bedforms to theorise on the development of the Moira Mounds in the mostly-inactive, mid-slope area (Foubert et al., 2011). As Foubert et al. (2011) claims the bedforms are moribund it is unclear if they represent contemporary processes and can therefore be used to determine the local environment with confidence around the mid-slope Moira Mounds. The aim of this chapter is to study the mostly-active Moira Mounds in the downslope area with respect to contemporary processes, and to understand the distribution and development of these Moira Mounds.

Various authors have contributed to this chapter. The project was funded through an award to Prof. Andy Wheeler whose initial ideas inspired this study. Prof. Wheeler was either chief scientist or, at least, involved in collection of all data for this research. He also supervised the research carried out and gave useful feedback on drafts. Dr. Veerle Huvenne was involved in both collection of the side scan sonar data set and for helpful advice on currents. Dr. Agostina Vertino and Dr. Silvia Spezzaferri were chief scientists on the Eurofleets cruise to collect box cores utilised in this chapter. Dr. Vertino further provided lab facilities for the analyses of these cores. Prof. Henk de Haas was chief scientist on the cruise which collected the side scan sonar data set. Aaron Lim wrote this chapter and developed the idea for this research, including the initial research questions, the chosen methodology and data interpretation. He regridded the bathymetry, and carried out all analyses on the spatial data sets. He assisted in collection of the video data and was solely responsible for the subsequent classification and analysis of this data set. He dissolved all carbonate and organic particles from the box cores and calculated the particle size distribution using a Malvern Mastersizer in University Milano Bicocca, Milan, Italy.

[a] School of Biological, Earth and Environmental Sciences, University College Cork, Ireland

[b] Irish Centre for Research in Applied Geosciences, University College Cork, Ireland

[c] Marine Geoscience, National Oceanography Centre, University of Southampton Waterfront Campus, European Way, Southampton SO14 3ZH, UK

[d] University of Milano-Bicocca, Department of Earth and Environmental Sciences, Piazza della Scienza 4, 20126 Milano, Italy

[e] Ghent University, Department of Geology, Renard Centre of Marine Geology, Krijgslaan 281 S8, B-9000 Gent, Belgium

[f] University of Fribourg, Department of Geosciences, Chemin du Musée, CH-1700 Fribourg, Switzerland

[g] NIOZ Royal Netherlands Institute for Sea Research, National Marine Facilities and Utrecht University, P.O. Box 59, 1790 AB Den Burg, The Netherlands

*corresponding author: alim2389@gmail.com

Abstract

Where sediment supply is significant, it acts as a major influence on the development of cold-water coral (CWC) reefs through sediment baffling by corals and hydrodynamic-topographic interactions. While previous work has demonstrated this effect on a regional scale or across large coral carbonate mound structures, this study examines a chain of small reefs, the westernmost (or downslope) chain of the Moira Mounds, and their sedimentary environment on a discrete area of seabed (<10 km in length) to better constrain the specific processes which affect CWC reef development and variability. An initial assessment of the western area of the Moira Mounds suggests that they vary in size and vitality (presence and status of CWCs) from south to north. Here, we utilise ROV-based video data, 30 kHz side-scan sonar backscatter, bathymetry, water column data (CTD's) and surface sediment samples to investigate mound development along this transect and how that relates to a local-scale environmental gradient. Three distinct zones are defined based on coral mound status, sedimentary environment and hydrodynamics. The main driver in this zonation is current speed, ranging from 30 - 41 cm s^{-1}, which corresponds to a change in mound size and surface morphology. At ~37 cm s^{-1}, conditions are favourable for isolated CWC colony development on dropstones, but not optimum for CWC reef development. At 39 - 41 cm s^{-1}, CWC reefs flourish but isolated colonies are rare.

Keywords: sediment transport, cold-water coral reef, currents, sedimentology, reef development

2.1 Introduction

A positive feedback mechanism, resulting in the formation of complex morphological structures on the seabed, is developed when framework-building cold-water corals (e.g. *Lophelia pertusa* and *Madrepora oculata*) and the local hydrodynamic regime interact (Dorschel et al., 2007a; Huvenne et al., 2009a; Roberts et al., 2009a; Rüggeberg et al., 2007; Wheeler et al., 2005a; Wheeler et al., 2008b). The resulting coral mound features in the north east Atlantic have been studied in detail, particularly on the Irish continental margin (De Mol et al., 2002; Huvenne et al., 2009b; Kano et al., 2007; Mienis et al., 2006; Pirlet et al., 2011b; Raddatz et al., 2014; Thierens et al., 2013b; Thierens et al., 2012; Thierens et al., 2010b; Titschack et al., 2009a). Large, hill-sized coral carbonate mounds (up to 350 m from base to summit) make up a significant component of these recent research efforts (Henriet et al., 2014 and references therein). However, in line with technological advances, mapping efforts are now imaging smaller features on the seabed to a higher resolution allowing for the identification of smaller cold-water coral reefs in water depths c.1000 m, e.g. the Moira Mounds and the Darwin Mounds (Fig. 1a) (Foubert et al., 2011a; Huvenne et al., 2009a; Wheeler et al., 2011d; Wheeler et al., 2008b). The terms "reef" and "mound" are used interchangeably here as all mounds studied in this paper support CWC reefs. The term mound is a topographic definition only and reef refers to a biogenic reef as defined in Roberts et al. (2009a) as being "long-lived, [with] their growth … balanced by (bio)erosion, [and forming] local topographic highs that alter hydrodynamic and sedimentary regimes, and they form structural habitats for many other species", although Wood (1999) offer a classical definition. The number of individual Moira Mound CWC reefs is significantly higher than the number of better-studied, neighbouring giant Belgica carbonate mounds (Figure 5B) (Wheeler et al., 2005a). Wheeler et al. (2011d) hypothesise that these small CWC reefs may represent an early-stage "start-up" phase of the nearby giant coral carbonate mounds, noting that the "footprints" of clusters of Moira Mounds have a comparable size to the base of the giant cold-water coral carbonate mounds and as such, may have formed through a coalescing of Moira-like Mounds at early stages of their development (also see De Mol *et al.*, 2005 and Huvenne *et al.*, 2005).

In the CWC-abundant north-east Atlantic, suitable hard substrates for coral settlement are widely available in the form of rock outcrops, glacial erratics & gravels (Dorschel et al., 2009b). Once settled, coral colonies may extend onto areas of soft sediment by recolonising coral rubble from previous colonies that have become physically broken (Roberts et al., 2003; Wilson, 1979b).

Lophelia pertusa is common amongst reef-building coral in the Porcupine Seabight (Foubert et al., 2005a; Henry and Roberts, 2007; Kozachenko, 2005b). This is also true at the Moira Mounds. *L. pertusa* has been proven to be tolerant of a wide range of salinities varying between 31.7 - 38.8 ‰ (Davies et al., 2008a; Fink et al., 2012 and references therein). It has been observed living between temperatures of 4°C - 13.9°C (Freiwald, 2002; Rogers, 1999), or even up to 15°C off the south-east US (Brooke et al., 2013). It can be exposed to rapid and frequent temperature fluctuations up to 1.6 °C (Mienis et al., 2009a).

As CWC are sessile and filter-feeding organisms, enhanced bottom currents are vital for coral growth by supplying food (Davies et al., 2009b; Duineveld et al., 2007a; Mueller et al., 2014b; Purser et al., 2010b) and keeping polyps free from smothering by fine sediment (Roberts et al., 2009a). All mound provinces along the European continental margin exist in areas where enhanced currents interact with topography and the rate of food encounter is increased (Mienis et al., 2009b). Evidence for strong bottom currents can be found within mound provinces along the north east Atlantic margin from the presence of contourite channels, sediment waves, scoured moats, sand sheets and ripples (Dorschel et al., 2007a; Dorschel et al., 2005c; Dorschel et al., 2009b; Hebbeln et al., 2016b; Kozachenko, 2005b).

Sediment supply seems to be a significant factor for vertical coral reef growth (Foubert et al., 2011a; IODP 307 Expedition scientists, 2005; Wheeler et al., 2005a) because, infilling the coral framework, it provides stability against strong bottom currents (Dorschel et al., 2009b) and protects the base of the coral colony from bioerosion (Beuck et al., 2010; Freiwald and Schönfeld, 1996). This sedimentation process has been observed, amongst others, in submarine dives at the Miami Terrace where corals are forming muddy mounds (Correa et al., 2012a; Neumann and Ball, 1970a). Furthermore, allogenic sediment can make up a dominant component of mound sediment. For instance, >50% of the Challenger Mound (Figure 5B) in the Porcupine Seabight consists of terrigenous sediment (Pirlet et al., 2011b; Thierens et al., 2013a) and 50 - 90% of the Darwin Mounds, northern Rockall Trough (Scottish Atlantic Margin), are composed of contourite sands (Huvenne et al., 2009a; Victorero et al., 2015). The importance of terrigenous sediment in CWC reefs and carbonate mounds as a driver for mound growth has previously been discussed (Pirlet, 2010; Pirlet et al., 2011b; Wheeler et al., 2011d). As currents flow through coral frameworks, frictional drag is created, slowing down the water flow. This allows current-suspended sediment to become deposited around the coral framework generating positive topographic growth (Roberts et al., 2009a; Wilson, 1979b; Wilson, 1975). This sediment-driven vertical reef growth then provides access for the corals to faster-flowing water with a greater POM to lithic ratio promoting further reef development (Roberts et al., 2008a; Roberts et al., 2003; Wheeler et al., 2005a).

However, despite this significant body of research over the last decade or so, a key question largely remains unanswered: what are the triggers that drive CWC colonisation from a situation of scattered colonies and thickets to the build-up of individual reefs and mounds? Here, a discreet patch of seabed from the Moira Mounds CWC habitat is examined with the aim of shedding light on the answer on a local-scale.

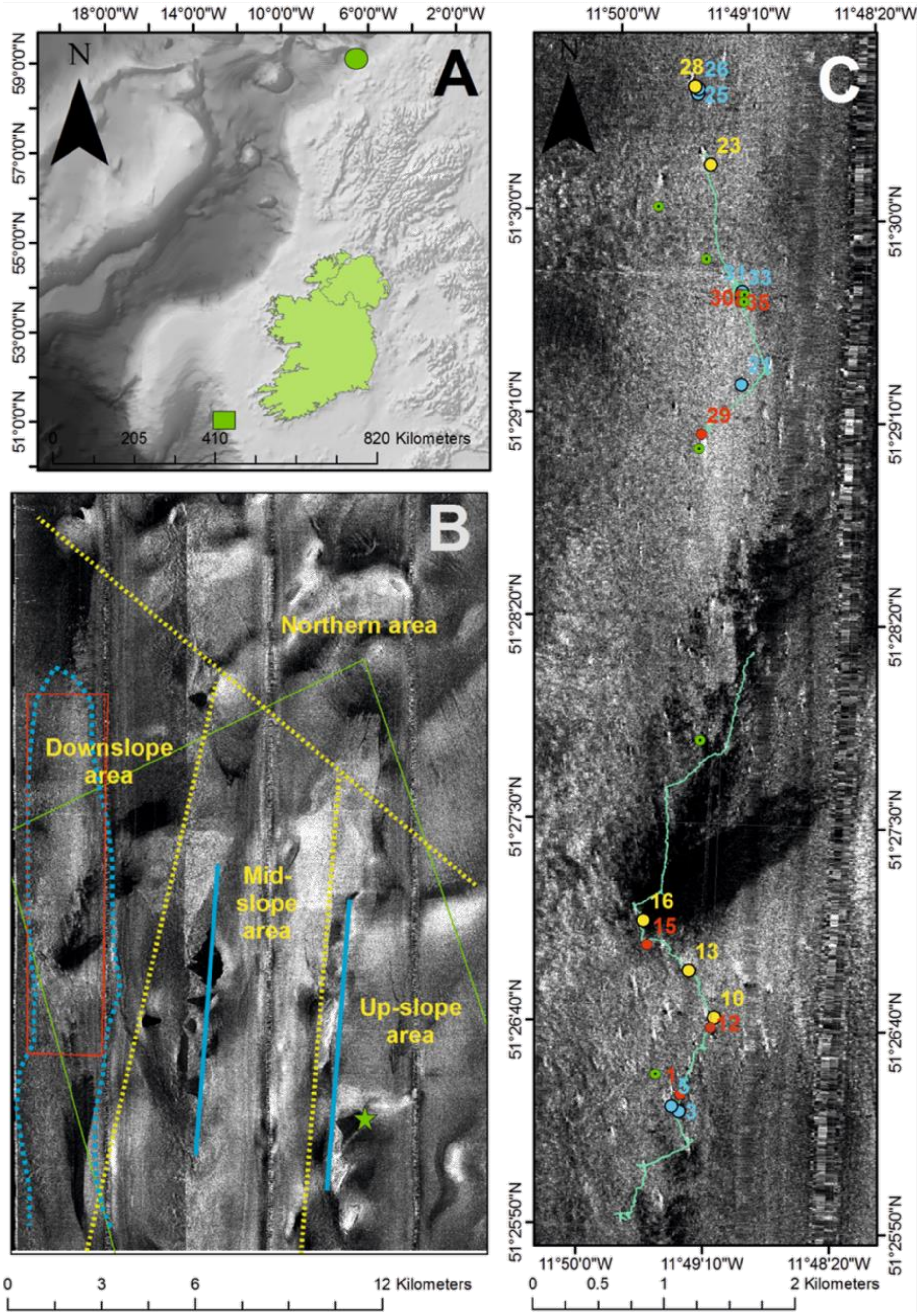

Figure 5 Location map of the study site.

(A) Location of the Belgica Mound Province (BMP) Special Area of Conservation (green box) and the Darwin Mounds (Green dot) (B) Study area (red box) within the BMP (green). Yellow dashed lines Moira Mound areas after Wheeler et al. (2011). Blue solid lines=two parallel chains of cold water coral carbonate mounds. Dashed blue line=location of Arwen Channel. Green star= Challenger Mound (C) Study area; green dots= CTD samples, numbered dots= box core samples (yellow= sand and biogenic hash, red= sediment and dropstones, blue= coral-bearing sediment) labelled by core number, blue line= ROV-video lines.

2.2 Regional Setting

The Belgica Mound Province (BMP) is located on the eastern margin of the Porcupine Seabight: a north-south, large embayment on the Irish continental margin, NE Atlantic (see Figure 5A) (Beyer et al., 2003a; Dorschel et al., 2007a; Henriet et al., 1998; Huvenne et al., 2002b; van Rooij et al., 2003b). Some of the BMP is within a Special Area of Conservation (SAC) designated under the EU Habitats Directive. The main modern-day Porcupine Seabight water mass which affects coral mound growth is the Mediterranean Outflow Water (MOW)(White et al., 2005). This can be characterised within the BMP by a salinity maximum between 600 m and 1100 m water depth (Dullo et al., 2008a; White and Dorschel, 2010a).

The BMP is characterised by its abundance of coral mound features which occur in the form of coral carbonate mounds and cold-water coral reefs (Foubert et al., 2005a; Wheeler et al., 2005a). Carbonate mounds occur in 2 distinct chains orientated parallel to the continental shelf (Figure 5B); the eastern chain is largely moribund (with a mainly dead coral cover; Foubert et al., 2005) while the western chain is mostly active with a profusion of live coral (De Mol et al., 2007a; Dorschel et al., 2007a; Eisele et al., 2008b). Carbonate mound morphologies range from conical to elongate ridge-like forms and are typically 1 km across and 100 m tall (Beyer et al., 2003a; Wheeler et al., 2005a). Contourite drifts have accumulated between the giant carbonate mounds and buried their upslope flanks (Van Rooij et al., 2003a). A blind channel, referred to as "Arwen Channel" (Figure 5B) (Murphy and Wheeler, 2017; Van Rooij, 2004b), formerly connected to the shelf break, runs through the province and now contains the westernmost Moira Mounds studied here (referred from here on as downslope Moira Mounds (sensu Wheeler et al., 2011d)).

Smaller CWC reefs, typically 30 m across and 10 m tall, are found throughout the BMP and are referred to as the Moira Mounds (Foubert et al., 2011a; Wheeler et al., 2011d). These are divided into 4 zones (Figure 5B) based on their geographic distribution: upslope area, down-slope area, mid-slope area and northern area (see Wheeler et al., 2011d). The Moira Mounds in the upslope area are described as dormant by Wheeler et al. (2011d) while the Moira Mounds in the mid-slope area are described as sediment stressed (Foubert et al., 2011a). Here, we present the first baseline study of the active Moira Mounds found in the downslope area.

2.3 Materials and Methods

To constrain the effect of local (10 m - 1 km scale) hydrodynamic and sedimentological processes on CWC reefs, sediment samples, remotely-sensed data (side-scan sonar and multibeam echosounder) and video data have been collected and analysed. This combination of data is used to delineate a number of zones based on attribute similarities (grain size, bed forms, mound size and stage of growth). Data were collected during the following surveys: VENTuRE survey (2011) on board *RV Celtic Explorer* with *ROV Holland 1* (Cruise number CE11009) (see Wheeler et al., 2011b), Eurofleets Moira Mounds survey (2012) on board *RV Belgica* (Cruise Number 2012/16) (see Spezzaferri et al., 2012), the TOBI sidescan sonar survey of cold-water coral mounds in the Porcupine Seabight and Rockall Trough on board the *RV Pelagia* in 2002 (Cruise Number 197; de Haas et al. (2002))

and the RV *Polarstern* cruise ANT XVII/4 as part of the GEOMOUND project (Beyer et al., 2003a).

2.3.1 Multibeam Echosounder

Multibeam Echosounder (MBES) bathymetry was collected onboard RV *Polarstern* cruise ANT XVII/4 using a Hydrosweep DS-2 operated at a frequency of 15.5 kHz. For more information regarding acquisition and processing of the MBES data see Beyer et al. (2003a). While these data do not resolve individual Moira Mounds (25 m pixel resolution), they are utilized here to look at gross seabed slope across the study site (1 km scale).

2.3.2 Side-scan sonar

Side-scan sonar (SSS) data were collected using the Towed Ocean-Bottom Instrument (TOBI) operated at 30 kHz. For more information regarding acquisition of the TOBI SSS data see de Haas et al. (2002). The data were processed using the NOC in-house PRISM software (Le Bas and Hühnerbach, 1999), achieving a pixel resolution of 6m x 6m (Huvenne et al., 2005a). Throughout this manuscript, high backscatter is represented by light tones, low backscatter by dark tones. While these data resolve Moira Mounds, ground-truthed by video in this study and by Wheeler et al. (2011d), they are utilized here to interpolate between box core locations based on similar backscatter reflectance properties and to estimate mound densities within the study area.

2.3.3 ROV video data

Video data were collected during the VENTuRE survey (CE11009) (Wheeler et al., 2011b) on board *RV Celtic Explorer* using an array of HD and colour composite cameras including aft, forward-facing and downward-facing mounted on the *HOLLAND 1 ROV*. Areas of investigation were selected based on tentative reef identification from the 30 kHz TOBI side-scan sonar backscatter (de Haas et al., 2002; Huvenne et al., 2005b). Two consecutive S-N video lines were recorded over the downslope Moira Mounds covering a length of 36.70 km at a speed of 0.2 - 0.4 kt (Figure 5C). Positioning was achieved using a *Sonardyne Ranger 2* USBL (ultra-short base line) with the aid of doppler velocity logging (DVL) using a 1200 kHz RDI workhorse. The ROV was aimed to be maintained at <2 m above the seabed during data acquisition. It is unlikely that this height was consistent for all acquisition so exact ROV height over the seabed was recorded using an altimeter. Using the USBL depth reading, this allows for calculation of mound height. Parallel lasers set at 11 cm apart were used to scale photographic and video imagery. The ROV's forward-facing (navigation) sonar guided the ROV over the summit of each mound feature.

Using the video data, a series of facies were identified based on similarities in sediment ripple type, seabed surface-sediment and coral presence (see Figure 6). These facies are: "homogeneous sediment" (sorted sediment with no identifiable bio- or lithic-clasts), "sediment and dropstones" (fine-grained sediment with larger pebble to boulder-sized, angular and rounded clasts), and "coral framework". The coral framework facies could be split into "isolated individual colonies", "thickets" (definition as per Squires (1964a), being "an aggregation of closely associated coral colonies … that are the second stage of structural development… and may be either monotypic or polytypic in composition, and is characterized by a definable extent and continuity of coral both laterally and vertically”) and "mounds" (referred to as “banks” in Squires (1964)). Ripple type (straight-crested, high sinuosity, low sinuosity, and lingoidal) was also noted. The start and end time of each facies was recorded. The heading of the ROV and downward-facing camera were used to determine ripple orientation while the laser scale was used to record feature size. Exact mound height was calculated as;

$$\text{Mound Height} = (d^{Rbase} + alt^{Rbase}) - (d^{Rsum} + alt^{Rsum}), \quad \text{(Eq. 1)}$$

where;

d^{Rbase} = Depth of the ROV at the base of the mound (from USBL),

alt^{Rbase} = Altitude of the ROV above the seabed at the base of the mound (from altimeter),

d^{Rsum} = Depth of the ROV at the summit of the mound (from USBL),

alt^{Rsum} = Altitude of the ROV above the seabed at the summit of the mound (from altimeter).

Using the start and end time of each facies and feature, the facies were synced with the easting and northing of the USBL. The facies and features were integrated within a geographic information system (GIS) and observed in relation to sample locations.

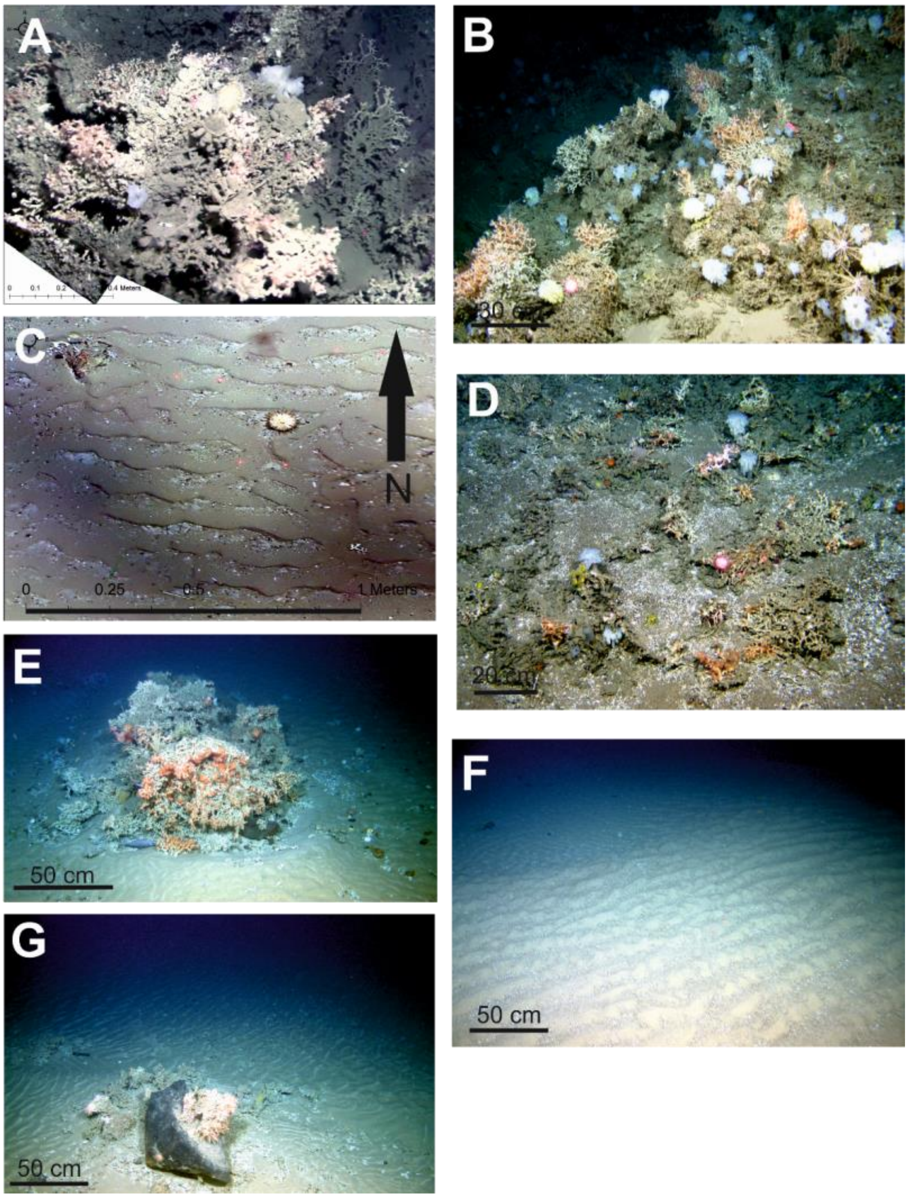

Figure 6 Example ROV imagery from the downslope Moira Mound area.

A) Summit of a mound in the north of the study area showing >1.5 m tall aggregation of L. pertusa, M. oculata and sponges. Laser scales = 11 cm. B) Flank of a mound dominated by live coral framework in the north of the study area. Note sediment trapped at the base of colonies, while coral polyps appear sediment free. Sponges and echinoderms are abundant. C) Off-mound (proximal to a mound base) in the north of study area. Note east-west orientation and sinuosity of ripples. D) Surface of a mound in the south of the study area. Note size of corals, sediment clogging and relatively smoother mound surface. E) Small thicket developing on and around a dropstone in the centre of the study area. Note abundance of newly-developed, coral-derived substrate around the thicket. A gentle slope is forming around the base of the thicket, highlighting the onset of sediment-trapping. F) Sandy, rippled-substrate in the south-central part of study area. Ripples have a low sinuosity with a ~10 cm wavelength. G) Colony growing on a dropstone in the south of the study area.

2.3.4 Box cores

Eighteen box cores from the downslope Moira Mounds were collected for this study (Figure 5C), targeting mounds, off-mound and mound-proximal areas. They are located in the southern and northern part of the study area; all coring attempts in the central part failed. Core samples were collected using a NIOZ-type box corer onboard *RV Belgica* in 980-1100 m of water, with *GAPS* Ultra Short Base Line (USBL) navigation to an accuracy of 0.5% of the slant range. Subcores were taken from each retrieved box core, and were stored at 4°C to preserve organic material and sedimentary structures.

Subcores were split, cleaned, photographed and lithologically described. For this study, only surface sediment samples from the box cores were used and the carbonate and organic dissolution technique procedure outlined by Pirlet (2010) was followed.

In each instance, approximately 1 cm^3 of sediment was extracted from each sample and oven-dried at 50°C for 24 hours. When dry, the sample was weighed (W1). At this point, any relatively large bioclasts (>2 mm) were removed using tweezers on visual observation. The sample was added to a beaker with 200 ml distilled water. 10 ml of 10% HCl was then added to the beaker to dissolve the carbonate fraction of the sediment sample. A further 10 ml of 10% H_2O_2 was added to the solution to dissolve the organic component of the sediment sample via oxidation. Distilled water was added to make the total volume of solution equal to 250 ml. The solution was heated on a hot plate at 90°C for a period of 2 hours. When the reaction was complete, the sample colour generally changed to beige/straw. In the case of an incomplete reaction, extra heat, HCl and H_2O_2 were added. The samples were rinsed with distilled water 3 times each to reach a neutral pH. After settling, any remaining solution was removed using a syringe, taking care not to remove any sediment. The sample was oven-dried at 50°C for a period of 24 hours. When dry, the sample was weighed (W2). Percentage carbonate and organic matter ($CaCO_3$ + Org) were calculated by the following equation;

(A) = (W2/W1)*100 (Eq. 2)

($CaCO_3$ + Org)% = 100 - A, (Eq. 3)

where W1 is the sample's dry weight before treatment, and W2 is the samples dry weight after treatment.

Subsequently, 0.05% sodium tetraphosphate was added to the remaining lithic component of the samples. The sample was shaken by hand and then sonicated for approximately 12 seconds to minimize flocculation of particles. Before particle-size analysis (PSA), the sample was mixed to ensure accurate representation of each sample. Laser granulometry was carried out at the Applied Geology Lab, University of Milano-Bicocca using a Malvern Mastersizer 2000. The sample was added to the Malvern Mastersizer 2000 by means of liquid (distilled water) dispersion. Before measurement, ultrasonic waves were passed through the liquid to ensure full deflocculation of particles. Each sample was measured 5 times. The results were then averaged.

Based on visual assessment, box core surface sediment samples were divided into 3 broad categories; a) sediment and dropstones, b) sediment with biogenic hash and c) coral-bearing sediment.

2.3.5 CTD (Conductivity - Temperature - Depth)

A series of CTD casts was collected during the Eurofleets Moira Mounds survey (2012) over the downslope Moira Mounds study site (Fig. 1c). Vertical CTD profiles were recorded using the Sea-Bird SBE09*plus* CTD profiler integrated with the Sea-Bird carousel water sampling system SBE32. Parameters recorded were water depth (m), temperature (°C), salinity (g/kg) and dissolved oxygen (µmol/kg^{-1}). Measurements were made at a rate of 24 samples per second. These data were averaged in the Sea-Bird deck unit over 0.5 second time intervals. A total of 24 vertical profiles were recorded in the area, each reaching from the surface down to approx. 5 m above the seabed. Recorded data were processed and managed using Sea-Bird software and stored in *.cnv format. The lowermost depth bin may represent the water mass in which the Moira Mounds are bathing. The average benthic water temperature was subsequently calculated by taking the average of these lowermost depth bins.

2.3.6 Quantification of current speeds

In order to understand the hydrodynamic regime around the Moira Mounds, erosional and depositional current thresholds were calculated after Soulsby (1997) (a detailed mathematical explanation can be found in Huvenne et al. (2009a)) to estimate current speeds where box cores have been retrieved (Table 2). The grain size distribution for each of these samples was used to estimate the critical current velocity 1 m above the seabed required to allow grains to settle or be transported in the water column. Grain sizes smaller than 10 µm were excluded from critical current velocity calculations as these are subject to flocculation (McCave et al., 1995). Where the erosional threshold is higher than the depositional one, grains will stay in suspended transport until the current reduces below the depositional threshold. Hence, a dominance of grains with such characteristics indicates that current regularly drops sufficiently to allow deposition. In order to mobilise these sediments again, current speeds have to increase above the erosional threshold again. In locations where the erosional threshold is lower than the depositional one (larger grainsizes), the final mobilisation of grains is through saltation, and the sedimentary regime is fully characterised by the erosional threshold.

Soulsby (1997) defines the formula to calculate the critical current velocity erosional threshold from particle size distributions as:

$\mathcal{U}_{100\ erosion} = \left(\frac{\mathcal{U}*_{cr}}{0.41}\right) \ln\left(\frac{z_{100}}{z_0}\right)$, where (Eq. 4)

z_{100} = level above seabed (1 m) (Eq. 4.1)

z_0 = roughness length, calculated = $\left(\frac{d}{12}\right)$ (Eq. 4.2)

d = grain diameter = mode of sample grain size curve (Eq. 4.2.1)

$\mathcal{U}_{cr}$ = critical shear velocity = $\mathcal{U}*_{cr} = \sqrt{\frac{\tau_{cr}}{\rho}}$, where (Eq. 4.3)

τ_{cr} = threshold bed shear stress (N/m^2) = (Eq. 4.3.1)

$g(\rho_2 - \rho)d.\left(\frac{0.30}{1+1.2D*} + 0.055[1 - \exp(-0.020D*)]\right)$ (Eq. 4.3.1)

$\rho =$ water density = 1027.4 kg / m^3 (Eq. 4.3.2)

$\rho_s =$ grain density = 2650 kg / m^3 (quartz) (Eq. 4.3.3)

D* = dimensionless grain size = $\left[\frac{g(\rho_s - \rho)}{\rho v^2}\right]^{\frac{1}{3}} d$ (Eq. 4.3.4) and to calculate the critical current velocity depositional threshold from particle size distributions as:

$$\mathcal{U}_{setl} = \frac{v}{d}\left[(10.36^2 + 1.049D_{*^3})^{\frac{1}{2}} - 10.36\right]\text{, where} \qquad \text{(Eq. 5)}$$

ν = kinematic viscosity of water = 1.4313 x 10^{-6} m^2/s (8°C and 35.1 g/kg)

The use of this approach assumes that particle size predominantly reflects the benthic current regime. In this area, where currents are strong, sediment ripples are common and testify to extensive bedload sediment transport and sediment reworking, this assumption appears valid. As a current velocity proxy, the results provide unrealistic precision (to several decimal places). Thus, results are rounded to the nearest cm s^{-1}.

These values were grouped geographically (Zone 1 in the south, Zone 2 in the centre and Zone 3 in the north (Table 2) and by sediment-type, and then averaged to represent the erosional and depositional value of that sample-type per zone. Sediment and dropstone samples are not utilized in current speed quantification as they are glacigenic muds exposed on the surface through winnowing and hence are non-representative of the contemporary hydrodynamic regime. Lithic sub-samples from Sediment with biogenic hash samples are included in the current speed quantification because they represent off-mound or mound-proximal samples that may represent the currents directly affecting the mounds. The mound-derived bioclasts are not *in situ* and therefore the sediment they are with has probably also moved and hence the erosional velocity values are taken into consideration as current speed indicators. Coral-bearing sediment samples are also considered for current speed calculations as they represent the current when it comes into contact with the mound structure. While the median of the erosional and depositional values is used, absolute values are also considered.

Where box cores are absent, bedforms (sinuous ripples and, in places, lingoidal ripples) combined with mean grain size (0.25-0.5 mm) as inferred from the TOBI SSS (Huvenne et al., 2005a; Masson et al., 2003b) are used to estimate current speeds by use of the bedform-velocity matrix graph after Stow et al. (2009).

Sediment-type	Sediment and Dropstones						Sediment and Biogenic Hash					Coral-bearing Sediment						
Sample ID	**BC_1**	**BC_12**	**BC_15**	BC_29	BC_35	BC_30	**BC_10**	**BC_13**	**BC_16**	BC_23	BC_28	**BC_3**	**BC_5**	BC_21	BC_33	BC_31	BC_25	BC_26
Mean grain size (>10 um)	116.5	54.01	100.5	43.61	25.97	96.34	278.8	293.5	321.6	267.8	441.3	57.45	119	215.4	111.8	209.5	225	176
Textural group (bulk)	Muddy Sand	Sandy Mud	Sandy Mud	Sandy Mud	Sandy Mud	Sandy Mud	Muddy Sand	Sand	Sand	Muddy Sand	Sand	Sandy Mud	Muddy Sand	Sand	Muddy Sand	Sand	Sand	Sand
($CaCO_3$ + Org)%	23	22	23	28	14	18	15	12	6	38	8	24	22	16	22	26	15	29
Erosional Velocity cm/s (Soulsby, 1997)	34.37	31.7	33.97	30.64	27.57	33.86	36.42	36.59	36.92	36.29	38.56	31.98	34.42	35.73	34.27	35.67	35.83	35.29
Depositional Velocity cm/s (Soulsby, 1997)	20	4.8	15.35	3.2	1.2	14.32	84.84	90.77	102	80.34	143.2	5.4	21.17	58.45	18.78	55.98	62.49	42.19
Zone	1	1	1	3	3	3	1	1	1	3	3	1	1	3	3	3	3	3

Table 2 Lithogenic sediment characteristics of surface sediments from all box core samples.

Grey represents samples in the north while white represents samples in the south.

2.4 Results

2.4.1 Multibeam echosounder bathymetry

The multibeam echosounder data set has previously been discussed (Beyer et al., 2003a) and the resolution of the data set (50 m) is too low to identify individual Moira Mounds. However, the gross morphology and slope of the seabed in the study site can be defined (Figure 7). The bathymetry shows the occurrence of the study site within a blind channel (Figure 5B). Furthermore, the slope of this blind channel is 1.2° except in the centre of the study site where it steepens to 2.3°.

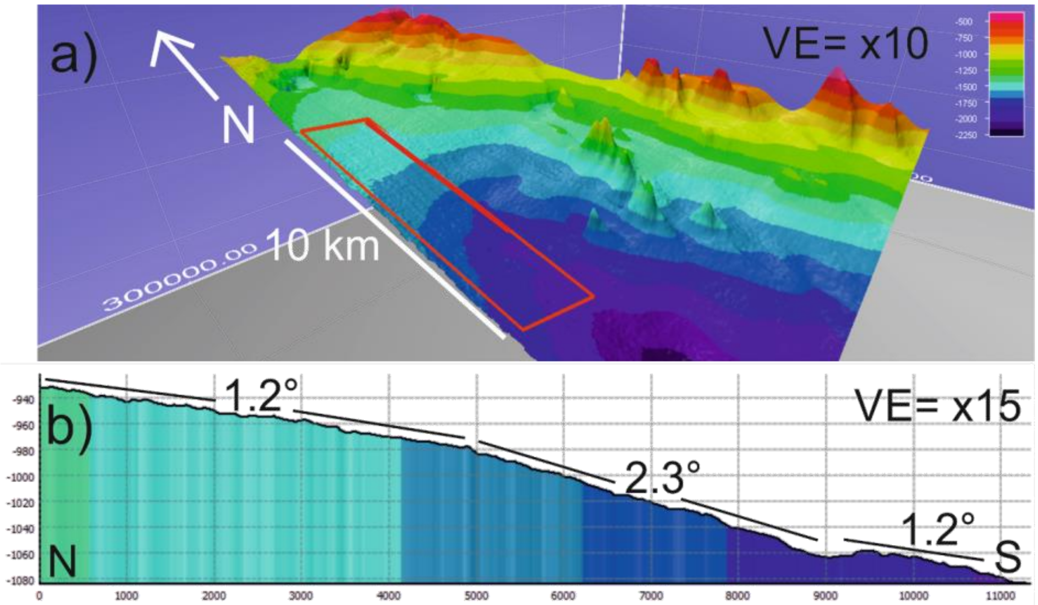

Figure 7 Geomorphology of the downslope Moira Mounds study site

a) Bathymetry (from Beyer et al. 2003) gridded at 50 m resolution. Red box = the study site. Note the location of the study site at the head of a blind channel (Arwen Channel) west of two chains of giant carbonate mounds; b) slope profile from north to south through the centre of the study area. Both the north and south of the study site have a slope of 1.2° while the centre is slightly steeper (2.3°).

2.4.2 Side-scan sonar imagery

The side-scan sonar imagery (Figure 5B and C) reveals the Moira Mounds as distinct ovoid areas of high backscatter (white) 10s of metres across. Fifteen of these mounds are now confirmed as CWC mounds by ROV-based video groundtruthing with a further 70 mounds inferred within the study area (Figure 8).

The seabed surrounding the mounds in the south, centre and north of the Moira Mound field shows distinctive backscatter signatures. The seabed to the south has a moderately high (light grey) backscatter with spatially dense Moira Mounds (9.1 mounds km^{-2}) and appear elongated. The centre of the study site has low (dark grey/black) backscatter with 2 of the 10 mounds groundtruthed (3.70 mounds km^{-2}) and the north has a medium to high (light grey) backscatter reflection with a relatively low-density number of mounds per unit area (3.75 mounds km^{-2}).

2.4.3 Video-detected data points and facies

The distribution of significant biological and geological seafloor features as well as the three main seabed facies (based on video observations and groundtruthed by the sediment samples), was compiled within a GIS. The results are shown in Figure 8 and are described below.

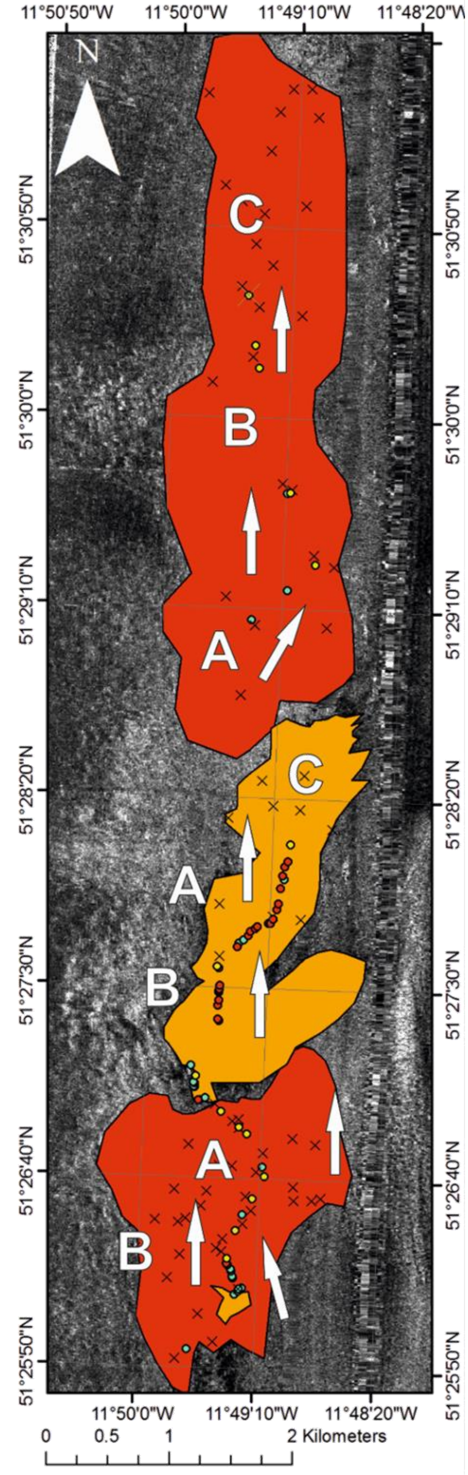

Figure 8 Map showing ROV-video observations.

Red dots=coral thickets; yellow dots=CWC reefs, blue dots=isolated individual CWC colonies; red polygons= "sediment and dropstone"-dominated seabed; *orange polygons= "homogeneous sand"*-dominated seabed; *white arrows=current direction inferred from ripple orientation; A=low sinuosity ripples; B=high sinuosity ripples; C=lingoidal ripples; X=Moira Mound as inferred from TOBI side scan sonar imagery.*

2.4.3.1 *Isolated coral colonies*

Twenty-five isolated coral colonies were imaged by the ROV (Figure 8 and Figure 6G). These colonies are live and attached to various-sized dropstones. Their occurrence decreases northwards; 13 in the south; 9 in the centre; 3 in the north. The trend in decreasing density of occurrence is similar to that found for thickets and mounds (see below).

2.4.3.2 *Thickets and mounds*

CWC mounds (Figure 8, Figure 6A, B and D) occur most frequently in the south and are relatively closely spaced, as is also visible on the TOBI side-scan sonar data. From the video data, it was noted that reefs are relatively small (6.4 m ± 1.9 in height above seabed) and are relatively sediment-clogged. In total, 8 mounds and 4 thickets were observed on approx. 18.2 km of ROV-video in the south of the study area (0.4 mounds km^{-1}; 0.2 thickets km^{-1}). It was observed that mounds in the south are dominated by dead coral framework.

In the north of the study area, CWC mounds are spaced further apart than in the south of the study area. Five mounds, 1 thicket and 2 coral-colonised sediment wave trains were observed on 11.02 km of ROV-video (0.5 mounds km^{-1}; 0.1 thickets km^{-1}; 0.2 coral-colonised sediment waves km^{-1}) (Figure 8). Furthermore, the largest reefs are found here reaching up to 11.8 m in height (7.8 m ± 3 in height above the seabed). Mounds in this area are dominated by complex, live coral frameworks. Coral colonisation occurs on the crest of some ridge-like features while bioclastic sediment accumulates in the troughs.

ROV-video acquired over the central area, corresponding to a low (dark-grey/black) backscatter on the SSS imagery, shows 23 coral thickets and just 2 CWC mounds per 7.3 km of ROV track (Figure 8) (0.1 mounds km^{-1}; 3.2 thickets km^{-1}). Mounds imaged in this area are between 3.2 and 2.1 m in height.

2.4.3.3 Sediment facies

ROV-video reveals that the southern and northern parts of the study area are dominated by "sediment and dropstones" while the central area is dominated by "homogeneous sediment" (sand). The area covered by "sediment and dropstones" corresponds to an area of high SSS backscatter while the "homogeneous sediment" in the centre corresponds to a low backscatter area (Figure 8). This type of backscatter signature recorded by TOBI SSS is typical of well-sorted sands with a mode of approx. 140 - 200 µm (Huvenne *et al*. 2005, Masson *et al*. 2003). Despite being rare, the higher (lighter-grey) backscatter patches in the centre zone also correspond to the rare occurrence of "sediment and dropstones".

2.4.3.4 Ripple orientation

Ripple orientation is predominantly east-west as observed on ROV-video with a northerly-directed ripple transport direction (Figure 8). This is particularly true for the central area. While the southern area is dominated by northerly-directed ripples, some minor occurrences of NW-directed ripples occur. Furthermore, some small sandy areas with no ripples can be found. The northern area is dominated to a much lesser extent by northerly-directed ripples. It also has a stretch of seabed measuring approx. 750 m which hosts NE and NNE-directed ripples. This stretch is located at the south of the northern area.

2.4.3.5 Ripple type

In the south, high-sinuosity ripples (relatively higher current velocity) are dominant (Figure 8). However, low-sinuosity ripples are also found and typically occur immediately north of mounds. Additionally, minor pockets of non-rippled seabed occur and are located immediately south of mounds.

Similarly, the south of the central area is dominated by high-sinuosity ripples. Six of the 23 thickets in the central area occur here. Towards the north of the central area, the seabed becomes dominated by the higher energy-related lingoidal ripples. Seventeen of the 23 central area thickets occur within the lingoidal ripples-dominated seabed.

In the north of the study area, the southern part is dominated by low sinuosity ripples, which corresponds to the only area of NE-directed ripples. North of this, and for the rest of the study area in the north, the seabed is dominated by high sinuosity ripples and sediment waves.

2.4.4 Box core surface sediment characterisation

The sediment samples can be classified into three distinct types *sensu* Vertino et al. (2015). These are: sediment with dropstones, sediment with biogenic hash and coral-bearing sediment. These three types of sampled deposits are comparable to the sediment facies observed by Douarin et al. (2013) for the Mingaley Reef complex (Scottish Shelf, NE Atlantic). The results of the lithic fraction analysis of each sediment type are described below and summarised in Table 1 and Figure 6.

Sampled deposits representative of the "sediment with dropstone" group show a general decreases in ($CaCO_3$ + Org)% northwards albeit variable. The >10 µm mean grain size (MGS) ranges from 25.97 - 116.5 µm. In absolute terms, the finest sediment is found in this sediment type. These samples represent the off-mound environment and may reflect a largely erosive or non-depositional regime, in which the regional poorly-sorted glacigenic muds are brought to the surface through winnowing of the overlying sediment (Figure 9, Figure 10 and Table 2 Lithogenic sediment characteristics of surface sediments from all box core samples.).

Generally, the >10 µm MGS of "sediment with biogenic hash" sediment type increases from south to north (278 - 441.3 µm) coinciding with a decrease in ($CaCO_3$ + Org)% of each sample. All samples are sand dominated. Following inspection of video data, sample BC23 was found to represent a different sedimentary environment (trough of a sediment wave).

In the "coral-bearing sediments" sediment type, MGS ranges from 57.45 - 225 µm, broadly increasing northwards. The ($CaCO_3$ + Org)% in these sediments range from 15-29 %wt. These sediments are sand-dominated but have a mud component in the south. They represent the on-mound cores.

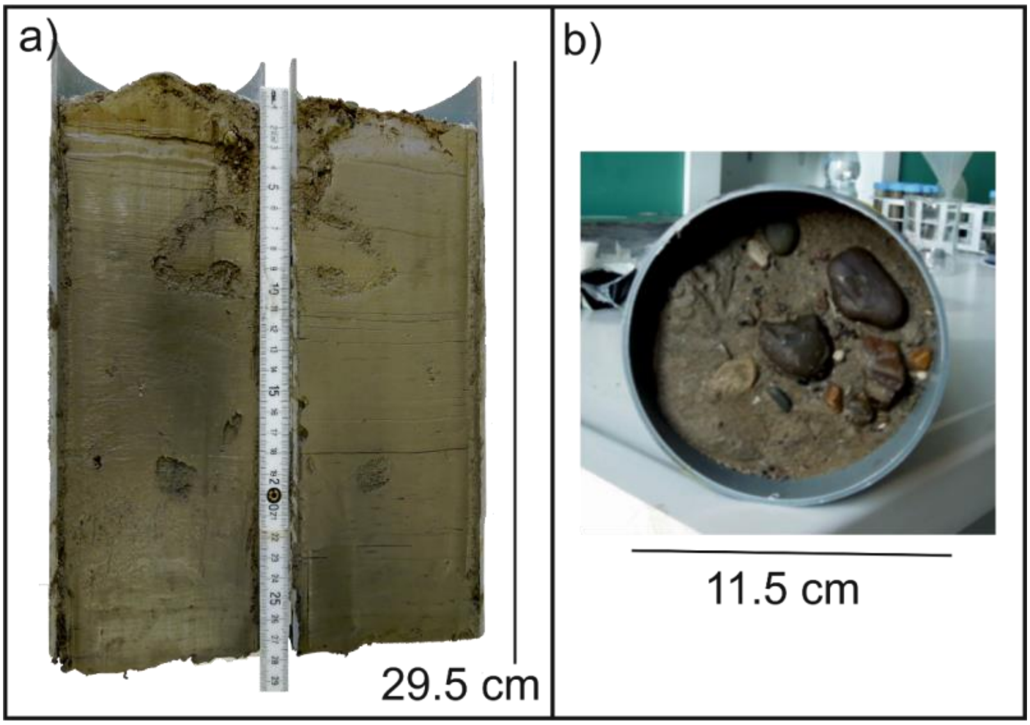

Figure 9 Box core photos.

a) Longitudinal section of split BC_15 b) top-down view of BC_15.

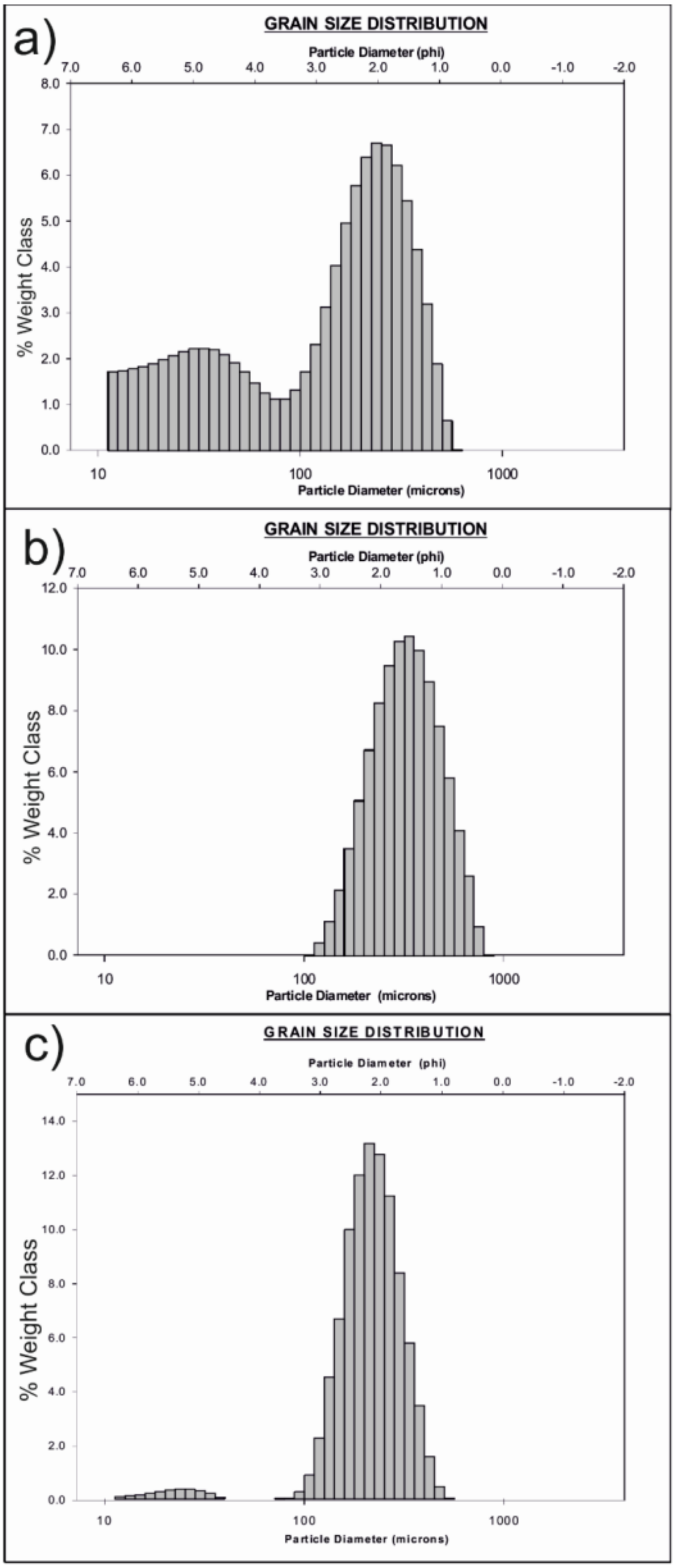

Figure 10 Example particle size distribution curves from the study site.

Typical histogram curve for the lithic component of the a) sediment and dropstones sediment-type b) sediment with biogenic hash sediment-type c) coral bearing sediment-type samples.

2.4.5 Hydrography

The average benthic water temperature recorded across the study area is 8.63°C with a standard deviation of 0.80°C; ranging from 9.0°C in the north to 8.2°C in the south (Table 3). Recorded salinity remains at 35.5 g/kg across the study site. O_2 saturation ranges from 6.4 - 6.5 ml/l^{-1}.

Station	Depth (m)	Temperature (°C)	Salinity (g/kg)	O_2 saturation (ml/l)
2	914.947	8.9	35.5	6.4
3	918.896	8.9	35.5	6.4
4	944.554	8.8	35.5	6.4
5	962.315	8.8	35.5	6.4
17	962.316	9	35.5	6.4
6	985.009	8.4	35.5	6.5
7	1023.485	8.4	35.5	6.5
8	1059.978	8.5	35.5	6.5
9	1105.343	8.4	35.5	6.5
10	1129.991	8.2	35.5	6.5

Table 3 bottom-water CTD data over the study area.

2.4.6 Current Speeds

Estimated current speeds characterising each zone are summarised in Table 4. The bedform-velocity matrix-derived current speeds were estimated across the full study site. However, the Soulsby (1997) equations were applied where possible (north and south) as these appear to yield more reliable results. The lowest current speeds can be found in the centre of the study site (a maximum of 30 cm s^{-1}). However, this increases to 40 cm s^{-1} in discreet places towards the north of the centre of the study site where lingoidal ripples begin to dominate. Using the Soulsby (1997) equations moderate current speeds (typically 37 cm s^{-1}) can be found in the south of the study site (Table 2). These values are in line with estimates from the bedform velocity matrix (~35 cm s^{-1}). The Soulsby (1997) equations reveal that the highest current speeds (39 cm s^{-1} to > 41 cm s^{-1}) are found in the north of the study site. Again, this is in line with estimation from the bedform velocity matrix (~40 cm s^{-1}).

Zone	Current Velocity (cm s^{-1}) after Soulsby (1997)	Current Velocity (cm s^{-1}) after Stow *et al.* (2009)
1	36.6	35
2	n/a	30
3	38.5-41.4	40

Table 4 Current velocity values for each zone based using Stow et al. (2009) and Soulsby (1997).

Current velocities from Soulsby (1997) are rounded to nearest decimal in text.

2.5 Discussion

2.5.1 Currents

Ripple orientation and type suggest a northerly-directed current at the time of video data acquisition that broadly increases towards the north of the study site (Figure 8). The study site occurs in a blind channel (Arwen Channel) (Murphy and Wheeler, 2017; Van Rooij, 2004b) where this increase in current speed appears to be further influenced by minute slope changes within the channel; the area to the centre of the study site has a relatively steep slope compared to the areas directly north and south of it (Figure 7B). It is also worth noting that while this northward-flowing residual current, generated by tidal rectification processes, is typical within the Porcupine Seabight (Pingree and LeCann, 1990; White, 2007), currents in this area may be susceptible to seasonal flow reversals (Pingree et al., 1999).

The south and north of the study site are dominated by the “sediment and dropstones” facies while the centre is dominated by the “homogeneous sand” facies (Figure 8 and Figure 6F). The dominance of dropstones in the north and south suggests erosion or non-deposition since their Pleistocene deposition (Kozachenko, 2005b). The homogeneous sands in the centre of the study site correspond to an area facing directly into the current with the steepest slope within the study site (Figure 7). The same area can be seen in Huvenne et al. (2005b) where this steepened slope can be seen on a 3.5 kHz sub-bottom profiler line showing a relatively thicker sediment package. The homogeneous sand, steepened slope facing directly into the current and thicker, stratified sub-seabed suggest a depositional environment, unlike the north and south of the area. Typically, areas with steeper slopes result in current acceleration and hence less deposition. However, when the slope changes over a short distance and has an aspect directly into the current, it may slow the current, creating extra turbulence and deposition of the sand load. This is comparable to the cyclical steps process identified by Cartigny et al. (2011) in submarine channels. The seabed in this depositional area coincides with a distinct low backscatter (dark tone) on the SSS imagery (Figure 5). The spectral signature of these TOBI SSS dark patches is typical of a well-sorted medium sand at least 10-15 cm thick (Huvenne et al., 2005b; Masson et al., 2003a).

Across the central area, a variety of bedforms are recorded, most notably ripples. While ripples require only a few hours to form, persistence and common occurrence suggests they reflect long-term mean velocity (Stow et al., 2009). Here, where sediment coring failed and current velocities were calculated by use of a Bedform-Velocity Matrix for deep water bottom currents as shown by Stow *et al*. (2009), the current is typically 30 cm s^{-1}. However, this may reach current speeds of up to 40 cm s^{-1} in discreet parts of the northern central area. This is evidenced by a change from sinuous ripple types in the south of the central area to lingoidal ripple types in the north of the central area (Figure 8).

Erosional and depositional velocities are calculated as per Soulsby (1997) (Table 2). Table 4 includes the estimated current speed in the north and south of the study site based on these values. In the south of the study site we estimate that the current speed regularly reaches at least ~37 cm s^{-1}. Figure 10a illustrates an important sand fraction in those sediments, with a mode of ~270 µm, which, based on our erosional velocity calculation, requires current speeds of 37 cm s^{-1} to be eroded. These sands are deposited in the vicinity of mounds (sediment with biogenic hash), where currents are slightly slowed down and deposits can build (Figure 10b, Table 2 Lithogenic sediment characteristics of surface sediments from all box core samples.). The north of the study site is interpreted as experiencing a current speed ranging from 39 cm s^{-1} to >41 cm s^{-1}. Non-deposition in this area suggests current speeds are higher than in the central zone.

2.5.2 Seabed zonation

Three seabed zones (Figure 11 Downslope Moira Mounds seabed zonation.) can be defined based on the spatial distribution of seabed facies, SSS backscatter and seabed slope. These zones reflect differences in the hydrodynamic and sedimentological regimes as manifested in changes in sediment types, coral occurrence and status, mound height and types of sediment ripples. The presence of migratory sedimentary bedforms (ripples), particularly in the north of the study area, highlights the intensity of currents in the area (see also the interpretation by Huvenne et al. (2005b)). However, while sand is evident on high-definition video data throughout the area, it appears to be a thin, mobile veneer in the north and south as illustrated in the split core (Figure 9). In fact, muddy-glacial sediments underlying these mobile sands were occasionally sampled (Figure 9Figure 10a), similar to findings by Foubert *et al*. (2011). These do not reflect the contemporary hydrodynamic regime.

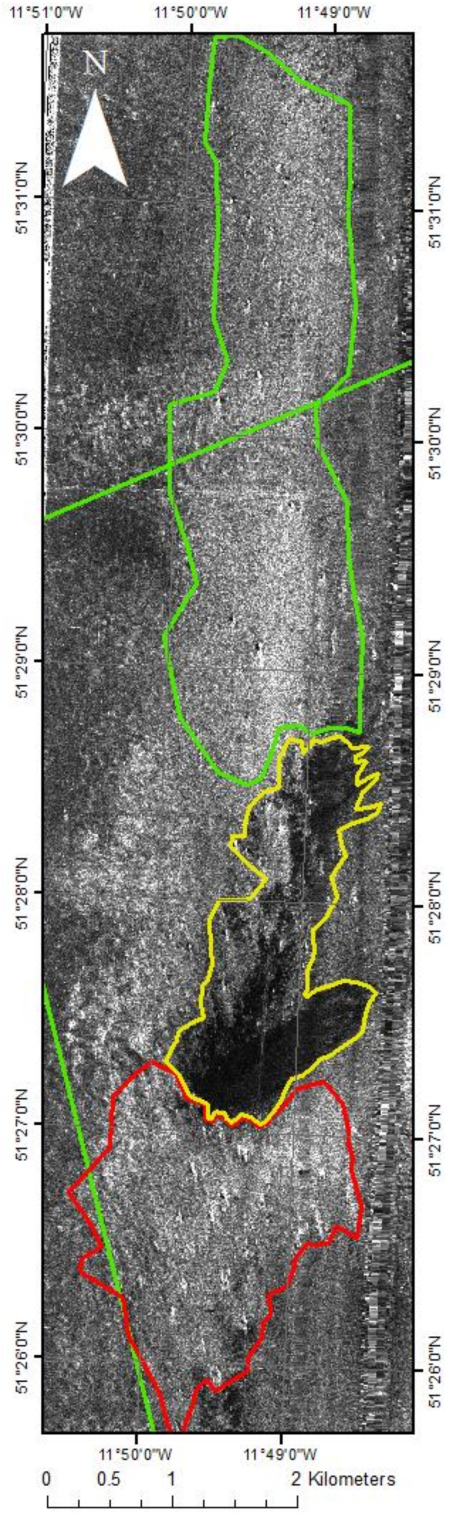

Figure 11 Downslope Moira Mounds seabed zonation.

Seabed zones as seen from differences in backscatter, bedforms, sediments and mound character. Zone 1 is in the red, zone 2 in the yellow and zone 3 is in the green polygon.

2.5.2.1 Zone 1

Despite having a higher density of mounds, the contemporary environment found in Zone 1 appears to be a sub-optimal area for CWC reef growth with significant amounts of dead coral-framework on- and around mounds. On-mound coral frameworks are also clogged and buried by this mud-dominated sediment (sediment-stressed). However, this zone is noted as having the highest number of off-mound, isolated coral colonies. While Zone 1 is the less-favourable zone for reef development showing signs of relatively lower energy than the northern-most counterpart, perhaps this is a contemporary example of how reefs and isolated coral colonies respond differently to the same hydrodynamic and sedimentological regime. In this lower-energy contemporary setting, the reefs have developed on a dropstone-dominated seabed. Unlike the off-mound area, the sediment baffling capability on-mound has caused them to become smothered by mud-dominated sediments and the coral frameworks are sediment-stressed. However, off-mound there are a relatively large number of live, isolated coral colonies. Paradoxically, these off-mound isolated coral colonies are able to grow and develop in this medium-strength current (~37 cm s^{-1}) before they become thickets and begin to trap significant amounts of sediment (Dorschel et al., 2007a). Purser et al. (2010b) indicate that in lower flow velocities, *Lophelia pertusa* colonies can capture zooplankton more efficiently. As observed, these colonies are growing in relatively large numbers. Perhaps, with time, this abundance of colonies will act as the nodal points for development, and possible coalescing of thickets and reefs as described by Wheeler et al. (2011d).

2.5.2.2 Zone 2

Zone 2 is characterised by the steepest seabed slope (2.3°), by the dominance of CWC thickets, a homogeneous, sandy substrate with fully developed ripples, and a distinct change in backscatter (dark grey/black). SSS suggests that CWC reefs are not common in this zone and ROV-video shows they are the smallest within the study area. Only 5 isolated colonies have been observed on the video data within this zone. Current speeds of 30 cm s^{-1} characterise this area while minor occurrences of lingoidal ripples toward the north of this zone suggest that currents can reach up to 40 cm s^{-1}.

Evidence shows (Figure 8) that the higher current velocity in the north of Zone 2 coincides with an increase in the occurrence of thickets. Zone 2 has the lowest current speeds in the study site with the smallest CWC reefs. In fact, as previously mentioned, CWC reefs are not common here (3.7 km^{-2}). Video evidence (Figure 6F) shows that the seabed surrounding the mounds in Zone 2 is predominantly "homogeneous sediment" (rippled sand) rather than "sediment and dropstones" commonly observed outside Zone 2. Furthermore, where dropstones are observed in Zone 2, they are colonised by coral thickets or isolated coral colonies which have not spread far from the initial dropstone substratum (Figure 6E). Thus, these thickets are not laterally extensive. It appears that mound development is curtailed to the thicket-stage due to substrate-restriction whereby their only mode of lateral spreading is dependent on the availability of mound-derived substrates (i.e. coral rubble and shell hash) as dropstones are not readily available. This form of horizontal spreading has been previously described by Roberts *et al*. (2003) and originally by Wilson (1979b). Given the dominance of a sandy substrate rather than a dropstone-dominated substrate, Zone 2 is interpreted as a substrate-restricted, thicket-dominated zone.

2.5.2.3 Zone 3

Zone 3 is characterised by the largest, most well-developed mounds, thickets and individual colonies. Furthermore, it is the only zone which displays sandwaves. Mounds here are the largest (~7.8 m ± 3.0) within the study area. The sedimentary environment surrounding the mounds, similar to that in the south (Zone 1), is predominantly dropstone-dominated. This is also reflected in the backscatter data. The seabed slope here is relatively flat (1.2°), similar to that of Zone 1.

Zone 3 is interpreted as the most favourable zone in the study area for reef development. Although mounds are less common here, they are larger (~7.8 m ± 3.0), with more complex frameworks than those in Zones 1 and 2 and they carry more live coral per mound. However, the number of isolated colonies is significantly lower in this zone (3). This supports the idea that colony initiation and reef development may have differing optimal hydrodynamic regimes. Up to now very little is known about larval biology of *Lophelia*, however Larsson et al. (2014) hint at relationships between flow speed and larval settlement. Similarly, the higher current speeds (39 - 41 cm s^{-1}) of Zone 3 could be too strong for larval settlement or even detach coral larvae from their initiation points (dropstones). Conversely, reefs appear to have grown larger, show no signs of sediment clogging and are dominated by live coral frameworks (in contrast to Zone 1).

2.5.3 Effect of hydrodynamics on CWC reef development

CTD (see 2.4.5), sediment samples (see 2.4.4) and ROV-video based observations (see 2.4.3) show that the downslope Moira Mounds are affected by an environmental gradient across the local-scale, 10 km study site, where the only variable is current speed as a result of the change in bathymetry and local slope (Figure 12). In the north (Zone 3) and south (Zone 1) of the study site, the slope is low (1.2°), the substrate is the same (dropstone-rich), and the benthic water temperature, salinity and O_2 saturation remain relatively constant (see Table 3). In quantifying current speeds in both Zones 1 (37 cm s^{-1}) and 3 (39 - 41 cm s^{-1}), a trend in mound surface morphology, on-mound carbonate and organic matter production and mound size is apparent. This trend seems to result from the increasing current speed across the study area. Zone 2 has the steepest slope, resulting in a slightly reduced current speed, which leads to the deposition of the coarsest sediment fraction and the build-up of a rippled sand sheet. Although the corals in this zone are healthy, they are substrate-restricted with regard to their settlement, and mainly occur in thickets. The number of mounds here are lower than in Zone 1 and Zone 3, and seem incapable of achieving sufficient size to slow down the currents and cause additional sediment deposition to drive mound build-up.

Mound surface morphology shows a progressive variation with current speed. At 37 cm s^{-1}, a relatively smoother mound surface is developed (Figure 6D) where coral frameworks are sediment clogged, toppled and buried with sediment. This contrasts with mound surface morphology in a 39 – 41 cm s^{-1} current speed regime where mound surfaces are more complex with larger erect coral frameworks and less sediment clogging. A similar result is found with on-mound carbonate and organic matter production. In Zone 3, there is an apparent difference in on-mound versus off-mound carbonate and organic matter content compared with that of Zone 1 (Table 2). We interpret this being due to the higher abundance of live scleractinians and the larger, more complex coral frameworks found on-mound in Zone 3 (Figure 6A and B) attracting more bioclast-producing organisms and further bioerosion. The average mound height in Zone 3 is also slightly higher than in Zone 1, which may also be a result of the difference in current speed. This size difference is also apparent in mound length as can be measured from the TOBI imagery (Table 6) where the mounds in Zone 1 are typically smaller than Zone 3. The increased current speed in Zone 3 is transporting coarser suspended sediments, and coral colonies are larger and more complex, trapping more sediment and food. This highlights the importance of hydrodynamics and sediment input as a driver for mound growth assuming that the spatial variation pattern in current speeds was maintained during the growth of the mounds. This seems reasonable as the current variation is regional and controlled by slope gradient and position in the channel, conditions that are unlikely to have changed during the mounds' existence.

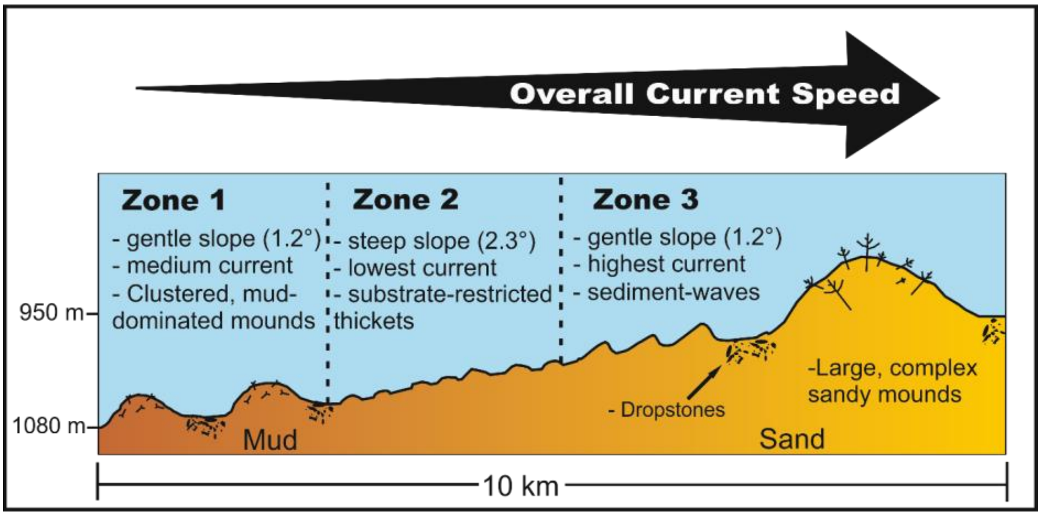

Figure 12 Interpretation of the seabed zonation at study site.

2.5.4 Comparison of current dynamics on other CWC reefs

Previously described as Scleractinian spaced cluster-macro reefs using a classification proposed by Riding (2002) (Wheeler et al., 2011d), the Moira Mounds exist between, and extend downslope of, chains of active and moribund, giant carbonate mound structures (e.g. De Mol et al., 2007a; Foubert et al., 2005a; Kozachenko, 2005b; Wheeler et al., 2005a; Wheeler et al., 2007a). They biogeologically grow upon Pleistocene muds and dropstones (Foubert et al., 2011a) and, based on our results, grow along a hydrodynamic gradient. Here, the downslope Moira Mounds are further divided into more defined zones which can now be more accurately compared to other CWC reef habitats (Table 5).

Site	**Study**	**Current velocity (cm s^{-1})**
Tisler CWC reef	Guihan *et al*. (2013); Wagne *et al*. (2011)	70
Galway Mound	Dorschel *et al*. (2007)	51 - 34
Moira Mounds Zone 3	*This study*	39 - 41
SW Rockall	Mienis *et al*. (2007); Mienis *et al*. (2009)	45
Moira Mounds Zone 2	*This study*	30 - 40
Viosca Knoll	Mienis *et al.* (2012)	38
Darwin Mounds	Huvenne *et al*. (2009); Wheeler *et al*. (2008); Masson *et al*. (2003)	35
SE Rockall	Mienis *et al*. (2007); Mienis *et al.* (2009)	30
Moira Mounds Zone 1	*This study*	37
Campeche Mound Province	Hebbeln *et al*. (2014)	30

Table 5 Summary of current velocities compared with Moira Mounds.

Moira Mounds Zones 1 and 3 are directly comparable as they are both affected by the same slope, substrate, temperature, salinity and dissolved O_2. These zones however, have a gradient in current velocity. When current velocity is ~ 37 cm s^{-1}

(Zone 1), mounds are relatively small and sediment-clogged. Further north where current velocity is 39 - 41 cm s^{-1} (Zone 3), mounds are larger, dominated by live *Lophelia*. Similarly, further north again at Galway Mound, a giant carbonate mound structure, Dorschel et al. (2007a) record a similar peak current velocities of 51 cm s^{-1} in areas of active coral growth (summit) and 34 cm s^{-1} in areas associated with vital coral growth (western flank). They also show a trend between current speed and the distribution of dead and live coral across the mound. However, despite being geographically proximal, Galway Mound occurs at 800 m water depth and summits 160 m above the seabed with a temperature range of 10.5 - 8.5 °C, a salinity range of 35.5 - 35.6 g/kg and reaching significantly higher in the water column than the Moira Mounds (Dorschel et al., 2007a). Mounds with higher densities of living corals (i.e. Galway Mound and Moira Mound Zone 3) coincide with areas of enhanced bottom currents. This suggests that within the BMP environment, current velocities of 34 - 50 cm s^{-1} are optimal for coral mound development.

Despite being geographically separated within the NE Atlantic, the Moira Mounds and Darwin Mounds are commonly compared based on their size (Huvenne et al., 2009a; Masson et al., 2003a; Wheeler et al., 2008b). Here, we show some new similarities and differences. Like the Darwin Mounds, Moira Mounds Zone 2 is substrate restricted, although this is not the case for Moira Mounds Zone 1 and 3. Both the western chain of Moira Mounds and Darwin Mounds occur at a similar depth range (900-1100 m) and temperature range (7.8 to 8.5°C: Masson *et al*., 2003; 8.6°C: this study). The number and distribution of Darwin Mounds and Moira Mounds are similar; both show an increase in size northwards; 300 Darwin Mounds (Huvenne et al., 2009a) and 256 Moira Mounds (Wheeler et al., 2011d).

Despite the Darwin Mounds and Moira Mounds showing a spatial morphometric gradation (Wheeler et al., 2008b), the Darwin Mounds have a significantly different H:L (Table 6) to the Moira Mounds. Assuming a common initiation period at the onset of the Holocene discussed by previous studies (Foubert et al., 2011a; Huvenne et al., 2009a; Victorero et al., 2015; Wheeler et al., 2011d) and a constant growth rate, then this may have implications for both Vertical Mound Growth Rates (VMGR) and Lateral Mound Growth Rates (LMGR). Wheeler *et al*. (2011b) speculate a VMGR of 30 cm ka^{-1} for the Moira Mounds assuming early Holocene initiation. Using the same method on this data set, a VMGR of 78 cm ka^{-1} can be calculated for Moira Mounds Zone 3 and a VMGR of 64 cm ka^{-1} can be calculated for Moira Mounds Zone 1. This suggests the downslope Moira Mounds have a higher VMGR to other mounds in the Porcupine Seabight (6.7 - 50 cm ka^{-1}; Dorschel *et al*., 2007b; Frank *et al*., 2005; Kano *et al*., 2007; Titschack *et al*., 2009).

Site	Height (m)	Length (m)	H:L	Slope (°)	Current Speed (cm s^{-1})
Darwin Mounds	5	75	1:15	7.60	35
Moira Mounds Zone 1	6.4	35	1:5.5	20.10	37
Moira Mounds Zone 3	7.8	65	1:8.3	13.50	39-41

Table 6 Morphometric comparison of Moira Mound Zones 1 and 3 and Darwin Mounds.

Slope calculated based on $\tan^{-1}(H/(L/2))$.

Moira Mounds Zone 3 and the Darwin Mounds have a similar diameter (65 m and 75 m respectively). Assuming constant growth and common initiation period, they have a comparable LMGR. It is possible that 34 - 50 cm s^{-1} is an optimum window for LMGR (or sediment accretion). This leads to other research questions: assuming current velocity continues to increase northwards, how does this impact mound growth and coral settlement? At what point does erosion become detrimental to mound growth? How does this affect mound growth, development and morphology?

Perhaps another CWC ecosystem comparable to the downslope Moira Mounds is the Viosca Knoll area, Gulf of Mexico. Similar to the downslope Moira Mounds, the Viosca Knoll CWC habitat hosts CWC thickets as well as a well-developed reef structure, "*Blue Reef*", but exists in a shallower setting (450 - 550 m), with a relatively high sediment input, dominated instead by river discharge (Davies et al., 2010; Mienis et al., 2012). Interestingly, the top of the Knoll, where thickets grow, experiences a similar peak current speed of 38 cm s^{-1} (Mienis et al., 2012) to that of the Moira Mounds Zones 1 and 3.

The Campeche Mound Province (CMP), Southern Gulf of Mexico is another CWC ecosystem which hosts many "small" (20 - 40 m tall) mounds. The area has a similar average current speed to the currents estimated at the Moira Mounds and also shows current aligned-elongation. However, despite similar current speeds, mound elongation and mound heights, there are some substantial dissimilarities. The CMP mounds occur in a depth range of 500 - 600 m with a slope of 30° (steeper than any of the Moira Mounds) and range in length from tens of meters to >1000 m (Hebbeln et al., 2014). They also occur in differing oceanographic conditions (temperature ranges from 9.5 - 7.5°C; salinity ranges from 35.1 - 34.9; dissolved O_2 is 2.7 ml l^{-1}).

2.6 Conclusions

ROV-video, sediment samples, CTD data, TOBI SSS and bathymetry allow for the measurement of relative hydrodynamic and sedimentological changes across a chain of cold-water coral reefs. The generated facies maps reflect the dominance of differing current-strengths across the area showing a broad increase in current velocity towards the north. When compared with CTD data, it appeared that the water column characteristics had no influence on CWC reef size, stage of growth or vitality. There is, however, a clear correlation between seafloor slope, current speed and the occurrence and size of thickets, reefs and live-coral dominated reefs. With current speeds quantified, we develop a seabed zonation where each zone suggests a differing set of environmental and sedimentological parameters influencing reef status and potential development.

Three sediment types were identified and classed as sediment and dropstones, bioclastic-hash and coral-bearing sediment. Sediment and dropstone samples represent off-mound samples and are deemed representative of either non-deposition or erosion. Bioclastic-hash samples represent mound-proximal samples while coral-bearing sediment samples represent on-mound samples. With this detailed zonation, the Moira Mounds can now be more accurately put into context with other CWC reefs. Current velocities between 34 - 50 cm s^{-1} appear optimum for reef development, potentially showing an equilibrium between erosion and deposition. Current velocities higher than this may curtail the lateral development of mounds as suggested by comparison of Moira Mounds Zone 3 and Darwin Mounds diameters and current velocities. Lower current velocities appear to lead to sediment clogging with a low LMGR or VMGR. In addition, we outline that differing hydrodynamic regimes are required for initial coral colony development and continued reef development. Initial coral colony development favours lower flow velocities whereas continued reef development favours higher flow velocities.

The western chain of Moira Mounds represents a favourable CWC habitat within the BMP. Further regional mapping will increase spatial coverage and may reveal how mounds react further north where current speeds may exceed 50 cm s^{-1} in an erosive environment.

2.7 Acknowledgements

The authors acknowledge Dr. Nicoletta Fusi, University Milano-Bicocca, Milano, Italy for help and use of the Malvern Mastersizer. A special thank you to the crew and officers of ROV Holland 1, RV Celtic Explorer, RV Belgica and RV Pelagia for assistance in collecting high resolution, accurately positioned data. Ship time on the RV Celtic Explorer was funded by the Marine Institute under the 2011 Ship Time Programme of the National Development Plan and by the National Geographic Society with additional support from National Geographic Television, National Oceanography Centre, UK, University of Southampton, UK, Geological Survey of Ireland, University College Cork and National University of Ireland, Galway. Ship time on the RV Belgica was funded by the European Union Seventh Framework Programme (FP7/2007-2013), under the Eurofleets grant agreement n° 228344. Ship time on RV Pelagia was undertaken with financial support of the European Union (EASSS III program) and the Porcupine Studies Group (PSG) of the Irish Petroleum Infrastructure Programme Group 3. V. Huvenne is funded by the ERC Starting Grant CODEMAP (Grant Agreement No 258482). The authors would like to acknowledge support from the COCARDE European Research Network community.

2.8 Chapter references

Beuck, L., Freiwald, A., Taviani, M., 2010. Spatiotemporal bioerosion patterns in deep-water scleractinians from off Santa Maria di Leuca (Apulia, Ionian Sea). Deep-Sea Research II 57, 458-470.

Beyer, A., Schenke, H.W., Klenke, M., Niederjasper, F., 2003. High resolution bathymetry of the eastern slope of the Porcupine Seabight. Marine Geology 198, 27-54

Brooke, S., Ross, S.W., Bane, J.M., Seim, H.E., Young, C.M., 2013. Temperature tolerance of the deep-sea coral Lophelia pertusa from the southeastern United States. Deep Sea Research Part II: Topical Studies in Oceanography 92, 240-248.

Cartigny, M.J.B., Postma, G., van den Berg, J.H., Mastbergen, D.R., 2011. A comparative study of sediment waves and cyclic steps based on geometries, internal structures and numerical modeling. Marine Geology 280, 40-56.

Correa, T.B.S., Eberli, G.P., Grasmueck, M., Reed, J.K., Correa, A.M.S., 2012. Genesis and morphology of cold-water coral ridges in a unidirectional current regime. Mar. Geol. 326–328, 14-27.

Davies, A.J., Duineveld, G.C.A., Lavaleye, M.S.S., Bergman, M.J.N., van Haren, H., Roberts, J.M., 2009. Downwelling and deep-water bottom currents as food supply mechanisms to the cold-water coral Lophelia pertusa (Scleractinia) at the Mingulay Reef Complex. Limnology and Oceanography 54, 620-629.

Davies, A.J., Duineveld, G.C.A., van Weering, T.C.E., Mienis, F., Quattrini, A.M., Seim, H.E., Bane, J.M., Ross, S.W., 2010. Short-term environmental variability in cold-water coral habitat at Viosca Knoll, Gulf of Mexico. Deep Sea Research Part I: Oceanographic Research Papers 57, 199-212.

Davies, A.J., Wisshak, M., Orr, J.C., Murray Roberts, J., 2008. Predicting suitable habitat for the cold-water coral Lophelia pertusa (Scleractinia). Deep Sea Research Part I: Oceanographic Research Papers 55, 1048-1062.

de Haas, H., Huvenne, V., Wheeler, A.J., Unnithan, V., crew, a.s.s., 2002. R.V. Pelagia Cruise 64PE197: A TOBI Side Scan Sonar Survey of Cold Water Coral Carbonate Mounds in the Rockall Trough and Porrcupine Sea Bight. Royal Netherlands Institute for Sea Research, Unpublished Cruise Report.

De Mol, B., Kozachenko, M., Wheeler, A., Alvares, H., Henriet, J.-P., Olu-Le Roy, K., 2007. Thérèse Mound: a case study of coral bank development in the Belgica Mound Province, Porcupine Seabight. Int J Earth Sci (Geol Rundsch) 96, 103-120.

De Mol, B., Van Rensbergen, P., Pillen, S., Van Herreweghe, K., Van Rooij, D., McDonnell, A., Huvenne, V., Ivanov, M., Swennen, R., Henriet, J.P., 2002. Large deep-water coral banks in the Porcupine Basin, southwest of Ireland. Marine Geology 188, 193-231.

Dorschel, B., Hebbeln, D., Foubert, A., White, M., Wheeler, A.J., 2007. Hydrodynamics and cold-water coral facies distribution related to recent sedimentary processes at Galway Mound west of Ireland. Marine Geology 244, 184-195.

Dorschel, B., Hebbeln, D., Ruggeberg, A., Dullo, W., Freiwald, A., 2005. Growth and erosion of a cold-water coral covered carbonate mound in the Northeast Atlantic during the Late Pleistocene and Holocene. Earth and Planetary Science Letters 233, 33-44.

Dorschel, B., Wheeler, A.J., Huvenne, V.A.I., de Haas, H., 2009. Cold-water coral mounds in an erosive environmental setting: TOBI side-scan sonar data and ROV video footage from the northwest Porcupine Bank, NE Atlantic. Marine Geology 264, 218-229.

Douarin, M., Sinclair, D.J., Elliot, M., Henry, L.-A., Long, D., Mitchison, F., Roberts, J.M., 2013. Changes in fossil assemblage in sediment cores from Mingulay Reef Complex (NE Atlantic): Implications for coral reef build-up. Deep Sea Research Part II: Topical Studies in Oceanography.

Duineveld, G.C.A., Lavaleye, M.S.S., Bergman, M.J.N., de Stigter, H., Mienis, F., 2007. Trophic structure of a cold-water coral mound community (Rockall Bank, NE Atlantic) in relation to the near-bottom particle supply and current regime. Bulletin of Marine Science 81, 449-467.

Dullo, C., Flögel, S., Rüggeberg, A., 2008. Cold-water coral growth in relation to the hydrography of the Celtic and Nordic European continental margin. Marine Ecology Progress Series 371, 165-176.

Eisele, M., Hebbeln, D., Wienberg, C., 2008. Growth history of a cold-water coral covered carbonate mound — Galway Mound, Porcupine Seabight, NE-Atlantic. Marine Geology 253, 160-169.

Fink, H.G., Wienberg, C., Hebbeln, D., McGregor, H.V., Schmiedl, G., Taviani, M., Freiwald, A., 2012. Oxygen control on Holocene cold-water coral development in the eastern Mediterranean Sea. Deep Sea Research Part I: Oceanographic Research Papers 62, 89-96.

Foubert, A., Beck, T., Wheeler, A., Opderbecke, J., Grehan, A., Klages, M., Thiede, J., Henriet, J.-P., 2005. New view of the Belgica Mounds, Porcupine Seabight, NE Atlantic: preliminary results from the Polarstern ARK-XIX/3a ROV cruise, in: Freiwald, A., Roberts, J.M. (Eds.), Cold-Water Corals and Ecosystems. Springer Berlin Heidelberg, pp. 403-415.

Foubert, A., Huvenne, V.A.I., Wheeler, A., Kozachenko, M., Opderbecke, J., Henriet, J.P., 2011. The Moira Mounds, small cold-water coral mounds in the

Porcupine Seabight, NE Atlantic: Part B—Evaluating the impact of sediment dynamics through high-resolution ROV-borne bathymetric mapping. Marine Geology 282, 65-78.

Freiwald, A., 2002. Reef-Forming Cold-Water Corals, in: Wefer, G., Billett, D.S.M., Hebbeln, D., Jørgensen, B.B., van Weering, T.C.E. (Eds.), Ocean Margin Systems, Hanse Conference on Ocean Margin Systems (2000: Delmenhorst, Germany) ed. Springer, Berlin Heidelberg New York, pp. 365-385.

Freiwald, A., Schönfeld, J., 1996. Substrate pitting and boring pattern of Hyrrokkin sarcophaga Cedhagen, 1994 (Foraminifera) in a modern deep-water coral reef mound. Mar. Micropaleontol. 28, 199-207.

Hebbeln, D., Van Rooij, D., Wienberg, C., 2016. Good neighbours shaped by vigorous currents: Cold-water coral mounds and contourites in the North Atlantic. Marine Geology.

Hebbeln, D., Wienberg, C., Wintersteller, P., Freiwald, A., Becker, M., Beuck, L., Dullo, C., Eberli, G.P., Glogowski, S., Matos, L., 2014. Environmental forcing of the Campeche cold-water coral province, southern Gulf of Mexico.

Henriet, J.-P., De Mol, B., Pillen, S., Vanneste, M., Van Rooij, D., Versteeg, W., Croker, P.F., Shannon, P.M., Unnithan, V., Bouriak, S., Chachkine, P., BELGICA 97 Shipboard scientific crew, 1998. Gas hydrate crystals may help build reefs. Nature 391, 648-649.

Henriet, J.P., Hamoumi, N., Da Silva, A.C., Foubert, A., Lauridsen, B.W., Rüggeberg, A., Van Rooij, D., 2014. Carbonate mounds: From paradox to World Heritage. Marine Geology 352, 89-110.

Henry, L.-A., Roberts, J.M., 2007. Biodiversity and ecological composition of macrobenthos on cold-water coral mounds and adjacent off-mound habitat in the bathyal Porcupine Seabight, NE Atlantic. Deep Sea Research Part I: Oceanographic Research Papers 54, 654-672.

Huvenne, V.A.I., Beyer, A., de Haas, H., Dekindt, K., Henriet, J.-P., Kozachenko, M., Olu-Le Roy, K., Wheeler, A.J., participants, T.P.c., participants, C.c., 2005a. The seabed appearance of different coral bank provinces in the Porcupine Seabight, NE Atlantic: results from sidescan sonar and ROV seabed mapping, in: Freiwald, A., Roberts, J.M. (Eds.), Cold-water Corals and Ecosystems. Springer-Verlag, Berlin Heidelberg, pp. 535-569.

Huvenne, V.A.I., Blondel, P., Henriet, J.P., 2002. Textural analyses of sidescan sonar imagery from two mound provinces in the Porcupine Seabight. Marine Geology 189, 323-341.

Huvenne, V.A.I., Masson, D.G., Wheeler, A.J., 2009a. Sediment dynamics of a sandy contourite: the sedimentary context of the Darwin cold-water coral mounds, Northern Rockall Trough. Int J Earth Sci (Geol Rundsch) 98, 865-884.

Huvenne, V.A.I., Van Rooij, D., De Mol, B., Thierens, M., O'Donnell, R., Foubert, A., 2009b. Sediment dynamics and palaeo-environmental context at key stages in the Challenger cold-water coral mound formation: Clues from sediment deposits at the mound base. Deep Sea Research Part I: Oceanographic Research Papers 56, 2263-2280.

Huvenne, V.I., Beyer, A., Haas, H., Dekindt, K., Henriet, J.-P., Kozachenko, M., Olu-Le Roy, K., Wheeler, A., 2005b. The seabed appearance of different coral bank provinces in the Porcupine Seabight, NE Atlantic: results from sidescan sonar and ROV seabed mapping, in: Freiwald, A., Roberts, J.M. (Eds.), Cold-Water Corals and Ecosystems. Springer Berlin Heidelberg, pp. 535-569.

IODP 307 Expedition scientists, 2005. Modern carbonate mounds: Porcupine drilling. IODP Prel. Rept., 307, p. 58.

Kano, A., Ferdelman, T.G., Williams, T., Henriet, J.-P., Ishikawa, T., Kawagoe, N., Takashima, C., Kakizaki, Y., Abe, K., Sakai, S., Browning, E.L., Li, X., Andres, M.S., Bjerager, M., Cragg, B.A., De Mol, B., Dorschel, B., Foubert, A.T.G., Frank, T.D., Fuwa, Y., Gaillot, P., Gharib, J.J., Gregg, J.M., Huvenne, V.A.I., Léonide, P., Mangelsdorf, K., Monteys, X., Novosel, I., O'Donnell, R., Rüggeberg, A., Samarkin, V.A., Sasaki, K., Spivack, A.J., Tanaka, A., Titschack, J., van Rooij, D., Wheeler, A.J., 2007. Age constraints on the origin and growth history of a deep-water coral mound in the northeast Atlantic drilled during Integrated Ocean Drilling Program Expedition 307. Geology 35, 1051-1054.

Kozachenko, M., 2005. Present and Past Environments of the Belgica Mounds (deep-water coral carbonate mounds), Eastern Porcupine Seabight, NE Atlantic, Department of Geology and Environmental Research Institute Cork. University College, Cork.

Larsson, A.I., Järnegren, J., Strömberg, S.M., Dahl, M.P., Lundälv, T., Brooke, S., 2014. Embryogenesis and Larval Biology of the Cold-Water Coral <italic>Lophelia pertusa</italic>. PLoS ONE 9, e102222.

Le Bas, T., Hühnerbach, V., 1999. PRISM Processing of remotely-sensed imagery for seafloor mapping operator’s manual version 3.1. Southampton Oceanography Centre, UK.

Masson, D.G., Bett, B.J., Billett, D.S.M., Jacobs, C.L., Wheeler, A.J., Wynn, R.B., 2003a. The origin of deep-water, coral-topped mounds in the northern Rockall Trough, Northeast Atlantic. Mar. Geol. 194, 159-180.

Masson, D.G., Bett, B.J., Billett, D.S.M., Jacobs, C.L., Wheeler, A.J., Wynn, R.B., 2003b. The origin of deep-water, coral-topped mounds in the northern Rockall Trough, Northeast Atlantic. Marine Geology 194, 159-180.

McCave, I.N., Manighetti, B., Robinson, S.G., 1995. Sortable silt and fine sediments size/composition slicing: Parameters for paleocurrent speed and palaeoceanography. Paleoceanography 10, 593-610.

Mienis, F., de Stigter, H.C., de Haas, H., van Weering, T.C.E., 2009a. Near-bed particle deposition and resuspension in a cold-water coral mound area at the

Southwest Rockall Trough margin, NE Atlantic. Deep Sea Research Part I: Oceanographic Research Papers 56, 1026-1038.

Mienis, F., de Stigter, H.C., de Haas, H., van Weering, T.C.E., 2009b. Near-bed particle deposition and resuspension in a cold-water coral mound area at the Southwest Rockall Trough margin, NE Atlantic. Deep Sea Res. Part I 56, 1026-1038.

Mienis, F., Duineveld, G.C.A., Davies, A.J., Ross, S.W., Seim, H., Bane, J., van Weering, T.C.E., 2012. The influence of near-bed hydrodynamic conditions on cold-water corals in the Viosca Knoll area, Gulf of Mexico. Deep Sea Research Part I: Oceanographic Research Papers 60, 32-45.

Mienis, F., van Weering, T., de Haas, H., de Stigter, H., Huvenne, V., Wheeler, A., 2006. Carbonate mound development at the SW Rockall Trough margin based on high resolution TOBI and seismic recording. Marine Geology 233, 1-19.

Mueller, C.E., Larsson, A.I., Veuger, B., Middelburg, J.J., van Oevelen, D., 2014. Opportunistic feeding on various organic food sources by the cold-water coral Lophelia pertusa. Biogeosciences 11, 123-133.

Murphy, P., Wheeler, A.J., 2017. A GIS-based application of drainage basin analysis and geomorphometry in the submarine environment: The Gollum Canyon System, North-east Atlantic, in: Bartlett, D., Celliers, L. (Eds.), Geoinformatics for Marine and Coastal Management. CRC Press, Taylor & Francis Group, Boca Raton, USA.

Neumann, A.C., Ball, M.M., 1970. Submersible Observations in the Straits of Florida: Geology and Bottom Currents. Geological Society of America Bulletin 81, 2861–2873.

Pingree, R.D., LeCann, B., 1990. Structure, strength and seasonality of the slope current in the Bay of Biscay region. Journal of the Marine Biological Association of the United Kingdom 70, 857-885.

Pingree, R.D., Sinha, B., Griffiths, C.R., 1999. Seasonality of the European slope current (Goban Spur) and ocean margin exchange. Continental Shelf Research 19, 929-975.

Pirlet, H., 2010. The Matrix of Cold-water Coral Mounds: Origin and Early-diagenetic Interactions, Faculty of Sciences. Ghent University, Ghent, Belgium, p. 179 pages.

Pirlet, H., Colin, C., Thierens, M., Latruwe, K., Van Rooij, D., Foubert, A., Frank, N., Blamart, D., Huvenne, V.A.I., Swennen, R., Vanhaecke, F., Henriet, J.-P., 2011. The importance of the terrigenous fraction within a cold-water coral mound: A case study. Marine Geology 282, 13-25.

Purser, A., Larsson, A.I., Thomsen, L., van Oevelen, D., 2010. The influence of flow velocity and food concentration on Lophelia pertusa (Scleractinia) zooplankton capture rates. Journal of Experimental Marine Biology and Ecology 395, 55-62.

Raddatz, J., Rüggeberg, A., Liebetrau, V., Foubert, A., Hathorne, E.C., Fietzke, J., Eisenhauer, A., Dullo, W.-C., 2014. Environmental boundary conditions of cold-water coral mound growth over the last 3 million years in the Porcupine Seabight, Northeast Atlantic. Deep Sea Research Part II: Topical Studies in Oceanography 99, 227-236.

Roberts, J.M., Henry, L.A., Long, D., Hartley, J.P., 2008. Cold-water coral reef frameworks, megafaunal communities and evidence for coral carbonate mounds on the Hatton Bank, north east Atlantic. Facies 54, 297-316.

Roberts, J.M., Long, D., Wilson, J.B., Mortensen, P.B., Gage, J.D., 2003. The cold-water coral Lophelia pertusa (Scleractinia) and enigmatic seabed mounds along the north-east Atlantic margin: are they related? Marine Pollution Bulletin 46, 7-20.

Roberts, J.M., Wheeler, A., Freiwald, A., Cairns, S., 2009. Cold-Water Corals: The Biology and Geology of Deep-Sea Coral Habitats. Cambridge University Press.

Rogers, A.D., 1999. The biology of Lophelia pertusa (Linnaeus 1758) and other deep-water reef-forming corals and impacts from human activities. International Review of Hydrobiology 84, 315-406.

Rüggeberg, A., Dullo, W.-C., Dorschel, B., Hebbeln, D., 2007. Environmental changes and growth history of a cold-water carbonate mound (Propeller Mound, Porcupine Seabight). International Journal of Earth Sciences 96, 57-72.

Soulsby, R., 1997. Dynamics of marine sands a manual for practical applications.

Spezzaferri, S., Vertino, A., Addamo, A.M., Backers, J., Baratti, V., Constandache, M., Camozzi, O., El Kateb, A., Gennari, G., Leuzinger, L., McGrath, M., Mc Hugh, S.K., Naudts, L., Savini, A., Stalder, C., 2012. E-CWC Moira (2012/16) RV Belgica: Cold-water coral ecosystems from the Moira Mounds (NE Atlantic): affinities and differences with modern and Pleistocene Mediterranean counterparts. University Freibourg, Switzerland, Unpublished Cruise Report.

Squires, D.F., 1964. Fossil Coral Thickets in Wairarapa, New Zealand. Journal of Paleontology 38, 904-915.

Stow, D.A.V., Hernández-Molina, F.J., Llave, E., Sayago-Gil, M., Díaz del Río, V., Branson, A., 2009. Bedform-velocity matrix: The estimation of bottom current velocity from bedform observations. Geology 37, 327-330.

Thierens, M., Browning, E., Pirlet, H., Loutre, M.F., Dorschel, B., Huvenne, V.A.I., Titschack, J., Colin, C., Foubert, A., Wheeler, A.J., 2013a. Cold-water coral carbonate mounds as unique palaeo-archives: The Plio-Pleistocene Challenger Mound record (NE Atlantic). Quaternary Science Reviews 73, 14-30.

Thierens, M., Browning, E., Pirlet, H., Loutre, M.F., Dorschel, B., Huvenne, V.A.I., Titschack, J., Colin, C., Foubert, A., Wheeler, A.J., 2013b. Cold-water coral carbonate mounds as unique palaeo-archives: The Plio-Pleistocene Challenger Mound record (NE Atlantic). Quaternary Science Reviews 73, 14-30.

Thierens, M., Pirlet, H., Colin, C., Latruwe, K., Vanhaecke, F., Lee, J.R., Stuut, J.B., Titschack, J., Huvenne, V.A.I., Dorschel, B., Wheeler, A.J., Henriet, J.P., 2012. Ice-rafting from the British–Irish ice sheet since the earliest Pleistocene (2.6 million years ago): implications for long-term mid-latitudinal ice-sheet growth in the North Atlantic region. Quaternary Science Reviews 44, 229-240.

Thierens, M., Titschack, J., Dorschel, B., Huvenne, V.A.I., Wheeler, A.J., Stuut, J.B., O'Donnell, R., 2010. The 2.6Ma depositional sequence from the Challenger cold-water coral carbonate mound (IODP Exp. 307): Sediment contributors and hydrodynamic palaeo-environments. Marine Geology 271, 260-277.

Titschack, J., Thierens, M., Dorschel, B., Schulbert, C., Freiwald, A., Kano, A., Takashima, C., Kawagoe, N., Li, X., 2009. Carbonate budget of a cold-water coral mound (Challenger Mound, IODP Exp. 307). Marine Geology 259, 36-46.

Van Rooij, D., 2004. An integrated study of Quaternary sedimentary processes on the eastern slope of the Porcupine Seabight, SW of Ireland, Renard Centre of Marine Geology. University Gent, Belgium, p. 355.

Van Rooij, D., De Mol, B., Huvenne, V., Ivanov, M., Henriet, J.P., 2003a. Seismic evidence of current-controlled sedimentation in the Belgica mound province, upper Porcupine slope, southwest of Ireland. Marine Geology 195, 31-53.

van Rooij, D., De Mol, B., Huvenne, V.A.I., Ivanov, M.K., Henriet, J.-P., 2003b. Seismic evidences of current-controlled sedimentation in the Belgica mound province, upper Porcupine slope, southwest of Ireland. Mar. Geol. 195, 31-53.

Vertino, A., Spezzaferri, S., Ruggeberg, A., Stalder, C., Wheeler, A.J., Party, t.E.C.-M.c.S., 2015. An Overview on Cold-Water Coral Ecosystems and Facies, in: Spezzaferri, S., Ruggeberg, A., Stalder, C. (Eds.), Atlas of benthic foraminifera from cold-water coral reefs. Cushman Foundation for Foraminiferal Research, pp. 12-19.

Victorero, L., Blamart, D., Pons-Branchu, E., Mavrogordato, M.N., Huvenne, V.A.I., 2015. Reconstruction of the formation history of the Darwin Mounds, N Rockall Trough: How the dynamics of a sandy contourite affected cold-water coral growth. Marine Geology.

Wheeler, A., Kozachenko, M., Beyer, A., Foubert, A., Huvenne, V.I., Klages, M., Masson, D., Olu-Le Roy, K., Thiede, J., 2005. Sedimentary processes and carbonate mounds in the Belgica Mound province, Porcupine Seabight, NE Atlantic, in: Freiwald, A., Roberts, J.M. (Eds.), Cold-Water Corals and Ecosystems. Springer Berlin Heidelberg, pp. 571-603.

Wheeler, A., Murton, B., Copley, J., Lim, A., Coughlan, M., Dorschel, B., Morris, K., Antoniacomi, A., Carlsson, J., Collins, P., Green, D., Nye, V., 2011a. Cruise Report CE11009: RV Celtic Explorer & Holland I ROV. VENTuRE Survey: VENTs and REefs deep-sea ecosystem study of the 45o North MAR hydrothermal vent field and the cold-water coral Moira Mounds, Porcupine Seabight. University College Cork, Ireland, Unpublished Report.

Wheeler, A.J., Beyer, A., Freiwald, A., de Haas, H., Huvenne, V.A.I., Kozachenko, M., Olu-Le Roy, K., Opderbecke, J., 2007. Morphology and environment of cold-water coral carbonate mounds on the NW European margin. Int J Earth Sci (Geol Rundsch) 96, 37-56.

Wheeler, A.J., Kozachenko, M., Henry, L.A., Foubert, A., de Haas, H., Huvenne, V.A.I., Masson, D.G., Olu, K., 2011b. The Moira Mounds, small cold-water coral banks in the Porcupine Seabight, NE Atlantic: Part A—an early stage growth phase for future coral carbonate mounds? Marine Geology 282, 53-64.

Wheeler, A.J., Kozachenko, M., Masson, D.G., Huvenne, V.A.I., 2008. Influence of benthic sediment transport on cold-water coral bank morphology and growth: the example of the Darwin Mounds, north-east Atlantic. Sedimentology 55, 1875-1887.

White, M., 2007. Benthic dynamics at the carbonate mound regions of the Porcupine Sea Bight continental margin. International Journal of Earth Sciences 96, 1-9.

White, M., Dorschel, B., 2010. The importance of the permanent thermocline to the cold water coral carbonate mound distribution in the NE Atlantic. Earth and Planetary Science Letters 296, 395-402.

White, M., Mohn, C., de Stigter, H.C., Mottram, G., 2005. Deep-water coral development as a function of hydrodynamics and surface productivity around the submarine banks of the Rockall Trough, NE Atlantic, in: Freiwald, A., Roberts, J.M. (Eds.), Cold-water Corals and Ecosystems. Springer, Berlin, Heidelberg, New York, pp. 503-514.

Wilson, J.B., 1979. 'Patch' development of the deep-water coral Lophelia Pertusa (L.) on Rockall Bank. Journal of the Marine Biological Association of the United Kingdom 59, 165-177.

Wilson, J.L., 1975. Carbonate Facies in Geologic History. Springer, New York.

Wood, R.A., 1999. Reef Evolution. Oxford Univ. Press, Oxford.

3 Cold-water coral reef spatial zonation, organisation and environmental controls: the case of the Piddington Mound, Porcupine Seabight, NE Atlantic

Aaron Lim [1], Andrew J. Wheeler [1] [2] and Aurélien Arnaubec [3]*

(Current status: in review, Marine Geology)

This chapter examines the contemporary processes leading to the current status of the Piddington Mound, a Moira Mound found in Zone 3 of the downslope Moira Mound area, named in honour of the late Mr. Ray Piddington, uncle to one of the author's, who passed away whilst this data was being collected at sea. Through an unprecedented investigation of the first cold-water coral reef-scale video mosaic, a reef-scale habitat zonation is developed and is linked to the findings of chapter 2. Numerous attempts have been made at understanding the spatial development of cold-water coral reefs and mounds (e.g. Dolan et al., 2009). However, none of these studies have a data set covering the entire reef or mound at the appropriate resolution and therefore results may not be representative. The aim of this chapter is to image the entire surface of the Piddington Mound at high-resolution to identify distributed facies. These facies are related to the mound-typical processes that generate these deposits and we therefore theorise how this mound developed in a spatio-temporal capacity. Another Moira Mound is examined to determine how representative this style of development is to the other Moira Mounds.

Various authors have contributed to this chapter. This project was funded through an award to Prof. Andy Wheeler. Prof. Wheeler was chief scientist on all cruises that collected this data set. He supervised all research carried out and gave useful feedback on drafts. Dr. Aurélien Arnaubec generated the video mosaic utilised in this chapter with the help of Aaron Lim. He also wrote the section on video mosaicking. Aaron Lim developed the classifiers used for this research. He applied the classification several times on various trial versions of the final video mosaic to test the accuracy and consistency of this classification. He ran all spatial statistics and the GIS component of the research. He wrote the chapter and created all figures and maps. He also planned the acquisition, acquired, processed and visualised the ROV-mounted multibeam bathymetry. He compared the downward and oblique video datasets utilised herein. All concepts and ideas developed from the data was by Aaron Lim.

[1)] *School of Biological, Earth and Environmental Sciences, University College Cork, Distillery Fields, North Mall, Cork, Ireland*

[2)] *Irish Centre for Research in Applied Geosciences, University College Cork, Ireland*

[3)]*Unité Systèmes sous-Marins, Centre de Méditerranée, Ifremer, Zone Portuaire de Brégaillon, CS 20330, 83507 La Seyne/Mer Cedex, France*

Abstract

Cold-water coral (CWC) reefs are biogenic build-ups formed by calcareous framework cold-water corals such as *Lophelia pertusa* and *Madrepora oculata*. In the North East Atlantic, CWC reefs and mounds have been studied in detail and reveal heterogeneous spatial on-mound organisation. However, these studies are limited by a paucity of remotely-sensed and video imagery at an appropriate resolution and coverage. This study is the first attempt to video mosaic an entire CWC reef (the Piddington Mound of the Moira Mounds, Porcupine Seabight, Irish margin). The mosaic is divided into 0.25 m^2 cells with a supervised classification applied to each within a GIS. Geostatistical analysis shows that cell distribution is not random but clustered significantly across the mound surface. These clusters of cells make up a ring-like facies pattern. Parallels to the Wilsons Ring model are invoked with caveats. Two models for this development are suggested, a biogenic Wilson Ring-like development or one developing similar spatial patterns due to changes in environmental controls over time. In a wider context, an additional

Moira Mound is assessed in a similar way and it appears that this spatial pattern is typical of the Moira Mounds in this area.

*Corresponding author: aaron.lim@ucc.ie

Keywords: cold-water coral, habitat mapping, spatial analysis, sediments, mound development

3.1 Introduction

Scleractinian cold-water corals (CWCs) are sessile, filter-feeding organisms that can baffle current-suspended sediment (Roberts et al., 2006a). *Lophelia pertusa*, the most common framework-forming CWC in the NE Atlantic, has been found as shallow as 39 m water depth and as deep as 4000 m water depth (Freiwald et al., 2004; Roberts et al., 2006a). It occurs in temperatures between 4 and 13°C (Freiwald, 2003) and has proven to be tolerant of a wide range of salinities, from 31.7 – 38.8 ‰ (Davies et al., 2008a). As the coral framework grows, it baffles sediment which can help to generate topographic features on the seabed called CWC reefs and, through successive periods of reef development, CWC carbonate mounds (Roberts et al., 2009a). CWC reefs and mounds are common in the NE Atlantic (Wheeler et al., 2007a), specifically where internal waves concentrate surface primary production which is delivered to CWCs by enhanced bottom currents (Dullo et al., 2008a; Mienis et al., 2009b; White and Dorschel, 2010a).

CWCs require a suitable, hard substrate by which to attach (Roberts et al., 2009a). In the NE Atlantic, this is usually in the form of glacial erratic's, rock outcrops and gravels (Dorschel et al., 2009a). After coral larvae settle and grow on a hard substrate, a colony develops. Squires (1964b) put forward 4 stages through which the CWC colony can develop into a CWC bank: colony to thicket to coppice and, finally, to bank. Building on this, Wilson (1979a), puts forward a general model for the understanding of CWC bank development under optimum conditions around a CWC colony. More recently, fossil assemblages, absolute dating (U/Th and AMS ^{14}C) and sedimentology of on- and off-mound cores (e.g. Dorschel et al., 2005b; Douarin et al., 2013), as well as seabed mapping (De Mol et al., 2007b; Foubert et al., 2011b), have been used to define various ways by which CWC mound features have developed. A summary model of which can be found in Roberts et al. (2006b) and .

Habitat mapping has proved to be a valuable, efficient and cost-effective tool in understanding the marine environment (e.g. Huang et al., 2011; Lamarche et al., 2011) including CWC habitats (Savini et al., 2014). Multibeam Echosounder (MBES) bathymetry and backscatter have been used extensively to characterise current dynamics and their influence on CWC mound morphology and development e.g. in the straits of Florida, west Atlantic (Correa et al., 2012a; Correa et al., 2012b) and the midslope Moira Mounds, Porcupine Seabight, NE Atlantic (Foubert et al., 2011b). Recently, more advanced approaches to MBES surveying have imaged CWC habitats in deep water using ROV-borne MBES (Dolan et al., 2008; Foubert et al., 2011b), on submarine terraces using AUV-borne MBES (Correa et al., 2012a) and on vertical cliff faces in submarine canyons using forward-facing ROV-borne MBES (Huvenne et al., 2011).

In the absence of adequate multibeam data, other studies (Dorschel et al., 2007a; Lim et al., *submitted;* Wheeler et al., 2008a) avail of current data, sediment types, video data and/or side scan sonar (SSS) surveying integrated within a Geographical Information System (GIS) to highlight the role of currents and sediment supply on CWC reefs and mounds. Seabed sediment samples are an effective way of studying CWC reefs although limited by the spatial representation of the sample (e.g. Day grab, <0.5 m^2). Video surveys can discriminate the seabed across substantial areas and are widely used in CWC habitat inspections (Foubert et al., 2005b; Huvenne et al., 2005a; Vertino et al., 2010a). Recent advances in underwater imaging have made high-resolution underwater imagery with accurate positioning in deep water environments possible (Kocak and Caimi, 2005). In addition, advances in image processing has led to the application of video mosaicking to marine habitat mapping (Rzhanov et al., 2000). For example, Lirman et al. (2007) accurately characterise a tropical coral reef in shallow water using an entire reef-scale video mosaic. However, no such study has been carried out on an entire CWC reef although small parts of CWC habitats have been manually photo mosaicked (Kozachenko, 2005a).

The need for more local-scale studies and data sets of comparable resolution have previously been highlighted (Dolan et al., 2008). The present study aims to answer some fundamental research questions relating to CWC reef spatial organisation and development, namely, does Piddington Mound show spatial organisation and what influences this organisation; is this organisation typical of other small-type CWC reefs?

3.2 Study Site

The Belgica Mound Province (BMP), partly enclosed with a Special Area of Conservation (SAC) designated under the EU Habitats Directive, is located on the eastern flank of the Porcupine Seabight, NE Atlantic (Figure 13) (Beyer et al., 2003b; Dorschel et al., 2007a; Huvenne et al., 2002a). It contains an abundance of (giant) CWC carbonate mounds, including the well-studied Galway Mound, Thérèse Mound and Challenger Mound (De Mol et al., 2007b; Dorschel et al., 2007a; Eisele et al., 2008a; Huvenne et al., 2009c; Kano et al., 2007; Thierens et al., 2010a; Titschack et al., 2009b; Wheeler et al., 2005c). Two distinct CWC carbonate mound chains have been identified, orientated roughly N-S (parallel to depth contours). Pre-existing bathymetry highlights their slight elongate to conical morphology and typical dimensions (approx. 1 km across and 100 m tall) (Beyer et al., 2003b). To the east, these CWC carbonate mounds are enclosed by the continental shelf and to the west, enclosed by a blind channel, the Arwen Channel, which runs through the BMP (Murphy and Wheeler, 2017; Van Rooij, 2004a).

The Moira Mounds are small-type CWC reefs (approx. 30 m across and 10 m tall) found throughout the BMP (Wheeler et al., 2005c). While no definitive dating has confirmed their age, it is speculated that they are Holocene features based on their size, seismic profiles and the surrounding seabed substrate (Foubert et al., 2011b; Huvenne et al., 2005a; Kozachenko, 2005a). The Moira Mounds in the BMP can be further subdivided into 4 areas or chains of mounds based on the distribution of approx. 256 Moira Mounds; the “up-slope area”, the “mid-slope area”, the “down-slope area” and the “northern area” (Wheeler et al., 2011c). While the number of Moira Mounds in the northern and the up-slope areas are relatively sparse, the main focus of research has been carried out on the mid- and down-slope areas. The mid-slope area occurs between the chain of CWC carbonate mound structures. The Moira Mounds here are thought to represent mound formation under "stressed" conditions due to high sediment flux (Foubert et al., 2011b).

The down-slope area is unique as it occurs within the Arwen Channel. Here, a N-S environmental gradient exists where Moira Mounds are influenced by changing current speeds. The area can be further subdivided into 3 zones based on these current speeds; Zone 1 to the south where the environmental conditions are thought to be unfavourable for mound development but more suitable for initial CWC growth; Zone 2 where CWC substrate-restricted thickets thrive and; Zone 3 where environmental conditions are thought to be favourable for mound development but not for initial CWC colony growth (Lim et al., *submitted*). The Piddington Mound is one of the Moira Mounds that occur in Zone 3 of the down-slope area and is actively trapping sands and producing bioclastic material on-mound (Lim et al., *submitted*).

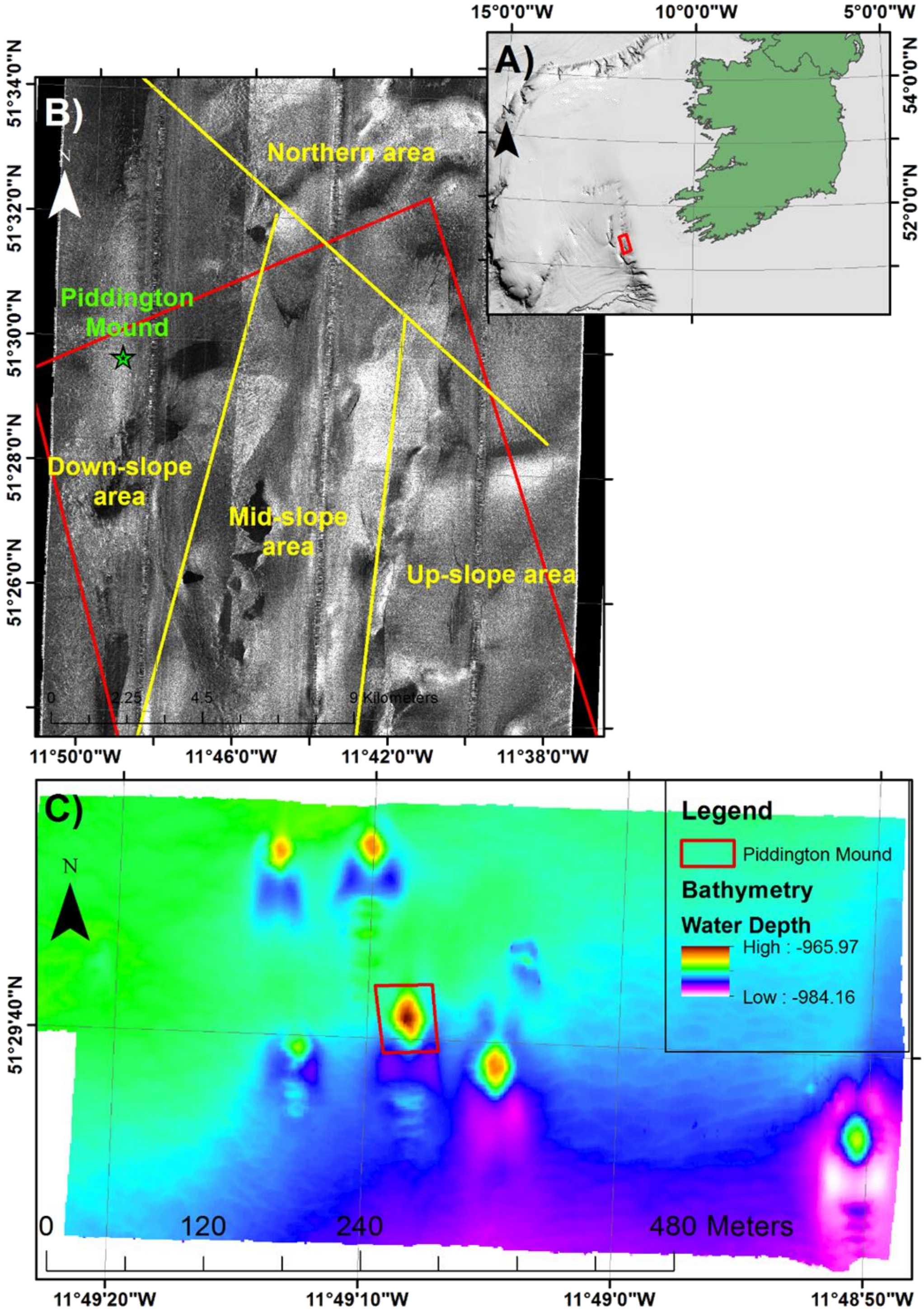

Figure 13 Study area location map.

A) Map showing the Belgica Mound Province (BMP) Special Area of Conservation (SAC) (red box) within the Porcupine Seabight relative to Ireland; B) the subdivision of Moira Mounds around the BMP SAC (red box) with the position of the Piddington Mound (green star); C) bathymetry of the Piddington Mound area.

3.3 Materials and Methods

3.3.1 ROV-borne Multibeam Echosounder (MBES)

ROV-borne MBES data was collected over the Piddington Mound and the surrounding seabed during the QuERCi survey (2015) on board *RV Celtic Explorer* with the *Holland 1 ROV* (cruise number CE15009: Wheeler et al. (2015). A high-resolution Kongsberg EM2040 MBES was integrated with a sound velocity probe and mounted on the front-bottom of the ROV. Data were acquired at a frequency of 400 kHz while the ROV maintained a height of 30 m above the seabed with a survey speed of approximately 2 knots. This achieved a swath width of ~ 160 m. Positioning and attitude were obtained using a Kongsberg HAINS inertial navigation system, ultra-short baseline (USBL) system (Sonardyne Ranger 2) and doppler velocity log (DVL). Data acquisition was carried out using SIS software, where calibration values, sensor offsets, navigation and attitude values were incorporated. Two adjacent 170 m long MBES lines were collected over Piddington Mound and the surrounding seabed. MBES data were stored as *.all and *.wcd files and were processed using CARIS HIPS and SIPS v9.0.14 to apply tidal corrections and clean anomalous data spikes. The cleaned data were saved as a single *.xyz and gridded to a 10 cm ArcView GRID.

The 10 cm MBES grid was imported into ArcMap 10.2 and projected in UTM Zone 29N. A 1 m contour *.shp file was generated using the Arc Toolbox Spatial Analyst Contour tool. Slope (degrees) and aspect were derived from the bathymetry using the Arc Toolbox Spatial Analyst tools.

3.3.2 ROV-video data collection

ROV-video data was collected over Piddington Mound during the VENTuRE survey (2011) on board *RV Celtic Explorer* with the *Holland 1 ROV* (cruise number CE11009: Wheeler and shipboard party, 2011). A downward-facing, high-definition camera was mounted on the bottom of the ROV. Positioning and navigation were achieved using a USBL (Sonardyne Ranger 2) and RDI Workhouse DVL. The ROV altimeter recorded and logged the height of the ROV from the seabed. The ROV recorded downward-facing HD video during a series of transects across the mound <2m off the seabed/mound surface.

Additional video data was collected during the same survey with the *Holland 1 ROV* with an oblique forward-facing camera. This is typically used for ROV exploratory investigations of the seabed. Oblique forward-facing video data was recorded over Piddington Mound and another Moira Mound (referred to here as "Venture Mound") 1.7 km NNW of Piddington Mound.

3.3.3 Georeferenced video mosaic generation

A georeferenced video mosaic has been generated using the IFREMER in-house *Matisse* software where the raw video data was imported and from which images have been extracted at a rate of 1 per second. Poor quality imagery, possibly due to an excessive fly height, and/or with a poor navigational lock were not included. The associated USBL navigation has been filtered with a sliding median filtering and 2^{nd} order polynomial model fit in order to lower trajectory noise. Image and navigation data have been synchronized so that each image has an initial approximate position. This position is refined later by the mosaicking process. For this refinement, the first process consists of feature detection and matching between images using the SIFT (Scale Invariant Feature Transform) algorithm (Lowe, 1999), known for its strong robustness and accuracy. Image matching alone would lead to a drifting mosaic and invalid scale, while USBL navigation alone is not accurate enough for high-quality local-overlapping but gives accurate global positioning. To benefit from the both image matching and USBL-navigation, we merged image and navigation information through a cost function minimization. This developed method is similar to Ferrer et al. (2007) except cost function weights are affected according to image and navigation data standard deviations so re-projection errors are minimized in the mosaicking plane rather than the image plane.

After this step, image positions are refined (with a global accuracy of ca. 1 m) and the mosaic can be drawn. This is carried out with state of the art seaming and blending techniques after Burt and Adelson (1983) and Kwatra et al. (2003). The resulting video mosaic is shown in Figure 14, holes in the mosaic are a result of data rejection.

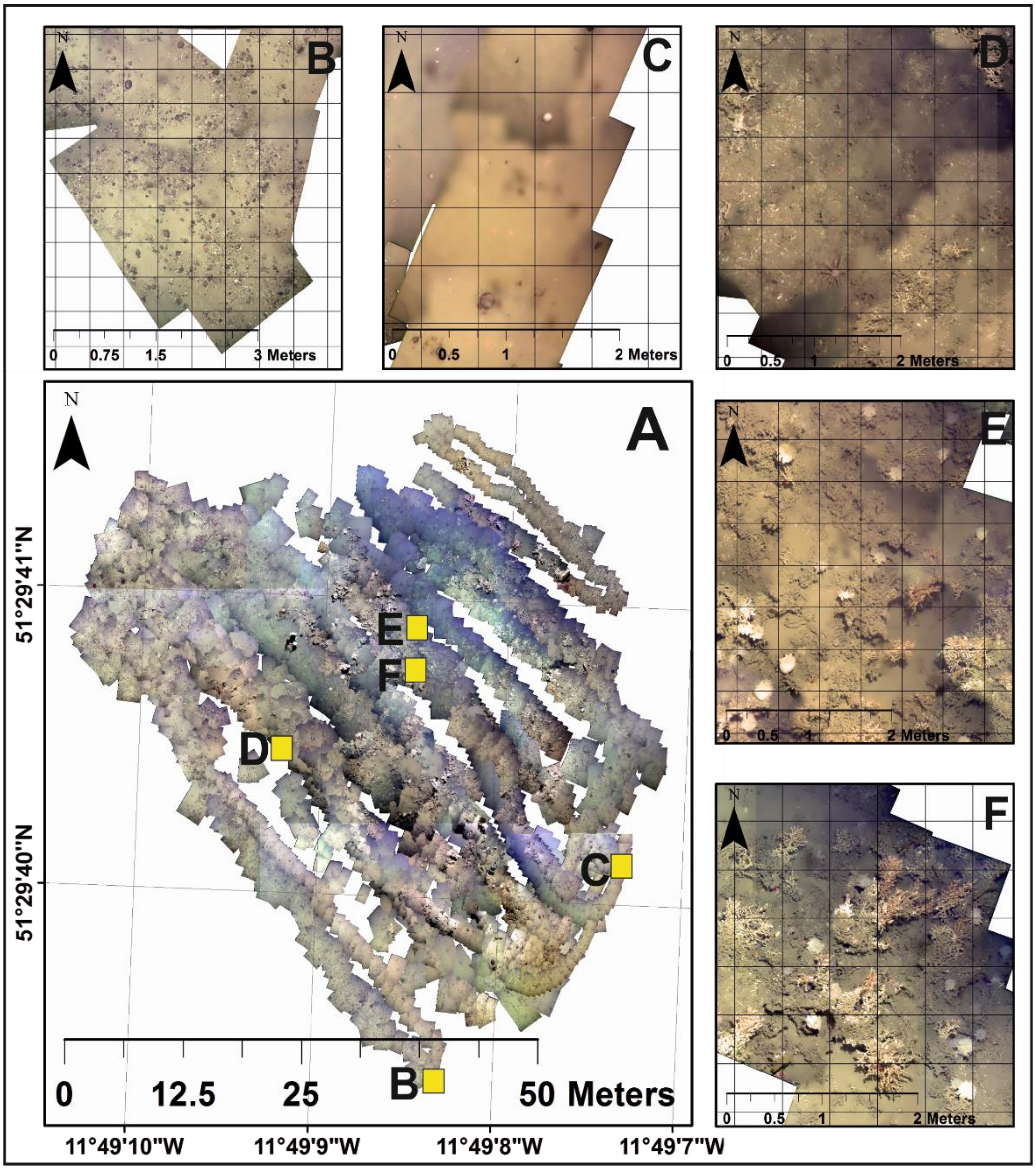

Figure 14 Georeferenced video mosaic of Piddington Mound

A) Map of georeferenced video mosaic with relative position of close-up images (yellow boxes); B) example close-up image of area dominated by "sediment and dropstone" cells with ArcGIS fishnet overlaid; C) example close-up image of area dominated by "sorted sediment" cells with ArcGIS fishnet overlaid; D) example close-up image of area dominated by "biogenic hash" cells with ArcGIS fishnet overlaid; E) example close-up image of area dominated by "dead coral framework" cell with ArcGIS fishnet overlaid; F) example close-up image of area dominated by "live coral framework" cells with ArcGIS fishnet overlaid.

3.3.4 Seabed classification

As the ROV could not be maintained at a constant height above the seabed in video surveying mode in strong currents, seawater-induced blue-shift varied across the video mosaic. Hence, an unsupervised (automatic) seabed classification could not be utilized. Instead, a supervised (manual) classification was applied to the entire video mosaic. An ArcMap fishnet with a cell size of 0.25 m^2 was overlaid on the video mosaic to manage the supervised classification at the highest resolution possible where each 0.25 m^2 cell can be inspected and classified (totally 18,980 cells).

Classifiers were based on CWC habitat facies from previous work (e.g. Dorschel et al., 2007a; Dorschel et al., 2009b; Douarin et al., 2013; Lim et al., *submitted;* Spezzaferri et al., 2012; Vertino et al., 2010b; Vertino et al., 2015) and a preliminary assessment of the video mosaic. The facies classifiers are: “sediment and dropstones”, “biogenic hash”, “sorted sediment”, “dead coral framework” and “live coral framework” (see Figure 14 for examples). The “sediment and dropstones” class can be characterised by the cell being dominated (>50 %) by dropstones and sediment (sand or mud). This class represents cells where erosion, non-deposition or non-coral growth has dominated since the deposition of dropstones (as the area is beyond the contemporary limit of icebergs it as assumed these early Holocene or older). The “biogenic hash” class can be characterised by a cell dominated (>50%) by recognisable bioclasts (i.e. shells, coral rubble) and sediment. This class represents cells whose most recent sedimentary process is dominated by the deposition of mound-derived sediments. The “sorted sediment” class can be characterised by the cell being dominated (>90%) by sorted sediment i.e. sand or mud with no recognisable bioclasts or dropstones. This class represents a cell where the deposition of sorted sediment under the influence of benthic currents is the most recent sedimentary process to take place. The “dead coral framework” class can be characterised by the cell being dominated (>50%) coral framework which has no identifiable living parts. This class represents a cell where coral grew, but currently does not support coral growth. The “live coral framework” class can be characterised by the cell being dominated (>50%) by coral framework with identifiable living parts (polyps or mucus-covered frameworks evident) although major proportions of the coral framework may be dead. This class represents a cell where coral is actively growing.

As each individual cell is inspected and a suitable class chosen, a value was assigned to an attribute table. Several preliminary classifications were applied to the video mosaic in different locations to test the individual classifiers and the classification itself. Some areas of the preliminary classification were re-classified and compared to their initial classification to ensure classification accuracy. The entire video mosaic was then classified and saved as a *.shp file.

The same classification was applied to the oblique video footage from both Piddington Mound and Venture Mound. At the start and end time of each facies type, the latitude, longitude and depth were also recorded. This data was stored in an unformatted excel file, imported into ArcMap and saved as a *.shp file.

3.3.5 Video-mosaic analysis

Spatial dependency can be measured by various spatial autocorrelation statistics (e.g. Moran’s *I*: Goodchild, 1986). However, these can be unrepresentative when spatial autocorrelation varies significantly over the study site. More suitably, Anselin (1995) developed local indicators for spatial association (LISA) which, in contrast to existing methods, measures local variation within patterns of spatial dependence that may not be represented in existing techniques. A widely-used LISA is the *G* statistic (Getis and Ord, 1992; Ord and Getis, 1995). This measures how concentrated high or low values are for a given study area by calculating a z-score (standard score) and p-value (calculated probability) of a set of geographical values. Here, it is utilised to measure the degree of clustering of the classified cells via the Arc Toolbox spatial statistics tools (High/Low clustering Tool) based on Euclidean distances.

The classified *.shp file was converted to a raster using the conversion tools in Arc Toolbox and imported to the Focal Statistics tool. This calculates, for each input cell location, a statistic of the value that occurs most often (majority) within a specified neighbourhood around it. The specified neighbour was calculated based on a potential navigational error of the ROV (<5 m). Therefore, the neighbourhood was defined as 2.5 m radius around each cell location.

3.4 Results

3.4.1 Bathymetry and slope

Figure 15A shows the derived bathymetry from Piddington Mound and the surrounding seabed. Piddington Mound exists in an area with several other mounds. It has a similar size (11.8 m tall, 60 m x 40 m across) and morphology (slightly elongated conical) as the surrounding mounds and it has substantial scouring (1 m - 3 m deep) at its southern limit. Sinuous megaripples (sediment waves) exist across the area around these mounds. They have a wavelength of ~10 m and a wave height of 20 cm – 75 cm. To the south of each mound, there are positive, ridge-shaped features 0.5 m - 2 m tall. These features are unlike the sediment waves as they have coral colonising them as shown by the oblique video footage (Figure 16).

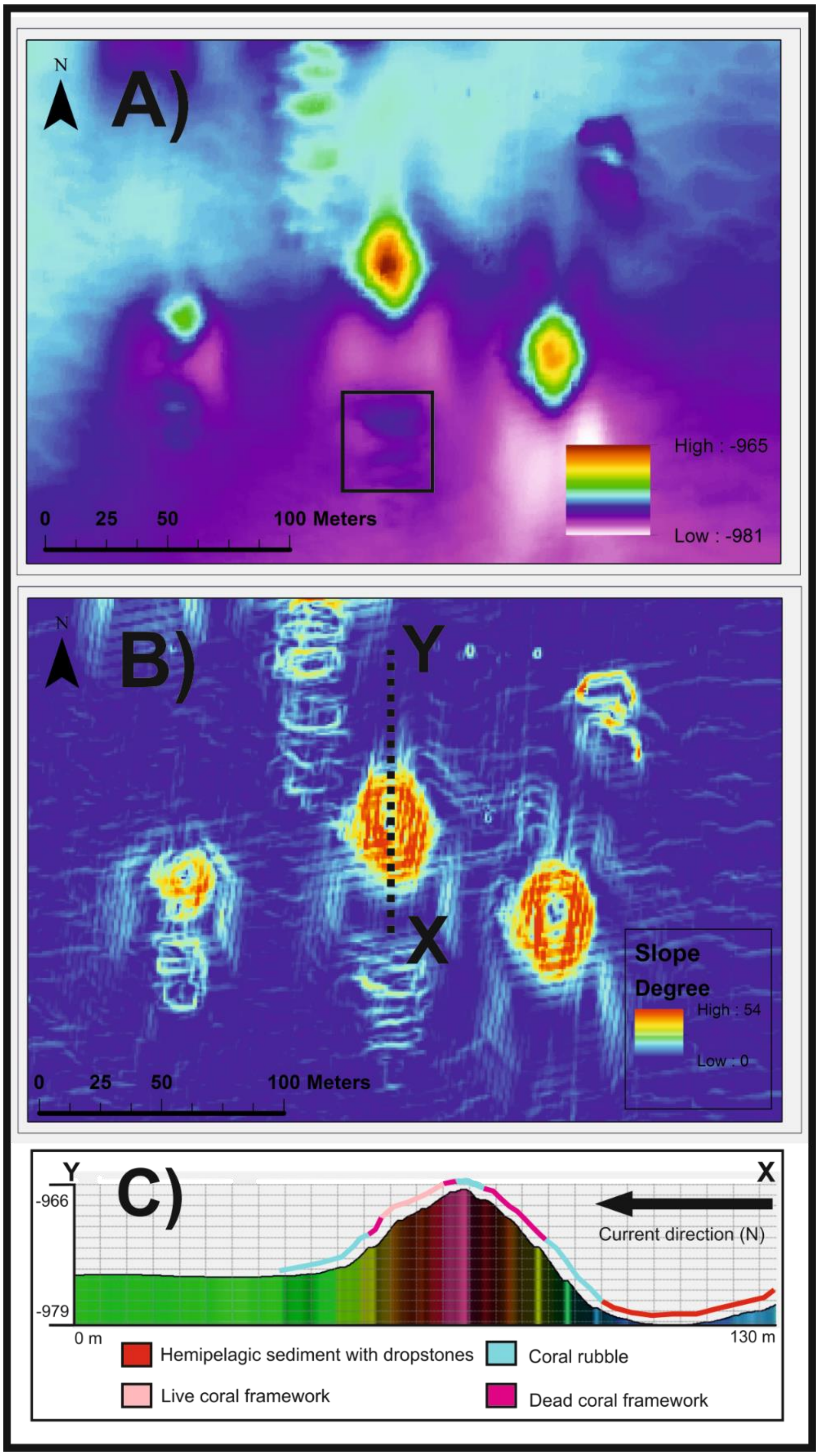

Figure 15 Bathymetry and slope of the Piddington Mound area

A) Bathymetry of the Piddington Mound (centre) area with coral ridge feature position identified (black box); B) ArcGIS-generated slope of the Piddington Mound area. Relatively flat areas in blue, relatively steep areas in red and line X-Y (Fig. 15C) indicated; C) Cross-profile of Piddington Mound with surface facies plotted.

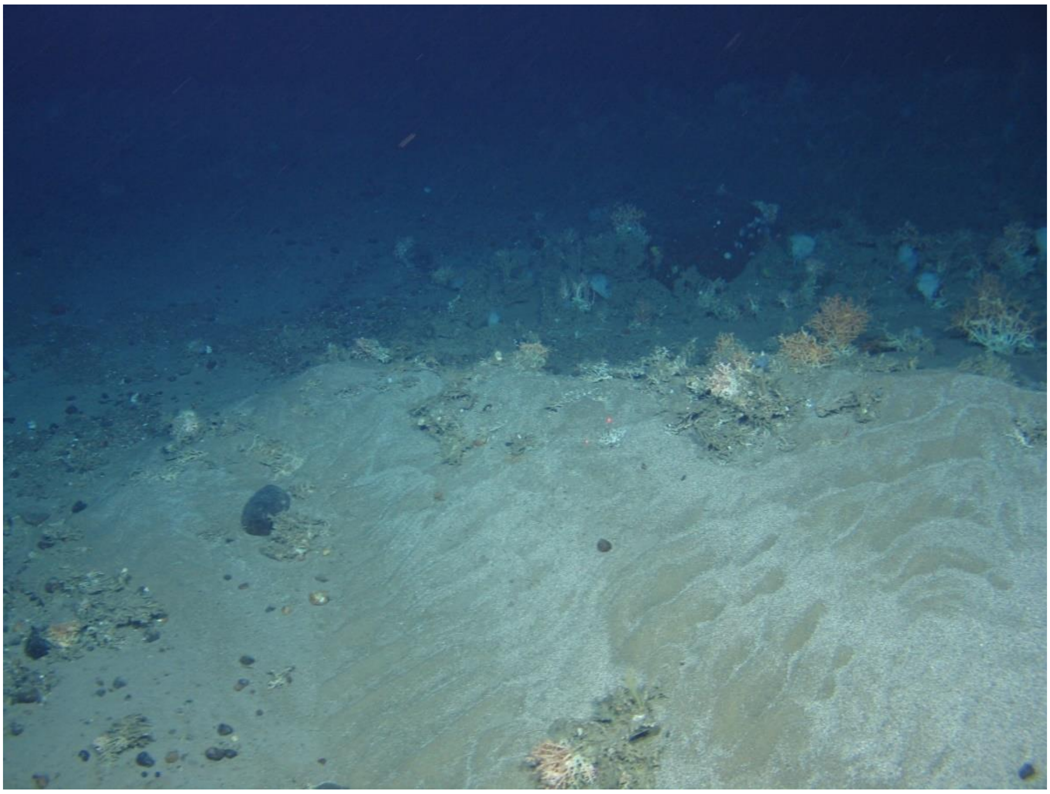

Figure 16 Image of coral ridge-form feature to the south of Piddington Mound. View to the north. Laser scalers = 11 cm. Ripple marks on the camera-facing side of the ridge indicate a northerly-directed current.

Figure 15B shows the slope raster layer generated in Arc Toolbox. The deep purple colour represents the flatter seabed while the green colour represents the steeper seabed area, all relative to this data set. Note that regional slope angle in this area is 1.2^{o} (Lim et al., *submitted*). The steepest areas can be found on the flanks of the mounds which are angled at ~55°. The summit of each mound is relatively flat as are areas away from the mounds (0° - 6°). This figure also includes the slip faces of mega ripples in the areas away from the mounds. These appear sinuous to cuspate with a wavelength of 7 m - 10 m and wave height of 4 cm - 20 cm with an east-west crest alignment. The larger coral colonised ridge-shaped features (0.5 m – 2 m tall) south of the mounds are morphologically distinct, with short east-west aligned linear crests and a wavelength of approx. 10 m. They diminish in size away from the mounds.

3.4.2 Seabed classification

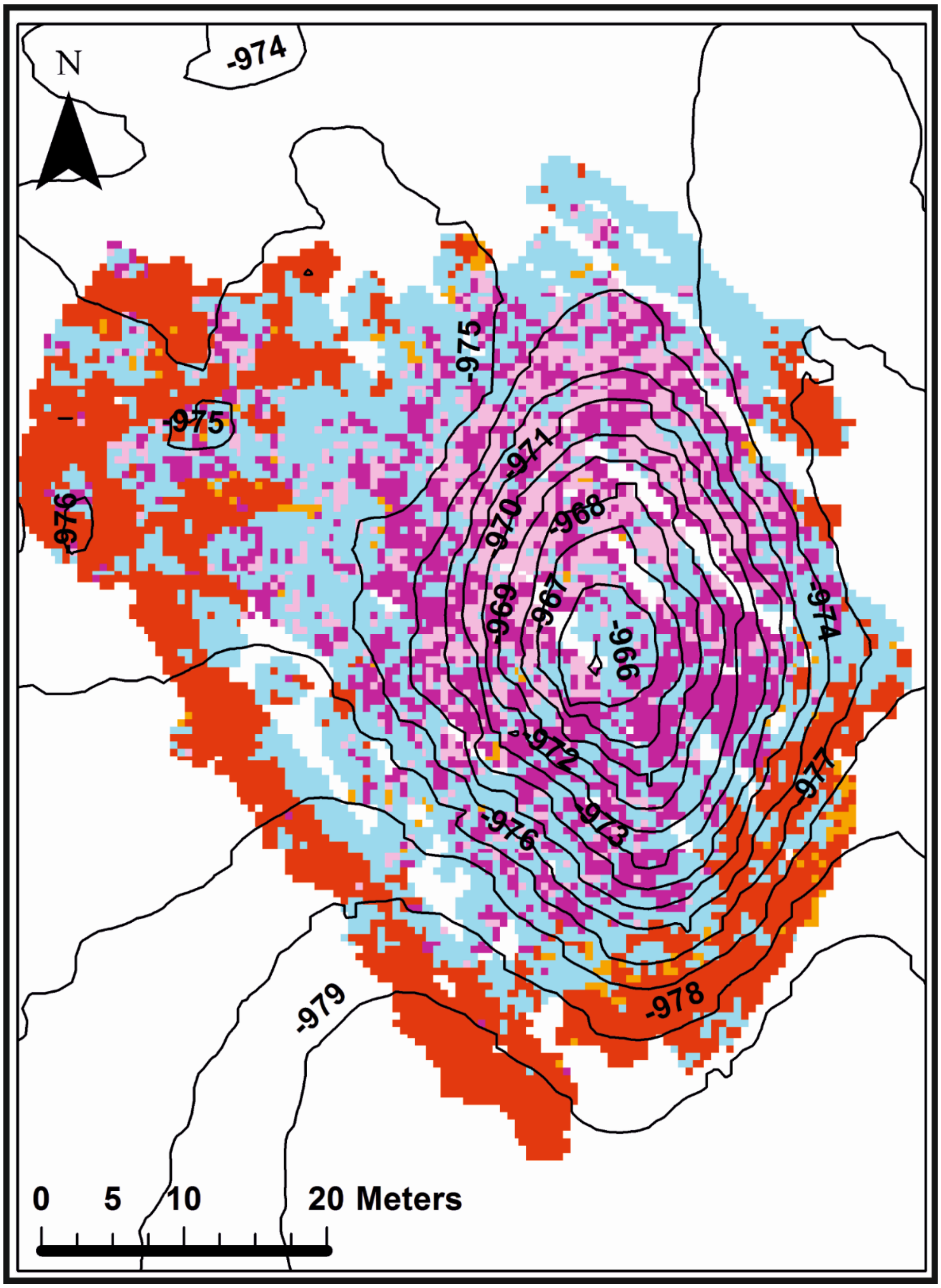

*Figure 17 Classified fishnet *.shp file with contours superimposed showing the distribution of facies types across thePiddington Mound mosaic*

(red = sediment and dropstones, orange = sorted sediment, blue = biogenic hash, purple = dead coral framework, and pink = live coral framework).

Figure 17 shows the shapefile which represents the classified video mosaic. The "sediment and dropstones" and "biogenic hash" classes are the most frequent classified cells in the video mosaic. The "sediment and dropstones" class occurs most commonly around the edges of the mosaic. The "biogenic hash" class most commonly occurs in a 10 m wide ring immediately enclosed by the "sediment and dropstones" classed cells. However, minor occurrences of this class exist to the centre of the video mosaic and outside of this ring. The least common class is "sorted sediment". This tends to occur in small clusters less than 0.75 m wide and appears to most commonly occur on the edges of the "biogenic hash" class. While the "live coral framework" class can be found throughout the video mosaic, it is concentrated in the northern central area. The "dead coral framework" class also occurs throughout the video mosaic but is concentrated in the centre and southern central area. While it appears that each class occurs in distinct areas, there is substantial heterogeneity within each area.

Supervised classification of the oblique video data from Piddington Mound shows a broad comparable trend (Figure 18A) although this may be affected by USBL-positioning, camera obliqueness and seabed slope. Sediment and dropstones are common in the observed off-mound area to the south west. Although biogenic hash can be seen on many parts of the video from Piddington Mound, it appears to be more common on the lower flanks, near the mound summit and to the north of the off-mound area. Live coral and dead coral frameworks are common across all the on-mound oblique video data. Where corals protrude into the water column, they make it more difficult to observe, record and classify flatter facies (e.g. biogenic hash). Dead coral framework appears to occur more often than live coral framework which occurs mostly on the upper northern mound flank. No sorted sediments were observed probably as these where hidden behind coral colonises.

The ROV progressed south west to north east across the Venture Mound where it observed flat, off-mound seabed, 3 m deep scour pits and the mound itself. The flat seabed and the flanks of the scour pits are dominated by sediment and dropstones while sorted sediment (sands) can be found within the deepest part of the scour pits. Biogenic hash can be found near the mound summit and the lower flanks of the mound, although there are some minor occurrences of coral framework found here. Dead coral frameworks dominate the mound flanks although some minor occurrences of live coral can also be seen here. Live coral is most common near the mound summit.

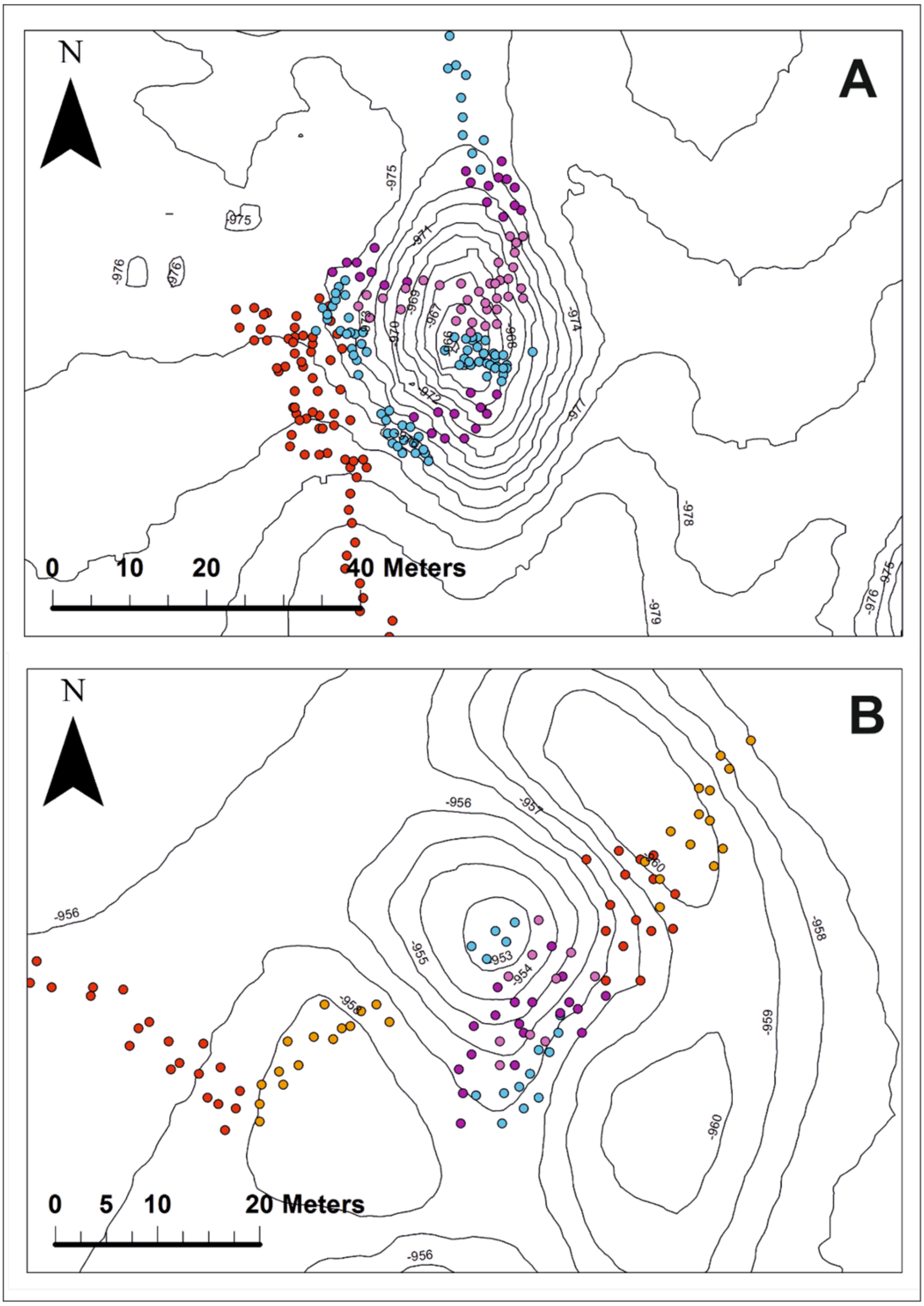

Figure 18 Oblique camera supervised classification of the Piddington Mound and the Venture Mound

A) Map showing the distribution of seabed facies across the Piddington Mound surface from oblique camera video data (red = sediment and dropstones, blue = biogenic hash, purple = dead coral framework, pink = live coral framework); B) Map showing the distribution of seabed facies across the Venture Mound surface from oblique camera video data (red = sediment and dropstones, orange = sorted sediment, blue = biogenic hash, purple = dead coral framework, pink = live coral framework).

3.4.3 Video-mosaic analysis

The High-Low Clustering (Getis-Ord General G) analysis reveals an observed General G score of 0.000276, a z-score of 168.89 and a p-value of <0.001. A high z-score and low p-value reveals that there is a highly-clustered cell distribution pattern with <1% chance that this could be the result of random chance.

The majority value of cells in the specified neighbourhood (2.5 m radius) (Figure 19) reveals 4 facies occurring in 5 areas: “Live coral framework” facies, “Dead coral framework” facies, “Biogenic hash” facies, and “Sediment and dropstone” facies (named after the cell-type that dominates the facies). This means that in these facies, a particular cell-type dominates, as shown by the focal statistic (majority) based on a 2.5 m radius. The distribution of these facies closely follows the distribution of observed common occurrence of the individual classified cells. These facies have a ring/annulus-like distribution.

The “Sediment and dropstone” facies exists in the outer rim of this ring/annulus shape. It has an area of 762 m^2 and a perimeter of 332.2 m. It is made up of 74.9% “sediment and dropstone” cells, 15.9% “biogenic hash” cells, 2.3% “dead coral framework” cells, 1.6% “sorted sediment” cells and 1.3% “live coral framework” cells (Figure 19B).

Immediately inside the “Sediment and dropstone” facies, the “Biogenic hash” facies exists. However, this facies also protrudes 11.5 m through this facies NW of the mound and exists on the highest point of the mound (at -968 m water depth) protruding 11.5 m towards the ENE. This zone has a total area of 1041 m^2 with a perimeter of 493.6 m. It is made up of 60.6% “biogenic hash” cells, 16.5% “dead coral framework" cells, 6.9% "live coral framework" cells, 6.3% "sediment and dropstone" cells and 1.6% "sorted sediment" cells (Figure 19B).

The "Dead coral framework" facies exists immediately inside the main body of the "Biogenic hash" facies ring. It has a U-shape where the centre of the "U" is broadly based around the highest point on the mound. It has an area of 491 m^2 and a perimeter of 315 m. This facies is made up of 53.1% "dead coral framework" cells, 24.3% "biogenic hash" cells, 17.4% "live coral framework" cells, 0.6% "sorted sediment" cells and 0.1% "sediment and dropstone" cells (Figure 19B).

Finally, the "Live coral framework" facies occurs 4.8 m north of the highest point on the mound, where it completes the U-shape of the "Dead coral framework zone" to make a complete ring, encircling the central "Biogenic hash" facies. This zone has an irregular morphology where the zone is intruded by minor occurrences of the "Dead coral framework" facies. It has an area of 207.8 m^2 and a perimeter of 150 m. It is made up of 47.8% "live coral framework" cells, 32.1% "dead coral framework" cells, 13.6% "biogenic hash" cells, 0.2% "sorted sediment" cells and 0% "sediment and dropstone" cells (Figure 19B).

As expected, the "sorted sediment" cells were not common enough in any neighbourhood (2.5 m) to develop its own facies in the focal statistics tool. However, their distribution in relation to these facies is noted.

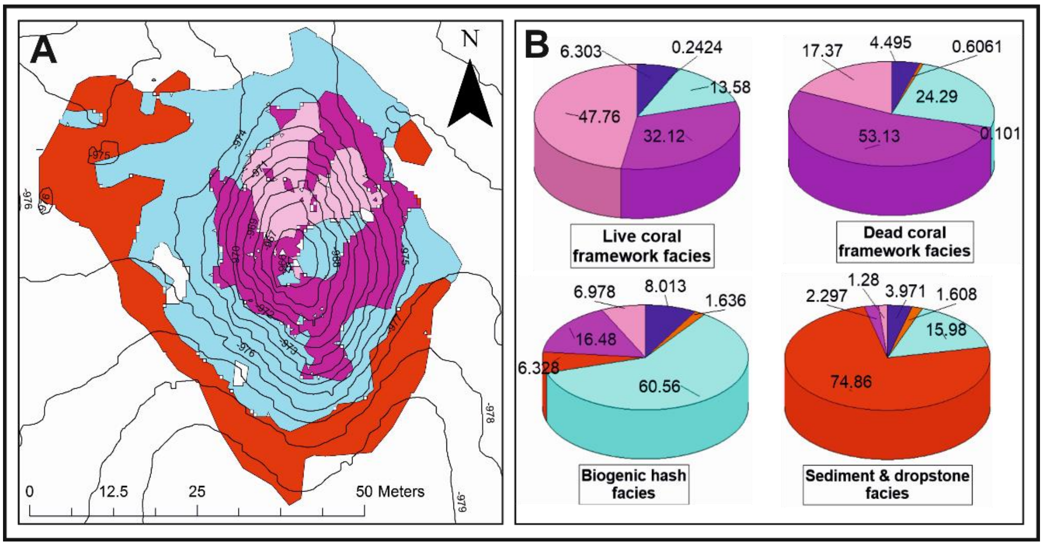

Figure 19 Focal statistics and facies proportions on the Piddington Mound

A) Map showing the focal statistics layer which shows the 4 identified facies occurring in 5 areas. Each facies represents where a cell-type is most dominant within a 2.5 m radius neighbourhood (red = "Sediment and dropstones" facies, blue = "Biogenic hash" facies, dark pink = "Dead coral framework" facies, light pink = "Live coral framework" facies); B) Pie charts showing the relative proportion and percentages of cells that define each facies.

3.5 Discussion

3.5.1 Local sedimentary environment

East-west orientated sediment waves surrounding Piddington Mound and its neighbouring mounds suggest a high-energy, hydrodynamically-influenced, sedimentary environment. In fact, Lim et al. (*submitted*) calculate a current speed of 38.8 - 41.4 cm s^{-1} in this area. The cross-profile morphology (steepened lee slope) of the sediment waves suggests a south to north prevailing current across the area (Figure 15B). Substantial scouring around the base of the mounds (Figure 15A) not only highlights the intensity of the currents but also exposes the underlying dropstone-dominated substrate. Piddington Mound and its neighbouring mounds have a current-orientated elongate morphology, probably owed to the dominance of currents in the area. The larger ridge-form features to the south of the mounds are not sediment transport features but rather biological in nature as shown by the presence of coral on them (see Figure 16). These are interpreted as small coral banks as noted by De Mol et al. (2007b) and Wheeler et al. (2007) at the base of the Therese Mound.

3.5.2 Piddington Mound spatial organisation

The G-statistic reveals that, despite the heterogeneous nature of the facies on Piddington Mound observed from the video mosaic at a 0.25 m^2 scale (broadly commensurate with a typical sediment sample footprint), there is a statistically significant clustered pattern. The focal statistics layer shows the geographic distribution of cell-type dominance (Figure 19A). The ring-like pattern of these dominating cell-types is clearly focussed around the positive topographic feature (Piddington Mound) observed in the bathymetric data (Figure 15A). This ring-like clustered pattern is made up of facies typical of CWC reefs and mounds ("Live coral framework", "Dead coral framework" and "Biogenic hash"). Similar facies have been identified at the nearby Galway Mound (Dorschel et al., 2007a), other Moira Mounds (Spezzaferri et al., 2012; Vertino et al., 2015), Atlantis Mound and Yellow Chain at the Santa Maria di Leuca Coral Province in the Mediterranean (Vertino et al., 2010a) and even through time at the Mingulay Reef Complex (Douarin et al., 2013). The distribution of these mound-typical facies closely follows the mound contours. Where the seabed becomes relatively flat (surrounding Piddington Mound) (Figure 15B), it is dominated by "Sediment and dropstones" facies. Thus, it is likely that the on-mound facies distribution can be attributed to mound development where each facies represents a dominant seabed/mound development process. The off-mound, sediment and dropstone-dominated seabed is typical of the Moira Mounds area (Foubert et al., 2011b; Kozachenko, 2005a; Lim et al., *submitted*) which is thought to represent dominant non-deposition or erosion since the deposition of the dropstones (presumed early Holocene or older). The “Live coral framework” area slightly to the north of the Piddington Mound summit is the area on the mound where coral framework growth dominates. The “Biogenic hash” area on the mound found near the summit and on the fringes of the reef are the areas where (bio) erosion of coral frameworks and biogenic sediment accumulation occurs. The “Dead coral framework” area found mainly on the flanks of the reef and are typically found where the “Biogenic Hash” and “Live coral framework” intersect. This area represents an area where live coral growth no longer dominates and older frameworks remain exposed.

Many spatial and temporal growth models have been put forward for CWC reef and mound development (De Mol et al., 2007b; Dorschel et al., 2005b; Douarin et al., 2013; Roberts et al., 2009a; Roberts et al., 2006b; Squires, 1964b; Wilson, 1979a), each based on differing criteria. Some growth models highlight the importance of currents (De Mol et al., 2007b; Dorschel et al., 2005b), sediment supply (Foubert et al., 2011b) and (bio)erosion (Douarin et al., 2013) in reef and mound development. Ring-like growth has previously been reported (Henriet et al., 1998; Wilson, 1979a). Henriet et al. (1998), however, link this ring-like reef development to speculated regional degassing of gas-hydrates. CWC reef and mound development with regard to gas hydrates and deep geological processes (Hovland et al., 1998; Hovland and Thomsen, 1997) has since been largely disregarded as a necessary or controlling process due to a paucity of evidence in favour of marine environmental conditions driving CWC reef and mound development (Roberts et al., 2009a).

Wilson (1979a) proposes a ring-like CWC reef development (Wilson Ring model), particularly focussed around the coppice stage (sensu Squires, 1964b). While there are substantial differences between the Wilson Ring model and our observations, some parallels can be made. Wilson (1979a) describe CWC reef development in optimum conditions, with limited sediment supply, where autogenic (biogenic) processes dominate; an isolated colony grows and successive rings of coral debris and colonies develop around this initial point (colony). This forms a circular CWC coppice made up of alternating rings of colonies and debris where, presumably, the centre is older than the edges of the structure.

The ring-like facies distribution on Piddington Mound is arguably a reef-scale Wilson Ring, based on the principals, rather than physical properties, of the Wilson Ring model (coral growth and decay as set out in the Wilson Ring model). Nevertheless, it should be noted that at the reef-scale, this is not in reference to patterns derived from individual colonies but rather areas dominated by coral-colonisation or bioclastic build-up. On Piddington Mound, there are coral framework-dominated facies ("Live Coral Framework" and "Dead Coral Framework") as well as a "Biogenic Hash" facies in a ring-like distribution, based around the mound summit. These facies represent differing processes; build up (Coral Framework); and breakdown (Biogenic Hash), which are similar to those processes described in the Wilson Ring Model (coral colonies where the structure builds up and coral debris where it breaks down). So, rather than individual colonies surrounded by debris which is surrounded by more colonies, for example, this research shows areas of Piddington Mound which are organised in a ring-like pattern, where each ring is dominated by a process. Thus, the distribution of facies and the processes they represent in principal are similar to the Wilson Ring model.

3.5.3 Influences on spatial organisation

Previous research highlights the nature of the Moira Mound hydrodynamic and sedimentary environment (Kozachenko, 2005; Wheeler et al., 2001) with the western Moira Mound chain being an area of non-deposition or even erosion adjacent to mounds, where glacially-deposited dropstones are still (re)exposed (Lim et al., *submitted*). This accounts for the dominance of dropstones surrounding the Piddington Mound.

The “sorted sediment” cell-type is uncommon across Piddington Mound (Figure 17), although its distribution is noted. In the literature, results from on-mound cores often associate layers of sediment which lack bioclasts (coral fragments or other fossil material) with a climate-induced reduction in currents and blanketing of the reef or mound by sediment (Dorschel et al., 2007b; Eisele et al., 2008a; Pirlet et al., 2011a). To the contrary, Piddington Mound is subjected to relatively high current speeds (39 - 41 cm s^{-1}) (Lim et al., *submitted*) yet this sediment class is present. Caution must therefore be applied in interpreting layers of sorted sediment in CWC mounds in palaeo-studies. Figure 17 shows that the “sorted sediment” cell-type occurs under this hydrodynamic regime in three scenarios. The first scenario is next to coral framework cell-types (“Dead coral framework” and “Live coral framework”) where the coral frameworks may produce localised areas of shelter from current inducing sedimentation. The second scenario is where the coral may act as a physical barrier to erosion for the already deposited sediment from a former lower hydrodynamic energy regime. The same scenario is highlighted by Douarin et al. (2013) at the Mingulay Reef Complex, northeast Atlantic. The third scenario is at the boundary between the “sediment and dropstone” cell-types and “biogenic hash" cell-types in the current-facing (southern) side of the mound. This build-up of "sorted sediment" may be explained by a sudden change in seabed rugosity slowing the current between these two cell-types, allowing the deposition of current-suspended sediment.

Walther's Law of Facies (Reading, 1996) implies that vertical facies sequences are the products of a migration of a series of depositional environments which lay laterally adjacent to each other. Several cycles of reef and mound development have previously been put forward, each showing a typical progression of live coral framework to dead coral framework to coral rubble (i.e. growing, aging and breakdown) (Douarin et al., 2013; Roberts et al., 2009a; Roberts et al., 2006b). Invoking Walther's Law, a similar facies association can be seen here expressed spatially on Piddington Mound: "Live coral framework" facies, "Dead coral framework" facies and "Biogenic hash" facies. In support of this progressive association, we find the "Live coral framework" facies next to the "Dead coral framework" facies followed by the "Biogenic hash" facies. In light of the outlined spatial organisation, two possible scenarios for the development of the observed distribution of mound-typical facies are put forward.

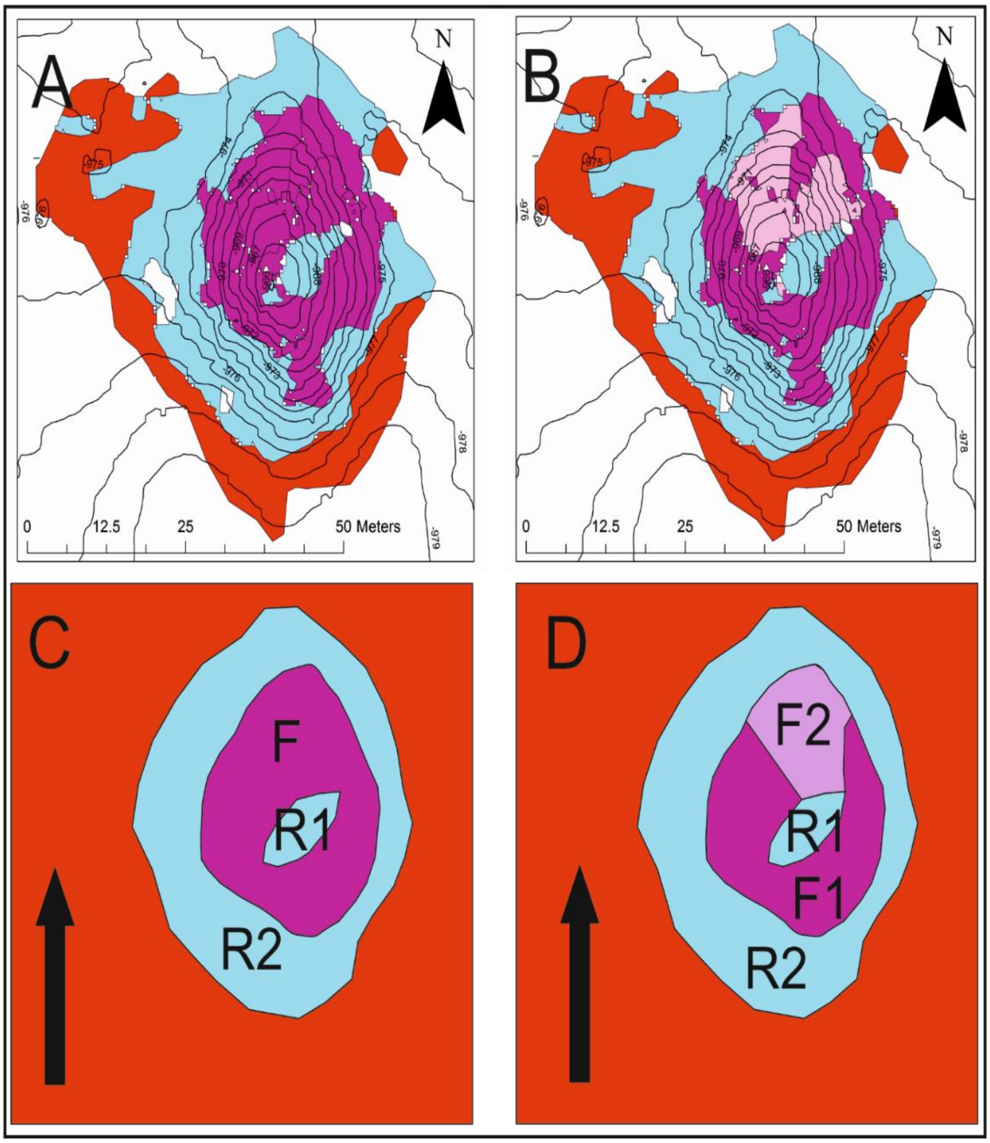

Figure 20 Idealised representation of facies across the Piddington Mound

A) map showing the distribution of facies across Piddington Mound without *differentiation between dead and live coral framework facies (red = sediment and dropstone facies, blue = biogenic hash facies, purple = combined coral framework facies). B) map showing the distribution of facies across Piddington Mound* with *differentiation between dead and live coral framework facies (red = sediment and dropstone facies, blue = biogenic hash facies, purple = dead coral framework facies, pink = live coral framework facies). C) Simplified drawing of Piddington Mound* without *differentiation between live and dead coral frameworks (red = sediment and dropstone facies, blue = biogenic hash facies, purple = combined coral framework facies, R1 & R2 = biogenic hash facies 2, F = combined coral framework facies, arrow = current direction). D) Simplified drawing of Piddington Mound* with *differentiation between live and dead coral frameworks (red = sediment and dropstone facies, blue = biogenic hash facies, purple = combined coral framework facies, R1 & R2 = biogenic hash facies 2, F1 = dead coral framework facies, F2 = live coral framework facies, arrow = current direction).*

3.5.3.1 Scenario 1: Biogenic reef-scale Wilson Ring-like development

The Wilson Ring model is based on CWC reef development in optimal conditions where colonies grow, age and breakdown. Thus, it is a biologically-driven (autogenic) model. In Figure 20A and C, we show the Piddington Mound without a differentiation between live and dead coral frameworks (F). This shows a ring of coral growth (F) surrounding and being surrounded by rings of coral breakdown (R1 and R2). In this scenario, R2 is interpreted as a former aggregation of coral framework that has since broken down to Biogenic hash forming an older substrate on which a reef-scale Wilson Ring-like structure develops. R2 is therefore the oldest facies on the Piddington Mound and "F" has settled upon this former "Biogenic hash" facies. According to the Wilson Ring model, F is the youngest facies of live coral dominated reef with an older core of the reef having died and is now broken down to biogenic hash (R1). So, in terms of age, R2 > R1 > F. If this model is correct then the future of Piddington Mound may see "R2" and "R1" act as a substrate for another coral framework facies while "F" may begin to breakdown.

Dividing "F" into "F1" ("Dead coral framework facies") and "F2" ("Live coral framework facies") more accurately reflects facies observed on Piddington Mound (Figure 20B and D), with the "Live coral framework" facies restricted to the northern flank. This complication provides, perhaps, the imperfect reality with F2 representing the start of the breakdown of the F ring into coral rubble but initially from the south.

3.5.3.2 Scenario 2: Reef-scale Wilson Ring-like development due to environmental change

Currents are well-known to influence facies distribution across CWC reefs and mound (Dorschel et al., 2007a). In fact, previous research on lithoherms show that even local-scale (bio)zonation may be primarily controlled by current flow over them (Messing et al., 1990). In this scenario, we consider currents as the dominant (allogenic) control on the distribution of facies across Piddington Mound. F1 and F2 (Figure 8C & D) develop relatively high on the mound where the corals benefit from enhanced food supply. It is noted that food flux is highest on the tops of mounds where it is undiluted by benthic sediment transport processes (Roberts et al, 2009). F1 and F2 also occur on the steepest part of the mound where physically and biologically eroded bioclasts may roll onto the flatter parts of the mound (predominately the downslope R2 although currents could push some fragments upslope to R1). Thus, F1 and F2 are the source of the bioclasts that make up the "Biogenic hash" facies in R2 and may also contribute somewhat to R1.

The location and distribution of the "Live coral framework" area is interesting as one would expect live coral framework to occur on the summit of mounds. In the case of the Piddington Mound, it occurs just north of the summit (Figure 19) on the lee side of the mound. In areas of excessively high current flow on the Porcupine Bank, cold-water corals have been found flourishing in the lee of mounds (Dorschel et al., 2009a). However, this is unlike other mounds in the eastern Porcupine Seabight (i.e. Galway Mound: Dorschel et al., 2007), and here the summit of Piddington Mound is dominated by Biogenic hash facies (R1). Figure 21 maps the facies types across the Piddington Mound bathymetric cross-profile. Lim et al. (*submitted*) calculate current speed here of 38.5 – 41.4 cm s^{-1} in this area, the highest noted for the western Moira Mounds chain. It may be that currents are simply too strong for live coral over most of Piddington Mound (F1 and R1) whilst live corals in F2 thrive in the shelter provided by the mound which acts as a physical barrier slowing the currents. Purser et al. (2010a) and Orejas et al. (2016) show that *Lophelia* capture food more effectively in lower flow velocities.

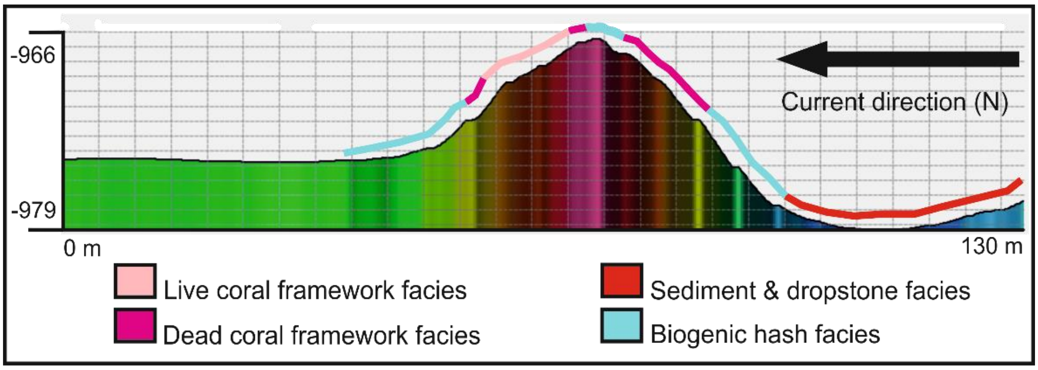

Figure 21 Cross profile of Piddington Mound with facies type plotted across the surface

The R1 "Biogenic hash" facies, if not solely derived by the upslope transport of bioclasts from F1 which seems unlikely, may represent a former "Live coral framework" facies. In this scenario, coral must once have thrived here but subsequently died due to a changing environmental conditions most probably due to an intensification of the current regime e.g. as a result of increasing benthic currents following the Little Ice Age (Foubert et al., 2011b).

The main loci for live coral growth on different mounds varies from setting to setting: on the summit (e.g. Galway Mound: Dorschel et al. (2007a), the lee side of the mound structure (e.g. Giant Mound and the Hedge Mounds: Dorschel et al., 2009; Piddington Mound: *this study*), and to the current-facing side of the mound structure (e.g. CWC reefs at Hola, offshore Norway: (Buhl-Mortenson et al., 2015). As the distribution of CWC's on reefs and mounds appear to be predominantly controlled by currents and are known as successful sediment baffling organisms, this highlights the complexity of their morphological development through time. Following the concept of developed mound morphologies (Wheeler et al., 2007), coral frameworks at the front of a mound will trap sediment and develop a different mound morphology to where the coral framework develops at the back of a mound. In addition to this, current speeds and directions may change through time as CWC mounds develop.

3.5.4 How representative is Piddington Mound?

Piddington Mound is 1 of 256 Moira Mounds noted in the BMP by Wheeler et al. (2005). To what extent is the spatial arrangement of coral facies and the subsequence inferences on mound development on the Piddington Mound typical of other Moira Mounds in the down slope area? Additional oblique camera ROV-video footage was used to survey a line across Piddington Mound to compare with other mounds (see Figure 18). Coral framework facies (dead and live) are substantially over-estimated with oblique camera due to the 3D structural habitat created by the coral framework. Conversely, the flatter facies (e.g. "Biogenic hash" and "Sorted sediment") are substantially underestimated (Figure 18A) where they are hidden behind upstanding coral colonies. The obliqueness of camera means that the exact position (taken from the ROV-mounted USBL) of the observed facies is not directly under the camera and height variation of the ROV, movement of the ROV around its own axis while in the same position and seabed slope influences the field of view. Nevertheless, by comparing Figure 17 with Figure 18A, we can see that the occurrence of facies in distinct areas and their location on the mound are similar to those seen with the downward facing camera. While "Biogenic hash" facies are underestimated, a small patch can be seen on the summit. Despite being over-estimated, coral framework facies (live and dead) surround this patch. On the margin of this, a small occurrence of “Biogenic hash” facies exists, clearly underestimated by the oblique camera. While this oblique view of Piddington Mound is not as spatially accurate as the downward-facing camera, a similar pattern can be observed.

Another Moira Mound (Venture Mound) within the down slope area, 1.7 km NNW of Piddington Mound was also surveyed by the same oblique camera (Figure 18B). The coral framework facies (live and dead) appear to be more dominant than “Biogenic hash” facies although this is probably caused by over-estimation due to camera obliqueness. The lower flanks of the Venture Mound are covered with biogenic hash while the upper flanks are dominated by live and dead coral framework in patches. While the summit of the mound is not 100% covered, like the oblique camera footage from Piddington Mound, there is evidence of “Biogenic hash” facies which is probably also underestimated. Off-mound, there is a substantial build-up of “sorted sediment”. While there are small amounts of this found on the on-mound/off-mound boundary at Piddington Mound, here it appears to be related to well-developed scouring, most probably being deposited within the scour pits.

The on-mound areas of both the Piddington and Venture Mounds show similarities in on-mound spatial facies patterns while the substantially more well-developed scouring off-mound could be related to a northward increase in current speed (Lim et al., *submitted*). This would suggest that the patterns of spatial zonation on Piddington Mound, and their implications for mound development, are applicable of all the Moira Mounds in the downslope area.

3.6 Conclusion

Although video mosaicking an entire CWC reef at this resolution is time consuming in data acquisition, processing and analysis, our preliminary investigation offers new, unique and detailed insights to CWC reef organisation and functioning. Despite mound surface heterogeneity, areas of the Piddington Mound surface (as small as 0.25 m^2) cluster significantly in a ring-like pattern focussed around the mound summit where each of these clusters represent a dominant process at that location. While ring-like growth has been reported at other CWC reefs and mounds (Henriet et al., 1998; Wilson, 1979a), the pattern of growth here is physically dissimilar. A definitive explanation cannot be put forward for the existence of this ring-like pattern however, with two possible scenarios invoked which incorporate previous reef and mound development models. The first scenario is based on the principals (ring-like growth and decay) of the Wilson Ring model while the second is based on the influences of the surrounding environment and environmental change.

Comparison of downward camera with the oblique camera video data from Piddington Mound show an under-estimation of flatter mound areas (coral debris-dominated areas). This is due to over-estimation of the 3D structure developed by the coral framework obscuring the field of view. Furthermore, the exact positioning of the field of view is hindered by camera obliqueness and seabed slope where the position of the observation is recorded near the camera (ROV-mounted for example) causing an inconsistent and inaccurate positioning error. Nevertheless, comparison of the oblique and downward cameras yield similar results.

In a wider context, another Moira Mound in the down slope area (the Venture Mound) was examined by oblique ROV video footage and demonstrated that the spatial patterns and inferred development scenarios for the Piddington Mound have regional implications.

3.7 Acknowledgements

The authors would like to thank the crew and officers of ROV Holland 1 and RV Celtic Explorer for assistance in collecting high resolution, accurately positioned data. Ship time on the RV Celtic Explorer was funded by the Marine Institute under the 2011 and 2015 Ship Time Programme of the National Development Plan. Funding. Aaron Lim is funded by the Irish Research Council Graduate of Ireland Scholarship IRC (2015 - 2016).

3.8 Chapter references

Anselin, L., 1995. Local Indicators of Spatial Association—LISA. Geographical Analysis 27, 93-115.

Beyer, A., Schenke, H.W., Klenke, M., Niederjasper, F., 2003. High resolution bathymetry of the eastern slope of the Porcupine Seabight. Mar. Geol. 198, 27-54.

Buhl-Mortenson, L., Hodnesdal, H., Thorsnes, T., 2015. The Norwegian Sea Floor. MAREANO 2015.

Burt, P.J., Adelson, E.H., 1983. A multiresolution spline with application to image mosaics. ACM Transactions on Graphics (TOG) 2, 217-236.

Correa, T.B.S., Eberli, G.P., Grasmueck, M., Reed, J.K., Correa, A.M.S., 2012a. Genesis and morphology of cold-water coral ridges in a unidirectional current regime. Mar. Geol. 326–328, 14-27.

Correa, T.B.S., Grasmueck, M., Eberli, G.P., Reed, J.K., Verwer, K., Purkis, S.A.M., 2012b. Variability of cold-water coral mounds in a high sediment input and tidal current regime, Straits of Florida. Sedimentology 59, 1278-1304.

Coughlan, M., Wheeler, A.J., Dorschel, B., Lordan, C., Boer, W., Gaever, P.v., Haas, H.d., Mörz, T., 2015. Record of anthropogenic impact on the Western Irish Sea mud belt. Anthropocene 9, 56-69.

Davies, A.J., Wisshak, M., Orr, J.C., Murray Roberts, J., 2008. Predicting suitable habitat for the cold-water coral Lophelia pertusa (Scleractinia). Deep Sea Research Part I: Oceanographic Research Papers 55, 1048-1062.

De Mol, B., Kozachenko, M., Wheeler, A.J., Alvares, H., Henriet, J.-P., Olu-Le Roy, K., 2007. Thérèse Mound: a case study of coral bank development in the Belgica Mound Province, Porcupine Seabight. International Journal of Earth Sciences 96, 103-120.

Dolan, M.F.J., Grehan, A.J., Guinan, J.C., Brown, C., 2008. Modelling the local distribution of cold-water corals in relation to bathymetric variables: Adding spatial context to deep-sea video data. Deep-Sea Research I 55, 1564-1579.

Dorschel, B., Hebbeln, D., Foubert, A., White, M., Wheeler, A.J., 2007a. Hydrodynamics and cold-water coral facies distribution related to recent sedimentary processes at Galway Mound west of Ireland. Marine Geology 244, 184-195.

Dorschel, B., Hebbeln, D., Rüggeberg, A., Dullo, W.-C., 2007b. Carbonate budget of a cold-water coral carbonate mound: Propeller Mound, Porcupine Seabight. International Journal of Earth Sciences 96, 73-83.

Dorschel, B., Hebbeln, D., Rüggeberg, A., Dullo, W.-C., Freiwald, A., 2005. Growth and erosion of a cold-water coral covered carbonate mound in the Northeast Atlantic during the late Pleistocene and Holocene. EPSL 233, 33-44.

Dorschel, B., Wheeler, A.J., Huvenne, V.A.I., de Haas, H., 2009a. Cold-water coral mounds in an erosive environmental setting: TOBI side-scan sonar data and ROV video footage from the northwest Porcupine Bank, NE Atlantic. Marine Geology 264, 218-229.

Dorschel, B., Wheeler, A.J., Huvenne, V.A.I., de Haas, H., 2009b. Cold-water coral mounds in an erosive environmental setting: TOBI side-scan sonar data and ROV video footage from the northwest Porcupine Bank, NE Atlantic. Mar. Geol. 264, 218-229.

Douarin, M., Sinclair, D.J., Elliot, M., Henry, L.-A., Long, D., Mitchison, F., Roberts, J.M., 2013. Changes in fossil assemblage in sediment cores from Mingulay Reef Complex (NE Atlantic): Implications for coral reef build-up. Deep Sea Research Part II: Topical Studies in Oceanography.

Dullo, C., Flögel, S., Rüggeberg, A., 2008. Cold-water coral growth in relation to the hydrography of the Celtic and Nordic European continental margin. Marine Ecology Progress Series 371, 165-176.

Eisele, M., Hebbeln, D., Wienberg, C., 2008. Growth history of a cold-water coral covered carbonate mound - Galway Mound, Porcupine Seabight, NE-Atlantic. Mar. Geol. 253, 160-169.

Ferrer, J., Elibol, A., Delaunoy, O., Gracias, N., Garcia, R., 2007. Large-area photo-mosaics using global alignment and navigation data, MTS/IEEE OCEANS Conference, Vancouver, Canada, pp. 1-9.

Foubert, A.T.G., Beck, T., Wheeler, A.J., Opderbecke, J., Grehan, A., Klages, M., Thiede, J., Henriet, J.-P., Polarstern ARK-XIX/3a shipboard party, 2005. New view of the Belgica Mounds, Porcupine Seabight, NE Atlantic: preliminary results from the Polarstern ARK-XIX/3a ROV cruise, in: Freiwald, A., Roberts, J.M. (Eds.), Deep-water corals and Ecosystems, . Springer-Verlag, Berlin Heidelberg, pp. 403-415.

Foubert, A.T.G., Huvenne, V.A.I., Wheeler, A.J., Kozachenko, M., Opderbecke, J., Henriet, J.-P., 2011. The Moira Mounds, small cold-water coral mounds in the Porcupine Seabight, NE Atlantic: Part B - Evaluating the impact of sediment dynamics through high-resolution ROV-borne bathymetric mapping Mar. Geol.

Freiwald, A., 2003. Reef-Forming Cold-Water Corals, in: Wefer, G., Billett, D., Hebbeln, D., Jørgensen, B.B., Schlüter, M., van Weering, T.C.E. (Eds.), Ocean Margin Systems. Springer Berlin Heidelberg, Berlin, Heidelberg, pp. 365-385.

Freiwald, A., Fosså, J.H., Grehan, A., Koslow, T., Roberts, J.M., 2004. Cold-water coral reefs. UNEP-WCMC, Cambridge, UK 84.

Getis, A., Ord, J.K., 1992. The Analysis of Spatial Association by Use of Distance Statistics. Geographical Analysis 24, 189-206.

Goodchild, M., 1986. Spatial Autocorrelation. Concepts and Techniques in Modern Geography 47. Norwich, UK: Geo Books.

Henriet, J.-P., De Mol, B., Pillen, S., Vanneste, M., Van Rooij, D., Versteeg, W., Croker, P.F., Shannon, P.M., Unnithan, V., Bouriak, S., Chachkine, P., BELGICA 97 Shipboard scientific crew, 1998. Gas hydrate crystals may help build reefs. Nature 391, 648-649.

Hovland, M., Mortensen, P.B., Brattegard, T., Strass, P., Rokoengen, K., 1998. Ahermatypic coral banks off mid-Norway: Evidence for a link with seepage of light hydrocarbons. Palaios 13, 189-200.

Hovland, M., Thomsen, E., 1997. Cold-water corals - are they hydrocarbon seep related? Mar. Geol. 137, 159-164.

Huang, Z., Brooke, B.P., Harris, P.T., 2011. A new approach to mapping marine benthic habitats using physical environmental data. Continental Shelf Research 31, S4-S16.

Huvenne, V.A.I., Beyer, A., de Haas, H., Dekindt, K., Henriet, J.-P., Kozachenko, M., Olu-Le Roy, K., Wheeler, A.J., participants, T.P.c., participants, C.c., 2005. The seabed appearance of different coral bank provinces in the Porcupine Seabight, NE Atlantic: results from sidescan sonar and ROV seabed mapping, in: Freiwald, A., Roberts, J.M. (Eds.), Cold-water Corals and Ecosystems. Springer-Verlag, Berlin Heidelberg, pp. 535-569.

Huvenne, V.A.I., Blondel, P., Henriet, J.-P., 2002. Textural analyses of sidescan sonar imagery from two mound provinces in the Porcupine Seabight. Mar. Geol. 189, 323-341.

Huvenne, V.A.I., Tyler, P.A., Masson, D.G., Fisher, E.H., Hauton, C., Hühnerbach, V., Le Bas, T.P., Wolff, G.A., 2011. A Picture on the Wall: Innovative Mapping Reveals Cold-Water Coral Refuge in Submarine Canyon. PLoS ONE 6, e28755.

Huvenne, V.A.I., Van Rooij, D., De Mol, B., Thierens, M., O'Donnell, R., Foubert, A.T.G., 2009. Sediment dynamics and palaeo-environmental context at key stages in the Challenger cold-water coral mound formation: Clues from sediment deposits at the mound base. Deep Sea Res. Part I 56, 2263-2280.

Kano, A., Ferdelman, T.G., Williams, T., Henriet, J.-P., Ishikawa, T., Kawagoe, N., Takashima, C., Kakizaki, Y., Abe, K., Sakai, S., Browning, E.L., Li, X., Andres, M.S., Bjerager, M., Cragg, B.A., De Mol, B., Dorschel, B., Foubert, A.T.G., Frank, T.D., Fuwa, Y., Gaillot, P., Gharib, J.J., Gregg, J.M., Huvenne, V.A.I., Léonide, P., Mangelsdorf, K., Monteys, X., Novosel, I., O'Donnell, R., Rüggeberg, A., Samarkin, V.A., Sasaki, K., Spivack, A.J., Tanaka, A., Titschack, J., van Rooij, D., Wheeler, A.J., 2007. Age constraints on the origin and growth history of a deep-water coral mound in the northeast Atlantic drilled during Integrated Ocean Drilling Program Expedition 307. Geology 35, 1051-1054.

Kocak, D.M., Caimi, F.M., 2005. The Current Art of Underwater Imaging – With a Glimpse of the Past and Vision of the Future. Marine Technology Society Journal 39, 5-26.

Kozachenko, M., 2005. Present and Past Environments of the Belgica Mounds (deep-water coral carbonate mounds) Eastern Porcupine Seabight, North East Atlantic (unpublished PhD Thesis), Department of Geography and Geology. University College Cork, Cork, p. 221.

Kwatra, V., Schödl, A., Essa, I., Turk, G., Bobick, A., 2003. Graphcut textures: image and video synthesis using graph cuts, ACM Transactions on Graphics (ToG). ACM, pp. 277-286.

Lamarche, G., Lurton, X., Verdier, A.-L., Augustin, J.-M., 2011. Quantitative characterisation of seafloor substrate and bedforms using advanced processing of multibeam backscatter—Application to Cook Strait, New Zealand. Continental Shelf Research 31, S93-S109.

Lim, A., Wheeler, A.J., Huvenne, V.A.I., Vertino, A., de Haas, H., Spezzaferri, S., *submitted*. Hydrodynamic and Sedimentological Influences on Cold-Water Coral Reef Development: The Moira Mounds, Porcupine Seabight, Irish-Atlantic margin. Mar. Geol.

Lirman, D., Gracias, N.R., Gintert, B.E., Gleason, A.C.R., Reid, R.P., Negahdaripour, S., Kramer, P., 2007. Development and application of a video-mosaic survey technology to document the status of coral reef communities. Environmental Monitoring and Assessment 125, 59-73.

Lowe, D.G., 1999. Object recognition from local scale-invariant features, Computer vision, 1999. The proceedings of the seventh IEEE international conference on. Ieee, pp. 1150-1157.

Messing, C.G., Neumann, A.C., Lang, J.C., 1990. Biozonation of deep-water lithoherms and associated hardgrounds in the northeastern Straits of Florida. Palaios 5, 15-33.

Mienis, F., de Stigter, H.C., de Haas, H., van Weering, T.C.E., 2009. Near-bed particle deposition and resuspension in a cold-water coral mound area at the Southwest Rockall Trough margin, NE Atlantic. Deep Sea Research Part I: Oceanographic Research Papers 56, 1026-1038.

Murphy, P., Wheeler, A.J., in press. A GIS-based application of drainage basin analysis and geomorphometry in the submarine environment: The Gollum Canyon System, North-east Atlantic, in: Bartlett, D., Celliers, L. (Eds.), Geoinformatics for Marine and Coastal Management. CRC Press, Taylor & Francis Group, Boca Raton, USA.

Ord, J.K., Getis, A., 1995. Local Spatial Autocorrelation Statistics: Distributional Issues and an Application. Geographical Analysis 27, 286-306.

Orejas, C., Gori, A., Rad-Menéndez, C., Last, K.S., Davies, A.J., Beveridge, C.M., Sadd, D., Kiriakoulakis, K., Witte, U., Roberts, J.M., 2016. The effect of flow speed and food size on the capture efficiency and feeding behaviour of the cold-water coral Lophelia pertusa. Journal of Experimental Marine Biology and Ecology 481, 34-40.

Pirlet, H., Colin, C., Thierens, M., Latruwe, K., Van Rooij, D., Foubert, A., Frank, N., Blamart, D., Huvenne, V.A., Swennen, R., 2011. The importance of the terrigenous fraction within a cold-water coral mound: A case study. Mar. Geol. 282, 13-25.

Purser, A., Larsson, A.I., Thomsen, L., van Oevelen, D., 2010. The influence of flow velocity and food concentration on *Lophelia pertusa* (Scleractinia) zooplankton capture rates. Journal of Experimental Marine Biology and Ecology 395, 55-62.

Reading, H., 1996. Sedimentary environments and facies. Blackwells Scientific. Oxford.

Roberts, J.M., Wheeler, A., Freiwald, A., Cairns, S., 2009. Cold-Water Corals: The Biology and Geology of Deep-Sea Coral Habitats. Cambridge University Press.

Roberts, J.M., Wheeler, A.J., Freiwald, A., 2006a. Reefs of the Deep: The Biology and Geology of Cold-Water Coral Ecosystems. Science 312, 543-547.

Rzhanov, Y., Linnett, L.M., Forbes, R., 2000. Underwater video mosaicing for seabed mapping, Image Processing, 2000. Proceedings. 2000 International Conference on, pp. 224-227 vol.221.

Savini, A., Vertino, A., Marchese, F., Beuck, L., Freiwald, A., 2014. Mapping Cold-Water Coral Habitats at Different Scales within the Northern Ionian Sea (Central Mediterranean): An Assessment of Coral Coverage and Associated Vulnerability. PLoS ONE 9, e87108.

Spezzaferri, S., Vertino, A., Addamo, A.M., Backers, J., Baratti, V., Constandache, M., Camozzi, O., El Kateb, A., Gennari, G., Leuzinger, L., McGrath, M., Mc Hugh, S.K., Naudts, L., Savini, A., Stalder, C., 2012. E-CWC Moira (2012/16) *RV Belgica*: Cold-water coral ecosystems from the Moira Mounds (NE Atlantic): affinities and differences with modern and Pleistocene Mediterranean counterparts. University Freibourg, Switzerland, Unpublished Cruise Report.

Squires, D.F., 1964. Fossil coral thickets in Wairarapa, New Zealand. Journal Paleontol. 38, 904-915.

Thierens, M., Titschack, J., Dorschel, B., Huvenne, V.A.I., Wheeler, A.J., Stuut, J.-B.W., O'Donnell, R., 2010. The 2.6 Ma depositional sequence from the Challenger cold-water coral carbonate mound (IODP Exp. 307): sediment contributors and hydrodynamic palaeo-environments. Mar. Geol. 271, 260-277.

Titschack, J., Thierens, M., Dorschel, B., Schulbert, C., Freiwald, A., Kano, A., Takashima, C., Kawagoe, N., Li, X., 2009. Carbonate budget of a cold-water coral mound (Challenger Mound, IODP Exp. 307). Mar. Geol. 259, 36-46.

Van Rooij, D., 2004. An integrated study of Quaternary sedimentary processes on the eastern slope of the Porcupine Seabight, SW of Ireland. Ghent University.

Vertino, A., Savini, A., Rosso, A., Di Geronimo, I., Mastrototaro, F., Sanfilippo, R., Gay, G., Etiope, G., 2010a. Benthic habitat characterization and distribution from two representative sites of the deep-water SML Coral Province (Mediterranean). Deep-Sea Research II 57, 380-396.

Vertino, A., Savini, A., Rosso, A., Di Geronimo, I., Mastrototaro, F., Sanfilippo, R., Gay, G., Etiope, G., 2010b. Benthic habitat characterization and distribution from two representative sites of the deep-water SML Coral Province (Mediterranean). Deep Sea Research Part II: Topical Studies in Oceanography 57, 380-396.

Vertino, A., Spezzaferri, S., Ruggeberg, A., Stalder, C., Wheeler, A.J., Party, t.E.C.-M.c.S., 2015. An Overview on Cold-Water Coral Ecosystems and Facies, in: Spezzaferri, S., Ruggeberg, A., Stalder, C. (Eds.), Atlas of benthic foraminifera from cold-water coral reefs. Cushman Foundation for Foraminiferal Research, pp. 12-19.

Wheeler, A.J., Beyer, A., Freiwald, A., de Haas, H., Huvenne, V.A.I., Kozachenko, M., Olu-Le Roy, K., Opderbecke, J., 2007. Morphology and environment of cold-water coral carbonate mounds on the NW European margin. Int J Earth Sci (Geol Rundsch) 96, 37-56.

Wheeler, A.J., Capocci, R., Crippa, L., Connolly, N., Hogan, R., Lim, A., McCarthy, E., McGonigle, C., O' Donnell, E., O' Sullivan, K., Power, K., Ryan, G., Vertino, A., Holland 1 ROV Technical Team, Officers and Crew of the RV Celtic Explorer, 2015. Cruise Report: Quantifying Environmental Controls on Cold-Water Coral Reef Growth (QuERCi). University College Cork, Ireland.

Wheeler, A.J., Kozachenko, M., Beyer, A., Foubert, A.T.G., Huvenne, V.A.I., Klages, M., Masson, D.G., Olu-Le Roy, K., Thiede, J., 2005. Sedimentary processes and carbonate mounds in the Belgica Mound province, Porcupine Seabight, NE Atlantic, in: Freiwald, A., Roberts, J.M. (Eds.), Cold-water Corals and Ecosystems. Springer-Verlag, Berlin Heidelberg, pp. 533-564.

Wheeler, A.J., Kozachenko, M., Henry, L.-A., Foubert, A.T.G., de Haas, H., Huvenne, V.A.I., Masson, D.G., Olu-Le Roy, K., 2011. The Moira Mounds, small cold-water coral banks in the Porcupine Seabight, NE Atlantic: Part A—an early stage growth phase for future coral carbonate mounds? Mar. Geol. 282, 53-64.

Wheeler, A.J., Kozachenko, M., Masson, D.G., Huvenne, V.A.I., 2008. Influence of benthic sediment transport on cold-water coral bank morphology and growth: the example of the Darwin Mounds, north-east Atlantic. Sedimentology 55, 1875-1887.

Wheeler, A.J., shipboard party, 2011. Vents & Reefs deep-sea ecosystem study of the 45˚ North MAR hydrothermal vent field and the cold-water coral Moira Mounds, Porcupine Seabight, Cruise report, p. 160.

White, M., Dorschel, B., 2010. The importance of the permanent thermocline to the cold water coral carbonate mound distribution in the NE Atlantic. Earth and Planetary Science Letters 296, 395-402.

Wilson, J.B., 1979. "Patch" development of the deep-water coral *Lophelia pertusa* (L.) on the Rockall bank. Journal of the Marine Biological Association of the United Kingdom 59, 165-177.

4 Determining seabed video-survey density and data temporal validity (shelf life) for best practice cold-water coral reef characterisation

(Current status: submitted, Deep Sea Research I)

Aaron Lim[1)], Adam Kane [1)], Aurélien Arnaubec [2)] and Andrew J. Wheeler [1), 3)]*

This chapter assesses the effectiveness of video surveying techniques and survey design through a thorough investigation of the facies observed on the surface of the Piddington Mound. This builds on the findings from the reef- (chapter 3) and reef-chain-scale (chapter 2) aspects of the research thus far. Many studies on cold water coral reefs and mounds (e.g. Correa et al., 2012; Vertino et al., 2010) compare and contrast their findings to other studies from these dynamic habitats. However, many of these studies use different camera angles and survey designs which has the potential to skew results and essentially make them incomparable. The aim of this chapter is to assess different survey designs on the Piddington Mound where the exact proportion of surface facies are known and make a series of recommendations on the practice of video and image surveying these seabed features. We apply the developed technique to the Piddington Mound on a dataset collected 4 years later to determine both the temporal variability of the mound and the comparability of imagery acquired at various temporal intervals.

Various authors have contributed to this chapter. This project was funded through an award to Prof. Andy Wheeler. Prof. Wheeler was chief scientist on all cruises that collected this data set. He supervised all research carried out and gave useful feedback on drafts. Dr. Aurélien Arnaubec generated the video mosaic utilised in this chapter with help from Aaron Lim and wrote parts of the video-mosaiking methodology. Dr. Adam Kane provided statistical advice on estimating sample sizes for multinomial population proportions and wrote the statistics methodology section. Aaron Lim carried out the classification of the video mosaic, the random sample classification of the mosaic and the classification of the repeat video coverage. He came up with the idea and methodology behind the research and applied to all video data. He wrote the paper, created the figures and maps. He created all survey designs and their spatial analysis within a GIS. All concepts and ideas developed from the data was by Aaron Lim.

[1)] *School of Biological, Earth and Environmental Sciences, University College Cork, Distillery Fields, North Mall, Cork, Ireland*

[2)]*Unité Systèmes sous-Marins, Centre de Méditerranée, Ifremer, Zone Portuaire de Brégaillon, CS 20330, 83507 La Seyne/Mer Cedex, France*

[3)] *Irish Centre for Research in Applied Geosciences, University College Cork, Ireland*

*Corresponding author: aaron.lim@ucc.ie

Keywords: cold water coral reef, survey design, video, sample size, sediments, GIS, habitat mapping

Abstract

Cold-water coral habitats are regarded as hotspots of biodiversity in the deep-sea although monitoring the effects of climate change, anthropogenic impact and natural variability through video-surveying in these habitats are still poorly-established. This study is the first attempt at standardising cost-effective video-survey campaign design specific to cold-water coral reefs in order to accurately determine the proportion of surface facies across an entire reef. The Piddington Mound of the Moira Mounds, Porcupine Seabight, offshore Ireland has been entirely imaged by downward-facing video in 2011 and 2015. The 2011 video data is navigated into a full-reef, georeferenced video mosaic. A quadrat-based supervised classification of this video mosaic at 0.25 m^2 resolution shows the exact

proportion of facies across the mound surface. The minimum number of randomly located images from the reef are determined to accurately characterise reef surface heterogeneity. This minimum sample size is used to test the effectiveness of various common survey designs for video-based reef investigations. Single-pass video lines are not representative of the mound surface whilst gridded survey designs yield best results similar to 100% reef coverage. The minimum sample size and supervised classification is applied to the 2015 video mosaicked data to show a 19% mound surface facies change over 4 years at 0.25 m^2 resolution. The proportion of coral, being sessile, slow-growing organisms, show little change where mobile and exposed substrates show most change. This defines a temporal decrease in survey data validity and implies that in 20 years, the mound surface will have almost entirely changed and video-survey “shelf life” has expired with the data obsolete.

4.1 Introduction

Cold-water corals (CWC) are sessile, filter-feeding organisms found in many parts of the world’s oceans, being common and well-studied in the NE Atlantic (Roberts et al., 2003; Roberts et al., 2006b). Also referred to as “deep-water” corals, their distribution actually covers a large depth range being found from 39 m to 2000 m water depth (Roberts et al., 2009b). As their name suggests, they typically exist in cooler waters from 4°C to 13°C (Freiwald, 2002) with the exception of *Oculina* spp., and within a salinity range of 31.7 ‰ - 38.8 ‰ (Davies et al., 2008b). *Lophelia pertusa* is the most well-studied framework-forming CWC and is reliant on currents for food supply (Orejas et al., 2016; Purser et al., 2010a) and can form carbonate mounds that benefit from its abilities to baffle currents and thereby enhance sedimentation (Wheeler et al., 2005c; Wheeler et al., 2008a). The complex hydrodynamic relationship between the CWC framework, food supply, currents and sedimentation often results in the generation of positive bathymetric features on the seabed called CWC biogenic reefs, also referred to as mounds or banks (De Mol et al., 2007b; Dorschel, 2003; Squires, 1964b; Wilson, 1979a). Elegantly described by Roberts et al. (2009b), a cold water coral carbonate mound can be formed through successive periods of CWC reef development, and can generate bathymetric features up to 350 m from base to summit (Henriet et al., 2014 and references therein).

The number of publications on the subject of CWC's has risen dramatically over the past 15 years, with 678 articles published between 2001 (n=5) and 2016 (n=64) (https://www.scopus.com). This has been attributed to the realisation of the true geographic extent of CWCs and their significance as speciose habitats. Furthermore, advances in marine survey technologies and techniques has fostered research opportunities (Roberts et al., 2009b). For example, marine remotely-sensed mapping of CWC habitats is becoming progressively more common through the use of side scan sonar (SSS) and multibeam echosounders (MBES). Huvenne et al. (2005a) examine the influence of currents and sediment dynamics on the growth of coral and mound development at a mound province scale whereas Dorschel et al. (2009a) provide an environmental context to cold-water coral carbonate mound development, both using regional SSS mapping (TOBI 30 kHz SSS). MBES has also proven an integral part of marine habitat mapping for CWC habitats using hull-mounted (Beyer et al., 2003b), ROV-mounted (Dolan et al., 2008), AUV-mounted (Correa et al., 2012a) and forward-facing MBES systems (Huvenne et al., 2011).

With recent advances in more accurate underwater positioning for deployed marine sampling/surveying equipment (Chitre et al., 2008; Kinsey et al., 2006), ground-truthing of marine remotely sensed mapping coverages is now possible with the effective positioning of still camera and video (ROV and drop frame). ROV video has proven useful in both covering large areas (Guinan et al., 2009; Huvenne et al., 2005a) and providing baseline studies (Vertino et al., 2010a) within CWC habitats.

Temporal variability across CWC habitats has been studied at various scales. Lavaleye et al. (2009) utilize long time-series datasets to understand CWC habitat functioning and its effect on the organic biochemistry of the reef-influencing water column. While anthropogenic impact (trawling activities and drill cutting) at CWC habitats have driven some temporal variability research, these studies reveal information about mound surface change over time and different approaches to effective video inspection at 1, 4 or 10 year timescales (Huvenne et al., 2016; Lundälv et al., 2008; Purser, 2015).

It is now common place to map (bathymetry and backscatter), physically sample (coring and grabs) and image (ROV video) CWC habitats for research purposes. Different combinations of these data types at differing resolutions in different geographic settings, and quite often with a temporal gap between sampling, are utilised to make parallels and contrasts between these habitats. Although not ideal, this is often done due to the financial and time-consuming nature of deep-water data acquisition under weather- and sea state-dependant conditions. However, a common finding of this research is the heterogeneity of these habitats (Vertino et al., 2010a; Wienberg et al., 2009) stressing the need for local-scale studies (Dolan et al., 2008) with a robust sampling density. In light of this, our aim is to identify the minimum amount of imagery needed to accurately characterise heterogeneous

CWC reefs and assess how to best collect this imagery in a representative manner. Furthermore, repeat mapping in high energy seabed environments such as CWC habitats shows that they can be highly-dynamic e.g. where sediment waves occur (Van Landeghem et al., 2012). Cold-water coral reefs exist in dynamic environments but how rapidly do reefs change? Growth rates of corals give us a clue but how does that translate into changing areas of coral colonisation? This study therefore also assesses relative temporal change in a reef facies and their proportions and uses this data to assess the temporal validity or "shelf life" of survey data.

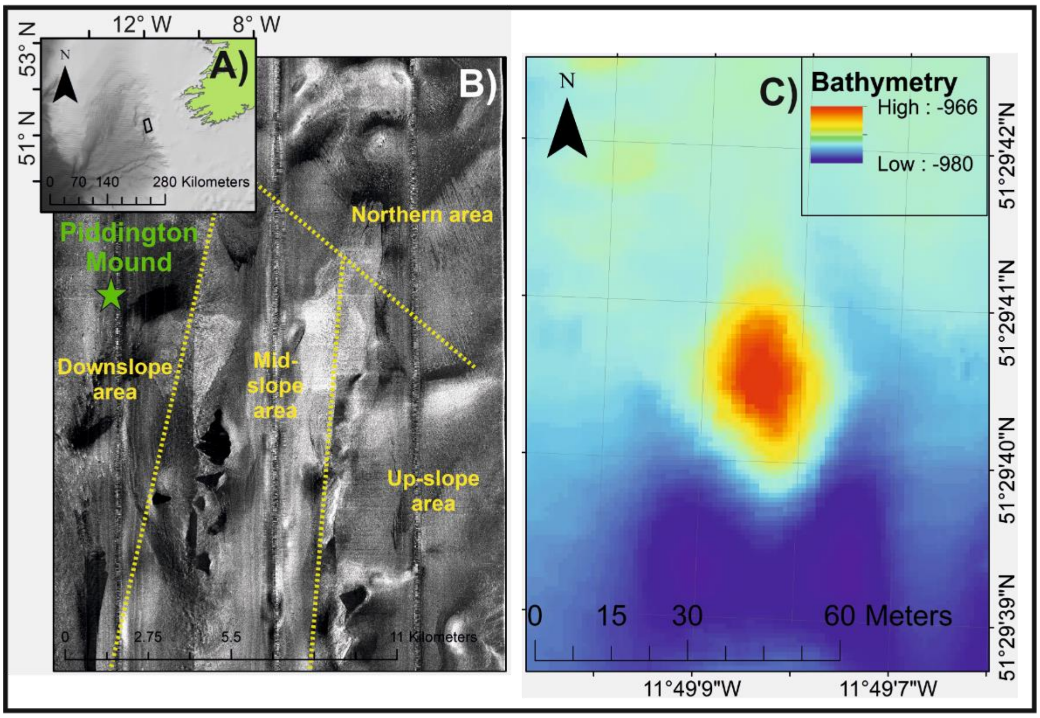

Figure 22 Location map of study area

A) Location of Belgica Mound Province (BMP) Special Area of Conservation (SAC) (black box), offshore SW Ireland; B) 30kHz TOBI side scan sonar imagery of the BMP SAC with areas defined by Wheeler et al., (2011) in yellow and location of Piddington Mound indicated by green star; C) Piddington Mound bathymetry.

4.2 Study Site

The Piddington Mound, a CWC reef in the Belgica Mound Province (BMP), has been selected for this study due to the existence of high-resolution imagery with good, sufficient spatial reef coverage as presented in Lim *et al*. (in review). The BMP is located on the eastern slope of the Porcupine Seabight, NE Atlantic (Figure 22). Previously designated as a Special Area of Conservation (SAC) under the EU Habitats Directive, the BMP hosts 2 chains of contour-parallel giant CWC carbonate mounds ranging in height from 50 m to 100 m and having a slight elongate to conical morphology (Wheeler et al., 2005c). A salinity maximum from 600 m to 1000 m water depth marks the depth range of the Mediterranean Outflow Water (MOW), the main mound-influencing water mass in the BMP (Dullo et al., 2008b; White, 2007).

Between and around these chains of giant CWC carbonate mounds, are approximately 250 CWC reefs, referred to as the "Moira Mounds" (Wheeler et al., 2011c) of which the Piddington Mound is an example. They are small (~10 m tall) with an ovoid to elongate morphology. It is speculated that they are Holocene in age (Huvenne et al., 2005a; Kozachenko, 2005a). They exist in various different settings: at the head of sediment wave trains, within a blind channel, around barchan sediment waves or on gravel ridges and occur as isolated or, more commonly, clustered examples (Lim et al., *submitted;* Wheeler et al., 2005b). They can be divided into 4 different areas based on their geographic distribution: the upslope area, the northern area, the downslope area and the midslope area. The Moira Mound CWC reefs within the downslope area, where the Piddington Mound resides, are concentrated within part of the Arwen Channel (Murphy and Wheeler, 2017; Van Rooij, 2004a). This area has been described as favourable for CWC reef development with current speeds of approximately 40 cm s^{-1} (Lim, 2017). The surrounding seabed is dominated by dropstones while the Piddington Mound itself is actively trapping sands and is dominated by *Lophelia pertusa* and *Madrepora oculata*. Lim et al. (in review) show that the mound has 4 distinct facies occurring in a ring-like distribution around the mound summit.

4.3 Materials and Methods

4.3.1 Video data

Two ROV video datasets were collected for this research. The first video dataset (referred to from here on as "T1") was collected during the *VENTuRE survey* (2011) on board *RV Celtic Explorer* with the *Holland 1 ROV* (cruise number CE11009: Wheeler and shipboard party, 2011). The second video dataset (referred to from here on as "T4") was collected during the *QuERCi survey* (2015) on board *RV Celtic Explorer* with the *Holland 1 ROV* (cruise number CE15009: Wheeler and shipboard party, 2015). Both research cruises collected video data over the Piddington Mound using a downward-facing HD camera mounted on the bottom of the ROV. Positioning and navigation for the ROV during dives were achieved using a Sonardyne Ranger 2 USBL (ultra-short baseline positioning system) corrected by RDI Workhouse doppler velocity logger. The ROV altimeter recorded and logged the height of the ROV (and therefore camera) above the seabed. The ROV recorded downward-facing HD video during a series of transects covering the entire surface of the Piddington Mound. To maintain a clear image of the mound surface, the ROV was flown <2 m above the mound surface at a survey speed of <2 knots. Several lights were attached to the ROV to achieve homogenous lighting across the camera field of view.

The T1 ROV video dataset was converted into a video mosaic (Lim et al., in review) using the IFREMER in-house software *Matisse* where the images were extracted at a rate of 1 per second. Poor quality video data (from imagery flown at over 2 m above the seabed, or collected in poor water quality or with poor navigation) were excluded from the image extraction process. To lower ROV trajectory noise, all the USBL navigation data were filtered using a sliding median filtering and 2nd order polynomial model fit. The extracted images and filtered navigation were then synced so each image had an approximate position, which is later refined by the mosaicking process. At this point, features in the extracted images are both detected and matched using a SIFT (Scale Invariant Feature Transform) Algorithm (Lowe, 1999). Image matching and USBL navigation are merged to give an accurate global position, correct scaling and sufficient local overlapping through a cost function minimisation. This method is similar to Ferrer et al. (2007) except cost function weights are affected according to image and navigation data standard deviations so re-projection errors are minimized in the mosaicking plane rather than the image plane. After the image positions are refined, the mosaic can be drawn incorporating seaming and blending techniques developed by Burt and Adelson (1983) and Kwatra et al. (2003). The resulting video mosaic is shown in Figure 14 (page 99).

The georeferenced T1 video mosaic was imported to ArcMap where a fishnet made up of 0.25 m^2 cells is overlaid on the Piddington Mound mosaic. A supervised classification was carried out on the mosaic using the following classifiers: “sediment and dropstones”, “biogenic hash”, “sorted sediment”, “dead coral framework” and “live coral framework” (see Figure 14, page 99 for examples).

Details of this classification can be found in Lim et al. (in review) and is summarised here in Table 7. The classified fishnet is saved as a shapefile and plotted in ArcMap (Figure 23).

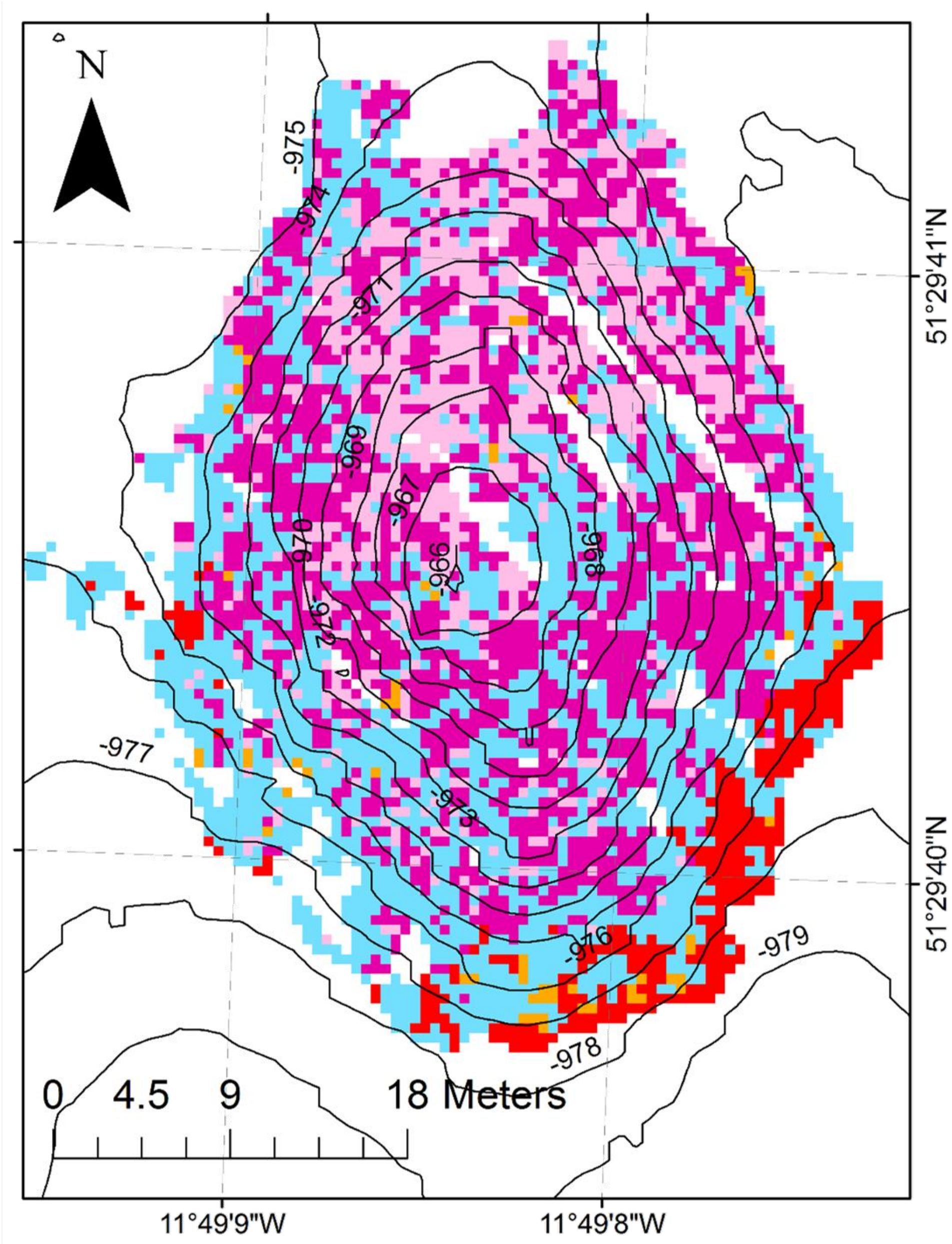

Figure 23 Classified mosaic

Blue=biogenic hash cells; red=sediment and dropstone cells; orange=sorted sediment cells; magenta=dead coral framework cells; and pink=live coral framework cells. Black lines represent 1 m contours.

Class	Description	Typical Environment
Sorted sediment	cell dominated (>90 % cell coverage) by hemipelagic sediment i.e. sand or mud with no recognisable bioclasts or dropstones	no dropstones nor deposition of biogenic material. Potentially deposition of a sorted sediment under the influence of benthic currents.
Biogenic hash	cell dominated (>50 % cell coverage) by recognisable biogenic material (i.e. coral rubble, shell fragments) and sediment	deposition of mound-derived material
Sediment with dropstones	cell dominated (>50 % cell coverage) by dropstones and sediment (sand or mud)	erosion, non-deposition or non-coral growth since the deposition of the dropstones
Dead coral framework	cell dominated (>50 % cell coverage) by coral framework which has no identifiable living parts	coral no longer grows
Live coral framework	cell dominated (>50 % cell coverage) by coral framework with identifiable living parts	coral growth

Table 7 Facies description

4.3.2 Image sampling analysis

To determine the minimum amount of still imagery needed from the Piddington Mound to accurately characterise the diversity of surface facies present, sample size estimation (specific to multinomial proportions) was carried out according to Thompson (1987). While other sample size estimation techniques exist (e.g. Angers, 1974), this particular technique is chosen for its robustness and accuracy even in worst case scenarios i.e. when the population proportions are all equal. The classified cells from the Piddington Mound describe a multinomial distribution with 6 different classes: “sediment and dropstones”, “biogenic hash”, “sorted sediment”, “dead coral framework”, “live coral framework” and “no data” (part of the mosaic where data quality was too low to mosaic). With this method, we specify the width of the confidence intervals by selecting an alpha level (α) and then choose a margin of error (d) for the confidence intervals. This allows us to govern the probability that population proportions of the whole reef are covered by the confidence intervals. Thompson (1987) provide a table that showing the minimum sample size required once these values are chosen (see Table 8). For this study, a confidence interval of 95% is chosen (i.e. α of 0.05) with a margin of error (d) of 0.05 allowing a sample size, *X* (n if d=0.05), to be determined (see Table 8). Note, both smaller values of α and smaller margins of error (d) would require larger sample sizes (*X*) and this method does not take into account spatial autocorrelation. This does not appear to be an issue as all results occur within the 95% confidence interval regardless.

alpha (α)	(d^2 * n)	m	*X* = (n if d = 0.05)
0.5	0.44129	4	177
0.4	0.50729	4	203
0.3	0.60123	3	241
0.2	0.74739	3	299
0.1	1.00635	3	403
0.05	1.27359	3	510
0.025	1.55963	2	624
0.02	1.65872	2	664
0.01	1.96986	2	788
0.005	2.28514	2	915
0.001	3.02892	2	1212
0.0005	3.3353	2	1342
0.0001	4.11209	2	1645

Table 8 Minimum sample size estimation table after Thompson (1987)

Alpha values (α) represents the significance level which can be used to calculate the confidence level (e.g. an alpha of 0.05 gives a confidence level of 95%), d is the margin of error, n is the sample size, m is the minimum number of categories required (see Thompson (1987) for further details on m), X is sample size.

To determine the best method for collecting images of the mound surface to most effectively capture mound heterogeneity, a series of potential survey designs were designed for the Piddington Mound in ArcMap and saved as *.shp files (Figure 24). These are used as a guide for a hypothetical drop camera system or ROV to acquire downward-facing stills or live video from which stills can be extracted. The survey designs include the following: a) SD1 - random points (to represent full-reef video mosaic coverage); b) SD2 - south to north transect; c) SD3 - east to west transect; d) SD4 - northwest-southeast diagonal transect; e) SD5 - horizontal grid; f) SD6 - spiral (circling from the mound base to the mound summit) and; g) SD7 - actual survey example (taken from ROV reconnaissance dive navigation over the Piddington Mound). Using the create random points tool in ArcMap, *X* number of random points were generated across the surface of the Piddington Mound (SD1). This represents the scenario of having full-reef video mosaic coverage. Then, to represent each of the other scenarios, *X* number of random points were generated across the fishnet but restricted to the lines defining each survey design *.shp file (SD2 to SD7: Figure 24). The proportion of cells of each class for each survey design was calculated. The total number of 0.25 m^2 cells in the fishnet from each class were also counted and the proportion of these cells calculated. This acts as the real-life control against which results from each survey design can be compared. The results were graphed and the number of “no data” values recorded within each survey design are used to generate proportional error bars for each individual class.

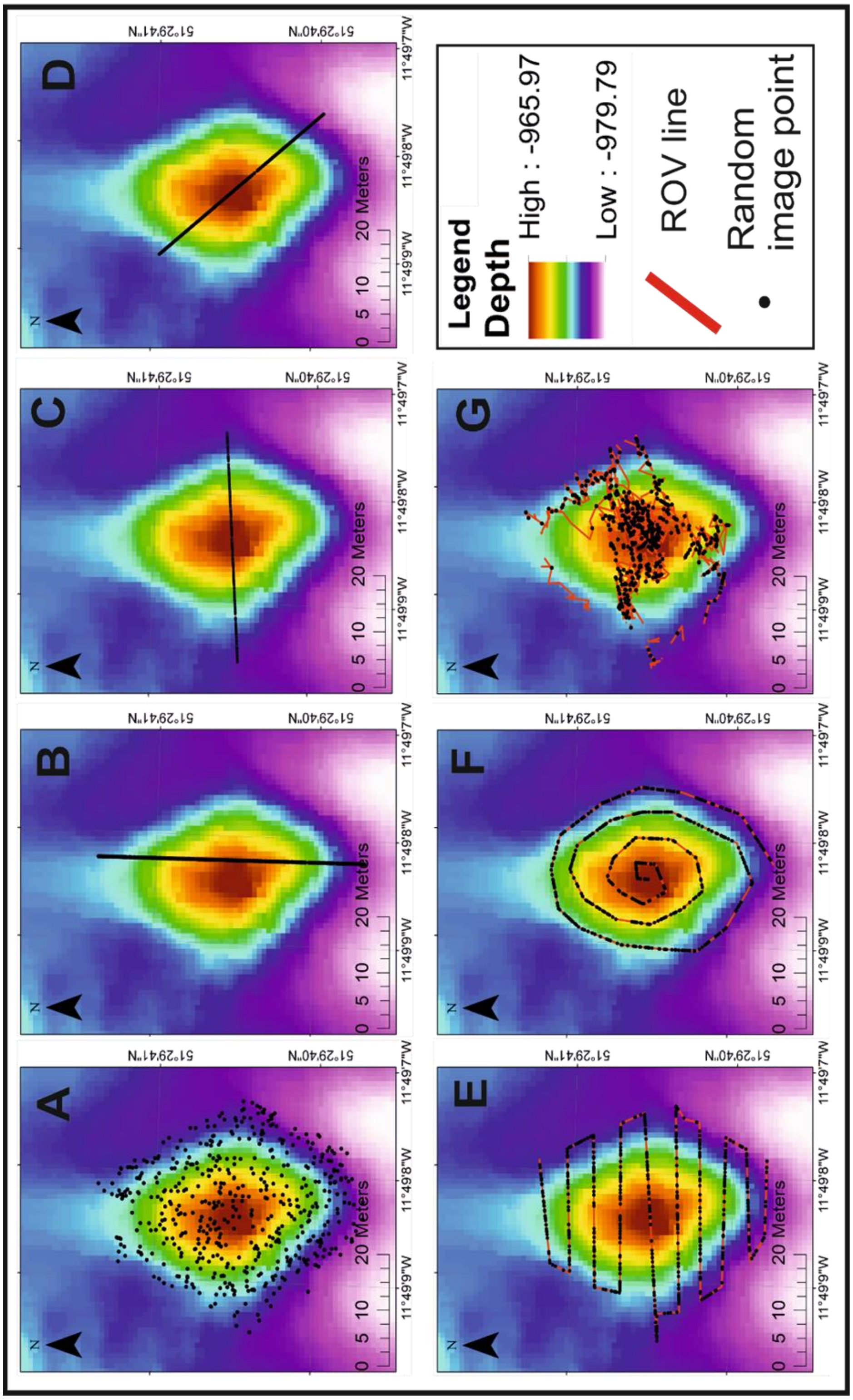

Figure 24 Video-survey designs facilitating the collection of X=510 random image points along the survey lines

A) random points (SD1), B) south-north transect (SD2), C) east-west transect (SD3), D) northwest-southeast diagonal transect (SD4), E) horizontal grid (SD5), F) spiral (SD6) and G) an actual survey transect from a reef reconnaissance dive (SD7).

4.3.3 Temporal variability analysis

A repeat survey of the Piddington Mound was undertaken four years after T1 and termed T4. The T4 survey comprises parallel north-south video lines covering the whole mound. In line with the image sampling analysis methodology, a minimum of number of images (*X*) were extracted from the T4 ROV video dataset with an equal number of images extracted from each video line to ensure a homogenous spread of images across the Piddington Mound surface. The video lines covering 100% of the reef, offer a comparison of the T1 Piddington Mound mosaic after a 4-year interval and in survey design is comparable to "SD1 - random points".

Each extracted image was manually inspected. A 25 cm^2 cell is overlaid around the area of the photo where the laser scales pointed (central field of view) and a supervised classification was applied using the same classifiers as the T1 ROV video data set: "sediment and dropstones", "biogenic hash", "sorted sediment", "dead coral framework" and "live coral framework". The total number of cells from each class are counted and their proportion determined.

4.4 Results

4.4.1 Seabed classification

Figure 23 shows the classified fishnet over the Piddington Mound. 6 classes exist: "sediment and dropstones", "biogenic hash", "sorted sediment", "dead coral framework", "live coral framework" and "no data". There are 5637 cells across the surface of Piddington Mound with the most common being "biogenic hash" (36.1 ± 2.9%) and "dead coral framework" (31.6 ± 2.5%). The least common cell-types are “sorted sediment” (1.1 ± 0.1%) and “sediment and dropstones” (6.7 ± 0.5%). The “live coral framework” cells cover 16.3 ± 1.3% of the mound surface. While the “biogenic hash” cell-type is found across the mound surface, it is typically concentrated around the mound perimeter and on the mound summit. The “live coral framework” cells occur most frequently towards the north of the mound. The “dead coral framework” can be found on the mound flanks. From here on, these proportions of observed cell-types on the Piddington Mound are referred to as the control proportion.

4.4.2 Image sampling analysis

Sample size estimation according to Thompson (1987), reveals a sample size, X (n if d=0.05), of 510 as a minimum sample size to reliably replicate, with a confidence level of 95%, the proportion of facies in the total of 5637 classified cells in the 0.25 m^2 fishnet overlay on the T1 Piddington Mound video-mosaic. The number of categories in our sample size is 6 which is greater than the required minimum of 3.

Table 9 shows the results of the image sampling analysis for each survey design. Survey design “SD1 - random points” represents maximum video coverage and thus the ability to drop 510 random points anywhere across the Piddington Mound surface. This survey design resulted in a 5.9% total difference to the control, namely of the actual proportion of all cells covering the Piddington Mound. The maximum difference in an individual class is 2.9% (“dead coral framework”) with an average class difference of 1.2%.

		No data	Sorted sediment	Biogenic Hash	Sediment with dropstones	Dead coral framework	Live coral framework	SUM
All T1 (control)	Count	455.0	64.0	2035.0	380.0	1782.0	921.0	5637.0
	%	8.1	1.1	36.1	6.7	31.6	16.3	100.0
	%±		0.1	2.9	0.5	2.6	1.3	
a) SD1 - random points	Count	41.0	6.0	192.0	39.0	147.0	85.0	510.0
	%	8.1	1.2	37.7	7.7	28.7	16.7	100.0
	%_Diff	0.0	0.0	1.6	0.9	2.9	0.4	5.9
	%±		0.1	3.0	0.6	2.3	1.3	
b) SD2 - south to north transect	Count	30.0	11.0	215.0	20.0	129.0	105.0	510.0
	%	5.9	2.2	42.0	3.9	25.3	20.6	100.0
	%_Diff	2.2	1.0	5.9	2.8	6.3	4.3	22.5
	%±		0.1	2.5	0.2	1.5	1.2	
c) SD3 - east to west transect	Count	57.0	5.0	190.0	5.0	163.0	90.0	510.0
	%	11.2	1.0	37.3	1.0	32.0	17.6	100.0
	%_Diff	3.1	0.2	1.2	5.8	0.3	1.3	11.8
	%±		0.1	4.2	0.1	3.6	2.0	
d) SD4 - northwest to southeast	Count	0.0	0.0	189.0	48.0	151.0	122.0	510.0
	%	0.0	0.0	37.1	9.4	29.6	23.9	100.0
	%_Diff	8.1	1.1	1.0	2.7	2.0	7.6	22.4
	%±		0.0	0.0	0.0	0.0	0.0	
e) SD5 - horizontal grid	Count	38.0	6.0	198.0	34.0	151.0	83.0	510.0
	%	7.5	1.2	39.0	6.7	29.3	16.3	100.0
	%_Diff	0.6	0.0	2.9	0.0	2.3	0.0	5.8
	%±		0.1	2.9	0.5	2.2	1.2	
f) SD6 - spiral	Count	54.0	3.0	168.0	19.0	182.0	84.0	510.0
	%	10.6	0.6	32.9	3.7	35.7	16.5	100.0
	%_Diff	2.5	0.5	3.2	3.0	4.1	0.1	13.4
	%±		0.1	3.5	0.4	3.8	1.7	
g) SD7 - actual survey	Count	39.0	0.0	182.0	0.0	168.0	121.0	510.0
	%	7.7	0.0	35.6	0.0	33.0	23.8	100.0
	%_Diff	0.4	1.1	0.5	6.7	1.4	7.4	17.7
	%±		0.0	2.7	0.0	2.5	1.8	

Table 9 Image sampling survey design results.

Relative class proportions determined by image sampling analysis for different survey design. The count column is the number of cells from a particular class. The % column is the percentage of that particular class. %± column is the potential error margin of this class based on the number of "no data" values (class 2). %_Diff column is the percentage that the particular class deviates from the control population. All values are rounded up to the nearest 1 decimal place.

Survey design "SD2 - south to north transect" represents 510 random image sampling points anywhere along a straight, individual ROV video line from the southern end to the northern end of the Piddington Mound. This survey design resulted in a total of 22.5% difference to that of the actual proportion of all cells covering the Piddington Mound. The maximum difference in an individual class is 6.3% ("dead coral framework") with an average class difference of 4.1%.

Survey design "SD3 - east to west transect" represents 510 random image sampling points anywhere along a straight, individual ROV video line from the eastern edge to the western edge of the Piddington Mound. This survey design resulted in a total of 11.8% difference to that of the actual proportion of all cells covering the Piddington Mound. The maximum difference in an individual class is 5.8% ("sediment and dropstones") with an average class difference of 1.7%.

Survey design "SD4 - northwest-southeast diagonal transect" represents 510 random image sampling points anywhere along a straight, individual ROV video line from the north-western edge to the south-eastern edge of the Piddington Mound. This survey design resulted in a total of 22.4% difference to that of the actual proportion of all cells covering the Piddington Mound. The maximum difference in an individual class is 7.6% ("live coral framework") with an average class difference of 2.9%.

Survey design "SD5 - horizontal grid" represents 510 random image sampling points anywhere along an east-west grid of ROV video lines covering the Piddington Mound. This survey design resulted in a total of 5.8% difference to that of the actual proportion of all cells covering the Piddington Mound. The maximum difference in an individual class is 2.9% ("biogenic hash") with an average class difference of 1.1%. It is also worth noting that there was 0% cell difference in 3 classes.

Survey design "SD6 - spiral" represents 510 random image sampling points anywhere along a spiral or conical ROV video line circling from the mound perimeter to the mound flank to the mound summit. This survey design resulted in a total of 13.4% difference to that of the actual proportion of all cells covering the Piddington Mound. The maximum difference in an individual class is 4.1% ("dead coral framework") with an average class difference of 2.2%.

Survey design "SD7 - actual survey example" represents 510 random image sampling points along an actual ROV reconnaissance dive video line over the Piddington Mound. This survey design resulted in a total of 17.7% difference to that of the actual proportion of all cells covering the Piddington Mound. The maximum difference in an individual class is 6.7% ("sediment and dropstones") with an average class difference of 3.4%.

Temporal variability analysis

Figure 25 and Table 10 show the results of the temporal variability of the Piddington Mound surface data based on a comparison to class determinations in the T1 and T4 video survey data. The minimum number of random samples needed to characterise the mound with a 0.95 probability of being within 0.05 of the class proportions is 510. Here, 622 images are used which marginally increases accuracy above 95% confidence. The most common T4 cell-types are "biogenic hash" (43.6%) and "dead coral framework" (37.3%). The "live coral framework" cell-type occurs 16.7% of the time. The least common cell types are "sorted sediment" (1%) and "sediment and dropstones" (1.4%).

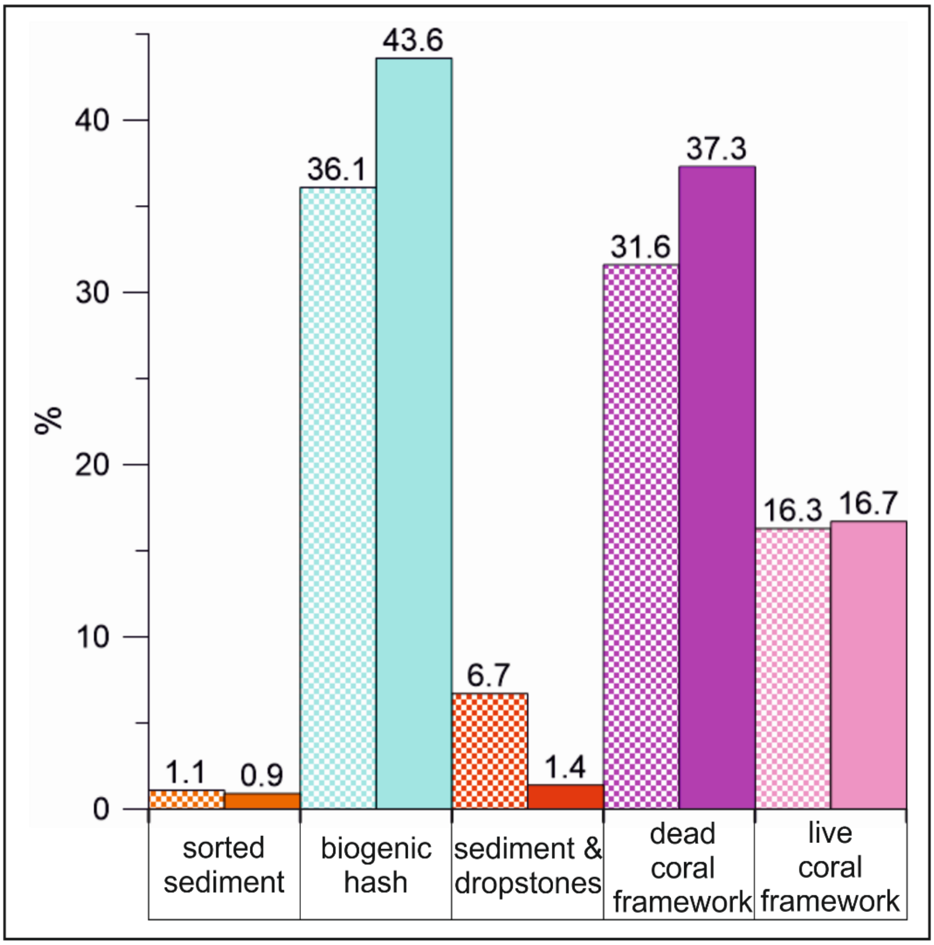

Figure 25 Temporal Variability graph.

T1 Piddington Mound cell-type proportions in checkered fill. T4 Piddington Mound cell-type proportions in solid fill.

Class	T1_%	T4_%	Δ_%
Sorted sediment	1.14	0.96	-0.18
Biogenic Hash	36.1	43.57	7.47
Sediment with dropstones	6.74	1.45	-5.29
Dead coral framework	31.61	37.3	5.69
Live coral framework	16.38	16.72	0.34

Table 10 Comparison of T1 Piddington Mound cell-type proportions (T1_%) with T4 Piddington Mound proportions (T4_%).

The Δ_% column represents the percentage change between T1 and T4. All values are rounded up to the nearest two decimal places.

4.5 Discussion

4.5.1 Seabed imagery for cold water coral reef characterisation

Numerous CWC reefs and mounds have been studied incorporating video observations from ROV-mounted camera systems in various different ways: oblique-angled, forward-facing camera (Foubert et al., 2005b), downward-facing camera (Huvenne et al., 2016), both downward-facing and oblique-angled, forward-facing cameras (Dolan et al., 2008; Guinan et al., 2009) and up to 3 cameras (Savini et al., 2014; Vertino et al., 2010a). Differences in the nature of the results from cameras at various angles have previously been highlighted with regard to local-scale studies (Lim *et al.,* in review). In this study, we focus only on downward facing cameras but question the effect of the amount of imagery used and the survey design by which it was collected which often varies from study to study. Here, the amount and survey design of seabed imagery acquisition is examined to put forward a survey-feasible methodology for characterising the surface of CWC reefs.

4.5.2 How much seabed imagery is needed to characterise the Piddington Mound?

In the deep sea, sampling and surveying opportunities are limited due to the availability, financial expense and weather-dependency of ship-time on research vessels. As a result, deep marine data collection is strictly prioritised by urgency of data needs, quite often to meet the needs of funding sources. As such, studies have used "single-pass" (individual line, typically straight) video lines across the surface of CWC reefs and mound to ground truth their surface (e.g. Foubert et al., 2005b; Huvenne et al., 2016). While this offers the opportunity to increase the geographical range of the study, it decreases the potential confidence and representativeness of the study. This leads to the question, how much imagery is actually needed to create a reliable representation of the surface of a CWC reef?

Based on the seabed classification (Figure 23), the proportion of 0.25 cm^2 cell-types on surface of the Piddington Mound are known. Assemblages of these cells represent dominant processes on various parts of the mound (Lim et al., in review; chapter 3). Our sample size estimation shows that 510 is the minimum number of 0.25 cm^2 images needed to accurately determine the proportion of identified classes on the Piddington Mound. Survey design "SD1 - random points" represents the ability to drop 510 random points anywhere on the Piddington Mound, thus utilizing the same video coverage as the T1 ROV video data set (full reef coverage). Therefore, it can be used to assess and ground-truth the accuracy of the determined sample size. A comparison of the control proportion (Table 9; all T1) with survey design “SD1 - random points” (Table 9) shows that this estimation is within 5.9% of the correct proportion of cell-types observed on the Piddington Mound, in line with the aimed probability (at least 0.95 that all estimates are within 0.05 of the multinomial proportions) of this dataset and give the most reliable representation of the reef surface of all the survey designs tested. The “SD1 - random points” survey could be accomplished by sub-sampling a video-mosaic which, perhaps not surprisingly, is the most robust approach to characterising the reef surface. However, this could alternative be accomplish by the use a yo-yo drop camera but the results suggest 510 images are needed to achieve reliable characterisation.

Vertino et al. (2010a) examine CWC meso- and macro-scale habitats at the Santa Maria di Leuca Coral Province, a clear example of the utilisation of dense ROV video coverage on CWC reefs to produce detailed studies. The detail revealed by studies with dense video coverage per CWC reef raises the question: are the spatial representation of “single-pass” video line surveys across CWC reefs enough? And conversely, with strict research cruise schedules, at what point does video coverage become excessive?

Single-pass ROV video lines across CWC reefs and mounds are common (i.e. Dolan et al., 2008; Lim et al., *submitted*). As such, 3 different straight line survey designs are tested here (“SD2 - south to north”, “SD3 - east to west” and “SD4 - northwest-southeast diagonal transect”) (Figure 24;Table 9). With an average of 18.9% total difference in cell-type proportions from the control proportion, single-pass surveys appear to yield the least representative results. This is expected given the reduced spatial representation of such survey designs. Two of these survey designs (“SD2 - south to north” and “SD4 - northwest-southeast diagonal transect”) produce a total difference of 22.5% and 22.4% in cell-type proportion from the control proportion, while “SD3 - east to west” produces a total difference of 11.8%. The ring-like cell-type clustering that exists on the Piddington Mound (Lim et al., in review; chapter 3) appears to have an influence on this result as the course of the east to west line happens to cover an area with similar proportions to the control proportion. This is evidenced by approximately 50% of the total difference of this survey design resulting from 1 individual facies.

Another common survey design is following the geomorphology of the CWC reef or mound (i.e. Guinan et al., 2009) or some other known characteristic. In the case of the Piddington Mound, survey design “SD6 - spiral” (Figure 24; Table 9) follows both the bathymetry and ring-like growth already observed on the Piddington Mound (Lim et al., in review; chapter 3), circling through the mound perimeter, flank and summit. This cone-like survey design yields a 13.4% total cell-type proportion difference from the control proportion. The accuracy of this result is probably due to the influence of prior knowledge on survey design.

Survey design “ SD7 - actual survey” defines the navigation path of an ROV on a reconnaissance dive over the Piddington Mound when it was first discovered and initially investigated (Wheeler and shipboard party, 2011) (Figure 24;Table 9). This survey design yields a 17.7% total cell-type proportion difference from the control proportion. It represents a real life example of survey design without the influence of prior knowledge or mapping of the CWC reef. This survey design (or lack of) resulted in relatively a large (7.6%) over-estimation of “live coral framework” cell-types. This sampling bias may be a typical result of reconnaissance video investigations when discovering new seabed features as the scientists preferentially concentrate the cameras on the live proportion of the feature that is of more interest to them. Another short-coming of this survey design, and probably a result of the same sampling bias, is that 2 entire classes were not seen in the video observation ("sediment and dropstones" and "sorted sediment").

Probably the most well-known survey design, but apparently least-applied in the case of CWC reefs and mounds is survey design "SD5 - horizontal grid" (Figure 24; Table 9). In this example, the grid is made up of a series of mound-traversing lines spaced approximately 5 m apart where the end of each line is connected to the start of the next line. This survey design yields a 5.8% total cell-type proportion difference from the control proportion, the most representative proportion of the study. An additional positive of this survey design is that it estimated the exact proportion of individual cell-types for 3 classes ("sediment and dropstones", "sorted sediment" and "live coral framework"). Interestingly, it also yields a similar result to survey design "SD1 - random points" (5.9%) which represents full-reef video coverage. With line spacing of approx. 1 m, it took ~8 hours to collect the full-reef video coverage (Wheeler and shipboard party, 2011). Assuming a survey speed of 0.5 knots to collect survey design "SD5 - horizontal grid" (line length of 319 m), it would take 20.6 minutes to collect this ROV video data, a vast improvement from ~8 hours for the same representation of surface facies proportions. In addition, this technique appears to be unbiased by the significant clustering found on the Piddington Mound (Lim et al., in review; chapter 3).

4.5.3 What is the temporal variability of Piddington Mound and its implication for samples?

The T4 ROV video dataset was collected over the Piddington Mound 4 years after the T1 survey (2015) and covered the entire mound surface at a slower survey speed to benefit image clarity. To assess mound surface change over this period, 622 random images are classified (a minimum of 510 are needed) according to the image sampling technique established above using the same classifiers. The survey design, similar to the T1 ROV video data set, covers the entire mound surface by a 1 m spaced line grid. Thus, the accuracy of this data is similar to that of survey design "SD1 - random points" (Table 9).

The T4 ROV video dataset exhibits a change of 19% of the total mound surface in comparison to the T1 ROV video dataset. This change has taken place over 4 years (2011 - 2015) and is evident at a 25 cm^2 resolution. The "live coral framework" cell-type remains relatively constant, increasing by only 0.4% over the 4 years (+0.1% per year). A minute increase is expected given the slow growth rates (~15 - 30 mm yr^{-1}) observed in *Lophelia* (Gass and Roberts, 2006; Larcom et al., 2014; Orejas et al., 2008). Similarly, Huvenne et al. (2016) show that after ten years, the amount of live coral found on the Darwin Mounds, the only other known example of small-sized CWC reefs in the NE Atlantic, also remains the same. The "normal" proportion of live coral per Darwin Mound is ~45-55%, sizably greater than that found here on the Piddington Mound.

The "sorted sediment" cell-type also remains relatively constant (-0.2% over 4 years). This facies is typically found in the lee of "live coral framework" cell-types (Figure 23) where it is protected from resuspension by the current (Lim et al., in review). Given the fact that the proportion of "live coral framework" cells have not changed, it seems likely that the proportion of "sorted sediment" cell-type would remain the same.

The "biogenic hash" cell-type increased the most (7.5%) at a rate of 1.9% per year, assuming a constant rate of change. Given the dominance of the "biogenic hash" cell-type on Piddington Mound in 2011, it is likely to see a change in the proportion of this class. The source of this biogenic hash is likely to be as a result of the biological or physical erosion of the "dead coral framework" class (Lim et al., in review) or (re)exposure and redistribution through benthic erosion and transport processes.

Interestingly, the proportion of "dead coral framework" cell-type increased by 5.7% (a rate of 1.4% per year). If this class is both contributing to the "biogenic hash" class and increasing relative to the T1 "dead coral framework" class, then it can be assumed that it changed by at least 5.7% and at a minimum of 1.4% per year. Given the low growth rate of *Lophelia* mentioned earlier, it is unlikely that the source of the increased "dead coral framework" coverage is entirely from the degradation of the "live coral framework" cell-type. It is therefore suggested that this increase is possibly through "dead coral framework" exhumation by currents removing covering sediment.

The proportion of the "sediment and dropstone" class decreases the most (-5.3%) at a rate of 1.3% per year. Given the mound-perimeter occurrence of this class and the dominance of the "biogenic hash" on the steepest parts of the mound (flanks), it is likely that this decrease is due to burial by biogenic hash where the biogenic hash (or freshly eroded biogenic hash from dead coral frameworks) roll from the steepened mound flanks to the edges of the mound where the slope decreases and "sediment and dropstone" cell-types are common (Lim et al., in review).

With a total mound surface change of 4.8% per year, then in just over 20 years, the entire Piddington Mound surface will change. Thus, if physical and image (video or photographic) samples are taken 5 years apart on Piddington Mound, a change of 25% (and 50% after 10 years) on the mound surface influences whether or not these samples consistently represent the mounds' status in the contemporary environment. This, coupled with the heterogeneity observed on the CWC reefs and mounds, positioning error margins (e.g. ~2 m with some calibrated USBL systems in deep water) and inconsistencies of repeat video acquisition (Purser, 2015) contests the validity of interpretation from surface samples on similar CWC reefs. It is therefore recommended that data from various survey campaigns should be treated cautiously as they may not represent the "contemporary" environment.

Centimetre-scale remotely-sensed mapping is becoming more common in the marine environment. As such, observations from video data should be equally as accurate. Oblique camera data acquisition induces positional errors where there is an offset between the field of view of the camera and the positioning beacon (e.g. USBL) thus giving an incorrect position for oblique camera video observation (Lim et al., in review). This error is a function of camera obliqueness, rotation of the camera-mounted platform (e.g. ROV) around its axis, seabed slope and height of camera from seabed and is therefore not constant nor easily reconciled. For relevant example, oblique camera data has been utilized in a temporal study of a CWC reef, offshore Norway, which highlights the inconsistencies of repeat surveys using oblique camera (e.g. viewing the same part of the reef from different angles) (Purser, 2015). As such, we would like to recommend the use of downward-facing camera for temporal-based studies of CWC habitats (and other dynamic marine habitats) as positioning of the camera is not influenced by rotation of the camera around its axis, the angle at which it views the seabed is always the same (0°) and is not influenced by seabed slope in the same way as oblique camera.

4.6 Conclusion

This study presents a standardised video survey technique applicable to CWC habitats to assess both differences in space and time. The technique presented is developed with particular consideration for the financial, temporal and sea-state dependant nature of deep sea research to maximise resolution and spatial coverage. Known proportions of CWC-typical facies on the Piddington Mound were used to determine the minimum number of images needed to characterise the surface of similar sized CWC reefs with the same number of classes using downward-facing camera. This allows for a standardised approach to surveying and studying CWC reefs through video and comparison of reefs in different geographic settings and in time at 25 cm^2 resolution. A comparison of different common survey designs show that single-pass video are the least representative and highly-influenced by the heterogeneity, typical of CWC reefs, despite being most commonly utilised in research. Following bathymetry or known features on CWC reefs and mounds is another common survey design but does not yield the most accurate results. The most representative results were yielded from either fully video mosaicking a reef or using a grid of spaced lines. However, a grid of lines in this case is 1/16 times faster than video mosaicking an entire reef while yielding similar results.

The developed technique was applied to the Piddington Mound 4 years later to assess the change in proportions of facies across the mound surface. With a mound surface change of 4.8% per year, the mound surface has changed by almost 20% from 2011 to 2015. The greatest change was in the "biogenic hash" class (7.5%) followed by "dead coral framework" and "sediment and dropstone" classes. These classes are affected by strong currents as mobile or exhumed substrates. Similar to other reefs, the proportion of "live coral framework" class remained the same over the 4-year period as anticipated for a sessile slow growing organism. In 20 years, this study anticipates 100% change in the surface of the Piddington Mound. Thus, samples taken from the mound 5 years apart (with a 25% mound surface change), makes the samples inconsistent and therefore not representative of the mound status. Finally, we highlight the suitability of downward-facing camera for high-resolution repeat surveys for temporal variability purposed due to the many short-comings of temporal-based, oblique-camera surveys.

4.7 Acknowledgements

The authors would like to thank the crew and officers of ROV Holland 1 and RV Celtic Explorer for assistance in collecting high resolution, accurately positioned data. Ship time on the RV Celtic Explorer was funded by the Marine Institute under the 2011 and 2015 Ship Time Programme of the National Development Plan. Funding. Mohit Tunwal (UCC) is thanked for mathematical proofing.

4.8 Chapter references

Angers, C., 1974. A graphical method to evaluate sample sizes for the multinomial distribution. Technometrics 16, 469-471.

Anselin, L., 1995. Local Indicators of Spatial Association—LISA. Geographical Analysis 27, 93-115.

Beuck, L., Freiwald, A., Taviani, M., 2010. Spatiotemporal bioerosion patterns in deep-water scleractinians from off Santa Maria di Leuca (Apulia, Ionian Sea). Deep-Sea Research II 57, 458-470.

Beyer, A., Schenke, H.W., Klenke, M., Niederjasper, F., 2003a. High resolution bathymetry of the eastern slope of the Porcupine Seabight. Marine Geology 198, 27-54.

Brooke, S., Ross, S.W., Bane, J.M., Seim, H.E., Young, C.M., 2013. Temperature tolerance of the deep-sea coral Lophelia pertusa from the southeastern United States. Deep Sea Research Part II: Topical Studies in Oceanography 92, 240-248.

Buhl-Mortenson, L., Hodnesdal, H., Thorsnes, T., 2015. The Norwegian Sea Floor. MAREANO 2015.

Burt, P.J., Adelson, E.H., 1983. A multiresolution spline with application to image mosaics. ACM Transactions on Graphics (TOG) 2, 217-236.

Cairns, S.D., 2007. Deep-water corals: an overview with special reference to diversity and distribution of deep-water scleractinian corals. Bulletin of marine Science 81, 311-322.

Chitre, M., Shahabudeen, S., Stojanovic, M., 2008. Underwater acoustic communications and networking: Recent advances and future challenges. Marine technology society journal 42, 103-116.

Correa, T.B.S., Eberli, G.P., Grasmueck, M., Reed, J.K., Correa, A.M.S., 2012a. Genesis and morphology of cold-water coral ridges in a unidirectional current regime. Mar. Geol. 326–328, 14-27.

Correa, T.B.S., Grasmueck, M., Eberli, G.P., Reed, J.K., Verwer, K., Purkis, S.A.M., 2012b. Variability of cold-water coral mounds in a high sediment input and tidal current regime, Straits of Florida. Sedimentology 59, 1278-1304.

Davies, A.J., Duineveld, G.C., Lavaleye, M.S., Bergman, M.J., van Haren, H., Roberts, J.M., 2009a. Downwelling and deep-water bottom currents as food supply mechanisms to the cold-water coral Lophelia pertusa (Scleractinia) at the Mingulay Reef complex. Limnology and Oceanography 54, 620.

Davies, A.J., Duineveld, G.C.A., van Weering, T.C.E., Mienis, F., Quattrini, A.M., Seim, H.E., Bane, J.M., Ross, S.W., 2010. Short-term environmental variability in cold-water coral habitat at Viosca Knoll, Gulf of Mexico. Deep Sea Research Part I: Oceanographic Research Papers 57, 199-212.

Davies, A.J., Wisshak, M., Orr, J.C., Roberts, J.M., 2008b. Predicting suitable habitat for the cold-water coral *Lophelia pertusa* (Scleractinia). Deep-Sea Research I 55, 1048-1062.

de Haas, H., Huvenne, V., Wheeler, A.J., Unnithan, V., crew, a.s.s., 2002. R.V. Pelagia Cruise 64PE197: A TOBI Side Scan Sonar Survey of Cold Water Coral Carbonate Mounds in the Rockall Trough and Porrcupine Sea Bight. Royal Netherlands Institute for Sea Research, Unpublished Cruise Report.

De Mol, B., Kozachenko, M., Wheeler, A., Alvares, H., Henriet, J.-P., Olu-Le Roy, K., 2007a. Thérèse Mound: a case study of coral bank development in the Belgica Mound Province, Porcupine Seabight. Int J Earth Sci (Geol Rundsch) 96, 103-120.

De Mol, B., Van Rensbergen, P., Pillen, S., Van Herreweghe, K., Van Rooij, D., McDonnell, A., Huvenne, V., Ivanov, M., Swennen, R., Henriet, J.P., 2002. Large deep-water coral banks in the Porcupine Basin, southwest of Ireland. Marine Geology 188, 193-231.

Dolan, M.F.J., Grehan, A.J., Guinan, J.C., Brown, C., 2008. Modelling the local distribution of cold-water corals in relation to bathymetric variables: Adding spatial context to deep-sea video data. Deep-Sea Research I 55, 1564-1579.

Dorschel, B., 2003. Late Quaternary Development of a deep-water Carbonate Mound in the northeast Atlantic, RCOM-Bremen. University of Bremen, bremen, p. 90.

Dorschel, B., Hebbeln, D., Foubert, A., White, M., Wheeler, A.J., 2007a. Hydrodynamics and cold-water coral facies distribution related to recent sedimentary processes at Galway Mound west of Ireland. Marine Geology 244, 184-195.

Dorschel, B., Hebbeln, D., Rüggeberg, A., Dullo, W.-C., 2007b. Carbonate budget of a cold-water coral carbonate mound: Propeller Mound, Porcupine Seabight. International Journal of Earth Sciences 96, 73-83.

Dorschel, B., Hebbeln, D., Rüggeberg, A., Dullo, W.-C., Freiwald, A., 2005a. Growth and erosion of a cold-water coral covered carbonate mound in the Northeast Atlantic during the Late Pleistocene and Holocene. Earth and Planetary Science Letters 233, 33-44.

Dorschel, B., Wheeler, A.J., Huvenne, V.A.I., de Haas, H., 2009a. Cold-water coral mounds in an erosive environmental setting: TOBI side-scan sonar data and ROV video footage from the northwest Porcupine Bank, NE Atlantic. Mar. Geol. 264, 218-229.

Douarin, M., Sinclair, D.J., Elliot, M., Henry, L.-A., Long, D., Mitchison, F., Roberts, J.M., 2014. Changes in fossil assemblage in sediment cores from Mingulay Reef Complex (NE Atlantic): Implications for coral reef build-up. Deep Sea Research Part II: Topical Studies in Oceanography 99, 286-296.

Duineveld, G., Lavaleye, M., Berghuis, E., 2004. Particle flux and food supply to a seamount cold-water coral community (Galicia Bank, NW Spain). Marine Ecology Progress Series 277, 13-23.

Duineveld, G.C.A., Lavaleye, M.S.S., Bergman, M.J.N., de Stigter, H., Mienis, F., 2007a. Trophic structure of a cold-water coral mound community (Rockall Bank, NE Atlantic) in relation to the near-bottom particle supply and current regime. Bulletin of Marine Science 81, 449-467.

Dullo, C., Flögel, S., Rüggeberg, A., 2008a. Cold-water coral growth in relation to the hydrography of the Celtic and Nordic European continental margin. Marine Ecology Progress Series 371, 165-176.

Eisele, M., Hebbeln, D., Wienberg, C., 2008a. Growth history of a cold-water coral covered carbonate mound - Galway Mound, Porcupine Seabight, NE-Atlantic. Mar. Geol. 253, 160-169.

Ferrer, J., Elibol, A., Delaunoy, O., Gracias, N., Garcia, R., 2007. Large-area photo-mosaics using global alignment and navigation data, MTS/IEEE OCEANS Conference, Vancouver, Canada, pp. 1-9.

Fink, H.G., Wienberg, C., Hebbeln, D., McGregor, H.V., Schmiedl, G., Taviani, M., Freiwald, A., 2012. Oxygen control on Holocene cold-water coral development in the eastern Mediterranean Sea. Deep Sea Research Part I: Oceanographic Research Papers 62, 89-96.

Foubert, A., Beck, T., Wheeler, A., Opderbecke, J., Grehan, A., Klages, M., Thiede, J., Henriet, J.-P., 2005a. New view of the Belgica Mounds, Porcupine Seabight, NE Atlantic: preliminary results from the Polarstern ARK-XIX/3a ROV cruise, in: Freiwald, A., Roberts, J.M. (Eds.), Cold-Water Corals and Ecosystems. Springer Berlin Heidelberg, pp. 403-415.

Foubert, A., Huvenne, V.A.I., Wheeler, A., Kozachenko, M., Opderbecke, J., Henriet, J.P., 2011a. The Moira Mounds, small cold-water coral mounds in the Porcupine Seabight, NE Atlantic: Part B—Evaluating the impact of sediment dynamics through high-resolution ROV-borne bathymetric mapping. Marine Geology 282, 65-78.

Foubert, A.T.G., Huvenne, V.A.I., Wheeler, A.J., Kozachenko, M., Opderbecke, J., Henriet, J.-P., 2011b. The Moira Mounds, small cold-water coral mounds in the Porcupine Seabight, NE Atlantic: Part B - Evaluating the impact of sediment dynamics through high-resolution ROV-borne bathymetric mapping Mar. Geol.

Frank, N., Lutringer, A., Paterne, M., Blamart, D., Henriet, J.-P., van Rooij, D., van Weering, T.C.E., 2005. Deep-water corals of the northeastern Atlantic margin: carbonate mound evolution and upper intermediate water ventilation during the Holocene, in: Freiwald, A., Roberts, J.M. (Eds.), Cold-water Corals and Ecosystems. Springer, Berlin, Heidelberg, New York, pp. 113-133.

Frederiksen, R., Jensen, A., Westerberg, H., 1992. The distribution of the scleractinian coral *Lophelia pertusa* around the Faroe Islands and the relation to internal tidal mixing. Sarsia 77, 157-171.

Freiwald, A., 2002. Reef-Forming Cold-Water Corals, in: Wefer, G., Billett, D.S.M., Hebbeln, D., Jørgensen, B.B., van Weering, T.C.E. (Eds.), Ocean Margin Systems, Hanse Conference on Ocean Margin Systems (2000: Delmenhorst, Germany) ed. Springer, Berlin Heidelberg New York, pp. 365-385.

Freiwald, A., Fosså, J.H., Grehan, A., Koslow, T., Roberts, J.M., 2004. Cold-water coral reefs. UNEP-WCMC, Cambridge, UK 84.

Freiwald, A., Hühnerbach, V., Lindberg, B., Wilson, J., Campbell, J., 2002. The Sula Reef Complex, Norwegian shelf. Facies 47, 179-200.

Freiwald, A., Schönfeld, J., 1996. Substrate pitting and boring pattern of *Hyrrokkin sarcophaga* Cedhagen, 1994 (Foraminifera) in a modern deep-water coral reef mound. Mar. Micropaleontol. 28, 199-207.

Freiwald, A., Wilson, J.B., 1998. Taphonomy of modern, deep, cold-temperate water coral reefs. Historical Biology 13, 37-52.

Gass, S.E., Roberts, J.M., 2006. The occurrence of the cold-water coral Lophelia pertusa (Scleractinia) on oil and gas platforms in the North Sea: Colony growth, recruitment and environmental controls on distribution. Marine Pollution Bulletin 52, 549-559.

Getis, A., Ord, J.K., 1992. The Analysis of Spatial Association by Use of Distance Statistics. Geographical Analysis 24, 189-206.

Goodchild, M., 1986. Spatial Autocorrelation. Concepts and Techniques in Modern Geography 47. Norwich, UK: Geo Books.

Guinan, J., Grehan, A.J., Dolan, M.F.J., Brown, C., 2009. Quantifying relationships between video observations of cold-water coral cover and seafloor features in Rockall Trough, west of Ireland. Marine Ecology Progress Series 375, 125-138.

Haas, H., Mienis, F., Frank, N., Richter, T., Steinacher, R., Stigter, H., Land, C., Weering, T.E., 2009. Morphology and sedimentology of (clustered) cold-water coral mounds at the south Rockall Trough margins, NE Atlantic Ocean. Facies 55, 1-26.

Hebbeln, D., Van Rooij, D., Wienberg, C., 2016a. Good neighbours shaped by vigorous currents: Cold-water coral mounds and contourites in the North Atlantic. Mar. Geol. 378, 171-185.

Hebbeln, D., Wienberg, C., Wintersteller, P., Freiwald, A., Becker, M., Beuck, L., Dullo, C., Eberli, G.P., Glogowski, S., Matos, L., 2014. Environmental forcing of the Campeche cold-water coral province, southern Gulf of Mexico.

Henriet, J.-P., De Mol, B., Pillen, S., Vanneste, M., Van Rooij, D., Versteeg, W., Croker, P.F., Shannon, P.M., Unnithan, V., Bouriak, S., Chachkine, P., BELGICA

97 Shipboard scientific crew, 1998. Gas hydrate crystals may help build reefs. Nature 391, 648-649.

Henriet, J.P., Hamoumi, N., Da Silva, A.C., Foubert, A., Lauridsen, B.W., Rüggeberg, A., Van Rooij, D., 2014. Carbonate mounds: From paradox to World Heritage. Marine Geology 352, 89-110.

Henry, L.-A., Roberts, J.M., 2007. Biodiversity and ecological composition of macrobenthos on cold-water coral mounds and adjacent off-mound habitat in the bathyal Porcupine Seabight, NE Atlantic. Deep Sea Research Part I: Oceanographic Research Papers 54, 654-672.

Hovland, M., Mortensen, P.B., Brattegard, T., Strass, P., Rokoengen, K., 1998. Ahermatypic coral banks off mid-Norway: Evidence for a link with seepage of light hydrocarbons. Palaios 13, 189-200.

Hovland, M., Thomsen, E., 1997. Cold-water corals - are they hydrocarbon seep related? Mar. Geol. 137, 159-164.

Huang, Z., Brooke, B.P., Harris, P.T., 2011. A new approach to mapping marine benthic habitats using physical environmental data. Continental Shelf Research 31, S4-S16.

Huvenne, V.A.I., Bett, B.J., Masson, D.G., Le Bas, T.P., Wheeler, A.J., 2016. Effectiveness of a deep-sea cold-water coral Marine Protected Area, following eight years of fisheries closure. Biological Conservation 200, 60-69.

Huvenne, V.A.I., Beyer, A., de Haas, H., Dekindt, K., Henriet, J.-P., Kozachenko, M., Olu-Le Roy, K., Wheeler, A.J., participants, T.P.c., participants, C.c., 2005a. The seabed appearance of different coral bank provinces in the Porcupine Seabight, NE Atlantic: results from sidescan sonar and ROV seabed mapping, in: Freiwald, A., Roberts, J.M. (Eds.), Cold-water Corals and Ecosystems. Springer-Verlag, Berlin Heidelberg, pp. 535-569.

Huvenne, V.A.I., Blondel, P., Henriet, J.-P., 2002a. Textural analyses of sidescan sonar imagery from two mound provinces in the Porcupine Seabight. Mar. Geol. 189, 323-341.

Huvenne, V.A.I., Masson, D.G., Wheeler, A.J., 2009a. Sediment dynamics of a sandy contourite: the sedimentary context of the Darwin cold-water coral mounds, Northern Rockall Trough. International Journal of Earth Sciences 98, 865-884.

Huvenne, V.A.I., Tyler, P.A., Masson, D.G., Fisher, E.H., Hauton, C., Hühnerbach, V., Le Bas, T.P., Wolff, G.A., 2011. A Picture on the Wall: Innovative Mapping Reveals Cold-Water Coral Refuge in Submarine Canyon. PLoS ONE 6, e28755.

Huvenne, V.A.I., Van Rooij, D., De Mol, B., Thierens, M., O'Donnell, R., Foubert, A., 2009b. Sediment dynamics and palaeo-environmental context at key stages in the Challenger cold-water coral mound formation: Clues from sediment deposits at the mound base. Deep Sea Research Part I: Oceanographic Research Papers 56, 2263-2280.

Huvenne, V.I., Beyer, A., Haas, H., Dekindt, K., Henriet, J.-P., Kozachenko, M., Olu-Le Roy, K., Wheeler, A., 2005b. The seabed appearance of different coral bank provinces in the Porcupine Seabight, NE Atlantic: results from sidescan sonar and ROV seabed mapping, in: Freiwald, A., Roberts, J.M. (Eds.), Cold-Water Corals and Ecosystems. Springer Berlin Heidelberg, pp. 535-569.

IODP 307 Expedition scientists, 2005. Modern carbonate mounds: Porcupine drilling. IODP Prel. Rept., 307, p. 58.

Kano, A., Ferdelman, T.G., Williams, T., Henriet, J.-P., Ishikawa, T., Kawagoe, N., Takashima, C., Kakizaki, Y., Abe, K., Sakai, S., Browning, E.L., Li, X., Andres, M.S., Bjerager, M., Cragg, B.A., De Mol, B., Dorschel, B., Foubert, A.T.G., Frank, T.D., Fuwa, Y., Gaillot, P., Gharib, J.J., Gregg, J.M., Huvenne, V.A.I., Léonide, P., Mangelsdorf, K., Monteys, X., Novosel, I., O'Donnell, R., Rüggeberg, A., Samarkin, V.A., Sasaki, K., Spivack, A.J., Tanaka, A., Titschack, J., van Rooij, D., Wheeler, A.J., 2007. Age constraints on the origin and growth history of a deep-water coral mound in the northeast Atlantic drilled during Integrated Ocean Drilling Program Expedition 307. Geology 35, 1051-1054.

Kinsey, J.C., Eustice, R.M., Whitcomb, L.L., 2006. A survey of underwater vehicle navigation: Recent advances and new challenges, IFAC Conference of Manoeuvering and Control of Marine Craft.

Kocak, D.M., Caimi, F.M., 2005. The Current Art of Underwater Imaging – With a Glimpse of the Past and Vision of the Future. Marine Technology Society Journal 39, 5-26.

Kozachenko, M., 2005a. Present and Past Environments of the Belgica Mounds (deep-water coral carbonate mounds) Eastern Porcupine Seabight, North East Atlantic (unpublished PhD Thesis), Department of Geography and Geology. University College Cork, Cork, p. 221.

Kwatra, V., Schödl, A., Essa, I., Turk, G., Bobick, A., 2003. Graphcut textures: image and video synthesis using graph cuts, ACM Transactions on Graphics (ToG). ACM, pp. 277-286.

Lamarche, G., Lurton, X., Verdier, A.-L., Augustin, J.-M., 2011. Quantitative characterisation of seafloor substrate and bedforms using advanced processing of multibeam backscatter—Application to Cook Strait, New Zealand. Continental Shelf Research 31, S93-S109.

Larcom, E.A., McKean, D.L., Brooks, J.M., Fisher, C.R., 2014. Growth rates, densities, and distribution of Lophelia pertusa on artificial structures in the Gulf of Mexico. Deep Sea Research Part I: Oceanographic Research Papers 85, 101-109.

Larsson, A.I., Järnegren, J., Strömberg, S.M., Dahl, M.P., Lundälv, T., Brooke, S., 2014. Embryogenesis and Larval Biology of the Cold-Water Coral <italic>Lophelia pertusa</italic>. PLoS ONE 9, e102222.

Lavaleye, M., Duineveld, G., Lundälv, T., White, M., Guihen, D., Kiriakoulakis, K., Wolff, G.A., 2009. Cold-Water Corals on the Tisler Reef-preliminary observations on the dynamic reef environment. Oceanography.

Le Bas, T., Hühnerbach, V., 1999. PRISM Processing of remotely-sensed imagery for seafloor mapping operators manual version 3.1. Southampton Oceanography Centre, UK.

Lim, A., Wheeler, A.J., Arnaubec, A., in review. Cold-water coral reef spatial zonation, organisation and environmental controls: the case of the Piddington Mound, Porcupine Seabight, NE Atlantic. Mar. Geol.

Lim, A., Wheeler, A.J., Huvenne, V.A.I., Vertino, A., de Haas, H., Spezzaferri, S., *submitted*. Hydrodynamic and Sedimentological Influences on Cold-Water Coral Reef Development: The Moira Mounds, Porcupine Seabight, Irish-Atlantic margin. Mar. Geol.

Lirman, D., Gracias, N.R., Gintert, B.E., Gleason, A.C.R., Reid, R.P., Negahdaripour, S., Kramer, P., 2007. Development and application of a video-mosaic survey technology to document the status of coral reef communities. Environmental Monitoring and Assessment 125, 59-73.

Lowe, D.G., 1999. Object recognition from local scale-invariant features, Computer vision, 1999. The proceedings of the seventh IEEE international conference on. Ieee, pp. 1150-1157.

Lundälv, T., Fosså, J.H., Buhl Mortensen, P., Jonsson, L.G., White, M., Guihen, D., Unnithan, V., 2008. Development in a trawl-damaged coral habitat (Tisler reef, NE Skagerrak) during four years of trawl protection, 4th International Symposium on Deep-Sea Corals, Wellington, New Zealand, December 2008.

Masson, D.G., Bett, B.J., Billett, D.S.M., Jacobs, C.L., Wheeler, A.J., Wynn, R.B., 2003a. The origin of deep-water, coral-topped mounds in the northern Rockall Trough, Northeast Atlantic. Marine Geology 194, 159-180.

Messing, C.G., Neumann, A.C., Lang, J.C., 1990. Biozonation of deep-water lithoherms and associated hardgrounds in the northeastern Straits of Florida. Palaios 5, 15-33.

Mienis, F., de Stigter, H.C., de Haas, H., van Weering, T.C.E., 2009a. Near-bed particle deposition and resuspension in a cold-water coral mound area at the Southwest Rockall Trough margin, NE Atlantic. Deep Sea Res. Part I 56, 1026-1038.

Mienis, F., Duineveld, G.C.A., Davies, A.J., Ross, S.W., Seim, H., Bane, J., van Weering, T.C.E., 2012. The influence of near-bed hydrodynamic conditions on cold-water corals in the Viosca Knoll area, Gulf of Mexico. Deep Sea Research Part I: Oceanographic Research Papers 60, 32-45.

Mienis, F., van Weering, T., de Haas, H., de Stigter, H., Huvenne, V., Wheeler, A., 2006. Carbonate mound development at the SW Rockall Trough margin based on high resolution TOBI and seismic recording. Marine Geology 233, 1-19.

Mortensen, P.B., Hovland, M.T., Fosså, J.H., Furevik, D.M., 2001. Distribution, abundance and size of *Lophelia pertusa* coral reefs in mid-Norway in relation to seabed characteristics. Journal of the Marine Biological Association of the UK Volume 81, Issue 04, Aug 2001, 581-597.

Mortensen, P.B., Rapp, H.T., 1998. Oxygen and carbon isotope ratios related to grows line pattern in skeletons of *Lophelia pertusa* (L) (Anthozoa,Scleractinia): Implications for determination of linear extension rates. Sarsia 83, 433-446.

Mueller, C., Larsson, A.I., Veuger, B., Middelburg, J., van Oevelen, D., 2014a. Opportunistic feeding on various organic food sources by the cold-water coral Lophelia pertusa. Biogeosciences 11, 123-133.

Murphy, P., Wheeler, A.J., 2017. A GIS-based application of drainage basin analysis and geomorphometry in the submarine environment: The Gollum Canyon System, North-east Atlantic, in: Bartlett, D., Celliers, L. (Eds.), Geoinformatics for Marine and Coastal Management. CRC Press, Taylor & Francis Group, Boca Raton, USA.

Neumann, A.C., Ball, M.M., 1970a. Submersible Observations in the Straits of Florida: Geology and Bottom Currents. Geological Society of America Bulletin 81, 2861–2873.

Ord, J.K., Getis, A., 1995. Local Spatial Autocorrelation Statistics: Distributional Issues and an Application. Geographical Analysis 27, 286-306.

Orejas, C., Gori, A., Gili, J.M., 2008. Growth rates of live Lophelia pertusa and Madrepora oculata from the Mediterranean Sea maintained in aquaria. Coral Reefs 27, 255-255.

Orejas, C., Gori, A., Rad-Menéndez, C., Last, K.S., Davies, A.J., Beveridge, C.M., Sadd, D., Kiriakoulakis, K., Witte, U., Roberts, J.M., 2016. The effect of flow speed and food size on the capture efficiency and feeding behaviour of the cold-water coral Lophelia pertusa. Journal of Experimental Marine Biology and Ecology 481, 34-40.

Pingree, R.D., LeCann, B., 1990. Structure, strength and seasonality of the slope current in the Bay of Biscay region. Journal of the Marine Biological Association of the United Kingdom 70, 857-885.

Pingree, R.D., Sinha, B., Griffiths, C.R., 1999. Seasonality of the European slope current (Goban Spur) and ocean margin exchange. Continental Shelf Research 19, 929-975.

Pirlet, H., 2010. The Matrix of Cold-water Coral Mounds: Origin and Early-diagenetic Interactions, Faculty of Sciences. Ghent University, Ghent, Belgium, p. 179 pages.

Pirlet, H., Colin, C., Thierens, M., Latruwe, K., Van Rooij, D., Foubert, A., Frank, N., Blamart, D., Huvenne, V.A., Swennen, R., 2011a. The importance of the terrigenous fraction within a cold-water coral mound: A case study. Mar. Geol. 282, 13-25.

Pirlet, H., Colin, C., Thierens, M., Latruwe, K., Van Rooij, D., Foubert, A., Frank, N., Blamart, D., Huvenne, V.A.I., Swennen, R., Vanhaecke, F., Henriet, J.-P., 2011b. The importance of the terrigenous fraction within a cold-water coral mound: A case study. Marine Geology 282, 13-25.

Purser, A., 2015. A Time Series Study of Lophelia pertusa and Reef Megafauna Responses to Drill Cuttings Exposure on the Norwegian Margin. PLOS ONE 10, e0134076.

Purser, A., Larsson, A.I., Thomsen, L., van Oevelen, D., 2010a. The influence of flow velocity and food concentration on *Lophelia pertusa* (Scleractinia) zooplankton capture rates. Journal of Experimental Marine Biology and Ecology 395, 55-62.

Raddatz, J., Rüggeberg, A., Liebetrau, V., Foubert, A., Hathorne, E.C., Fietzke, J., Eisenhauer, A., Dullo, W.-C., 2014. Environmental boundary conditions of cold-water coral mound growth over the last 3 million years in the Porcupine Seabight, Northeast Atlantic. Deep Sea Research Part II: Topical Studies in Oceanography 99, 227-236.

Reading, H., 1996. Sedimentary environments and facies. Blackwells Scientific. Oxford.

Roberts, J.M., Henry, L.A., Long, D., Hartley, J.P., 2008a. Cold-water coral reef frameworks, megafaunal communities and evidence for coral carbonate mounds on the Hatton Bank, north east Atlantic. Facies 54, 297-316.

Roberts, J.M., Long, D., Wilson, J.B., Mortensen, P.B., Gage, J.D., 2003. The cold-water coral Lophelia pertusa (Scleractinia) and enigmatic seabed mounds along the north-east Atlantic margin: are they related? Marine Pollution Bulletin 46, 7-20.

Roberts, J.M., Wheeler, A., Freiwald, A., Cairns, S., 2009a. Cold-Water Corals: The Biology and Geology of Deep-Sea Coral Habitats. Cambridge University Press.

Roberts, J.M., Wheeler, A.J., Freiwald, A., 2006b. Reefs of the Deep: The Biology and Geology of Cold-Water Coral Ecosystems. Science 312, 543-547.

Rogers, A.D., 1999. The biology of *Lophelia pertusa* (Linnaeus 1758) and other deep-water reef-forming corals and impacts from human activities. International Review of Hydrobiology 84, 315-406.

Rüggeberg, A., Dullo, W.-C., Dorschel, B., Hebbeln, D., 2007. Environmental changes and growth history of a cold-water carbonate mound (Propeller Mound, Porcupine Seabight). International Journal of Earth Sciences 96, 57-72.

Rzhanov, Y., Linnett, L.M., Forbes, R., 2000. Underwater video mosaicing for seabed mapping, Image Processing, 2000. Proceedings. 2000 International Conference on, pp. 224-227 vol.221.

Savini, A., Vertino, A., Marchese, F., Beuck, L., Freiwald, A., 2014. Mapping Cold-Water Coral Habitats at Different Scales within the Northern Ionian Sea

(Central Mediterranean): An Assessment of Coral Coverage and Associated Vulnerability. PLoS ONE 9, e87108.

Soulsby, R., 1997. Dynamics of marine sands a manual for practical applications.

Spezzaferri, S., Vertino, A., Addamo, A.M., Backers, J., Baratti, V., Constandache, M., Camozzi, O., El Kateb, A., Gennari, G., Leuzinger, L., McGrath, M., Mc Hugh, S.K., Naudts, L., Savini, A., Stalder, C., 2012. E-CWC Moira (2012/16) *RV Belgica*: Cold-water coral ecosystems from the Moira Mounds (NE Atlantic): affinities and differences with modern and Pleistocene Mediterranean counterparts. University Freibourg, Switzerland, Unpublished Cruise Report.

Squires, D.F., 1964a. Fossil Coral Thickets in Wairarapa, New Zealand. Journal of Paleontology 38, 904-915.

Stow, D.A.V., Hernández-Molina, F.J., Llave, E., Sayago-Gil, M., Díaz del Río, V., Branson, A., 2009. Bedform-velocity matrix: The estimation of bottom current velocity from bedform observations. Geology 37, 327-330.

Thierens, M., Browning, E., Pirlet, H., Loutre, M.F., Dorschel, B., Huvenne, V.A.I., Titschack, J., Colin, C., Foubert, A., Wheeler, A.J., 2013a. Cold-water coral carbonate mounds as unique palaeo-archives: the Plio-Pleistocene Challenger Mound record (NE Atlantic). Quaternary Science Reviews 73, 14-30.

Thierens, M., Pirlet, H., Colin, C., Latruwe, K., Vanhaecke, F., Lee, J.R., Stuut, J.B., Titschack, J., Huvenne, V.A.I., Dorschel, B., Wheeler, A.J., Henriet, J.P., 2012. Ice-rafting from the British–Irish ice sheet since the earliest Pleistocene (2.6 million years ago): implications for long-term mid-latitudinal ice-sheet growth in the North Atlantic region. Quaternary Science Reviews 44, 229-240.

Thierens, M., Titschack, J., Dorschel, B., Huvenne, V.A.I., Wheeler, A.J., Stuut, J.-B.W., O'Donnell, R., 2010a. The 2.6 Ma depositional sequence from the Challenger cold-water coral carbonate mound (IODP Exp. 307): sediment contributors and hydrodynamic palaeo-environments. Mar. Geol. 271, 260-277.

Thompson, S.K., 1987. Sample size for estimating multinomial proportions. The American Statistician 41, 42-46.

Titschack, J., Thierens, M., Dorschel, B., Schulbert, C., Freiwald, A., Kano, A., Takashima, C., Kawagoe, N., Li, X., 2009a. Carbonate budget of a cold-water coral mound (Challenger Mound, IODP Exp. 307). Marine Geology 259, 36-46.

Van Landeghem, K.J., Baas, J.H., Mitchell, N.C., Wilcockson, D., Wheeler, A.J., 2012. Reversed sediment wave migration in the Irish Sea, NW Europe: A reappraisal of the validity of geometry-based predictive modelling and assumptions. Mar. Geol. 295, 95-112.

van Oevelen, D., Mueller, C.E., Lundälv, T., Middelburg, J.J., 2016. Food selectivity and processing by the cold-water coral Lophelia pertusa. Biogeosciences 13, 5789.

Van Rooij, D., 2004a. An integrated study of Quaternary sedimentary processes on the eastern slope of the Porcupine Seabight, SW of Ireland. Ghent University.

Van Rooij, D., De Mol, B., Huvenne, V., Ivanov, M., Henriet, J.P., 2003a. Seismic evidence of current-controlled sedimentation in the Belgica mound province, upper Porcupine slope, southwest of Ireland. Marine Geology 195, 31-53.

Vertino, A., Savini, A., Rosso, A., Di Geronimo, I., Mastrototaro, F., Sanfilippo, R., Gay, G., Etiope, G., 2010a. Benthic habitat characterization and distribution from two representative sites of the deep-water SML Coral Province (Mediterranean). Deep-Sea Research II 57, 380-396.

Vertino, A., Spezzaferri, S., Ruggeberg, A., Stalder, C., Wheeler, A.J., Party, t.E.C.-M.c.S., 2015. An Overview on Cold-Water Coral Ecosystems and Facies, in: Spezzaferri, S., Ruggeberg, A., Stalder, C. (Eds.), Atlas of benthic foraminifera from cold-water coral reefs. Cushman Foundation for Foraminiferal Research, pp. 12-19.

Victorero, L., Blamart, D., Pons-Branchu, E., Mavrogordato, M.N., Huvenne, V.A.I., 2015. Reconstruction of the formation history of the Darwin Mounds, N Rockall Trough: How the dynamics of a sandy contourite affected cold-water coral growth. Marine Geology.

Wheeler, Kozachenko, M., Henry, L.A., Foubert, A., de Haas, H., Huvenne, V.A.I., Masson, D.G., Olu, K., 2011a. The Moira Mounds, small cold-water coral banks in the Porcupine Seabight, NE Atlantic: Part A—an early stage growth phase for future coral carbonate mounds? Marine Geology 282, 53-64.

Wheeler, A., Bett, B., Billett, D., Masson, D., 2000. High resolution side-scan sonar mapping of deep-water coral mounds: surface morphology and processes affecting growth. Eos, Transactions, American Geophysical Union 81, F638.

Wheeler, A., Kozachenko, M., Beyer, A., Foubert, A., Huvenne, V.I., Klages, M., Masson, D., Olu-Le Roy, K., Thiede, J., 2005a. Sedimentary processes and carbonate mounds in the Belgica Mound province, Porcupine Seabight, NE Atlantic, in: Freiwald, A., Roberts, J.M. (Eds.), Cold-Water Corals and Ecosystems. Springer Berlin Heidelberg, pp. 571-603.

Wheeler, A., Murton, B., Copley, J., Lim, A., Coughlan, M., Dorschel, B., Morris, K., Antoniacomi, A., Carlsson, J., Collins, P., Green, D., Nye, V., 2011b. Cruise Report CE11009: RV Celtic Explorer & Holland I ROV. VENTuRE Survey: VENTs and REefs deep-sea ecosystem study of the 45o North MAR hydrothermal vent field and the cold-water coral Moira Mounds, Porcupine Seabight. University College Cork, Ireland, Unpublished Report.

Wheeler, A.J., Beck, T., Thiede, J., Klages, M., Grehan, A., Monteys, F.X., Polarstern ARK XIX/3a Shipboard Party, 2005b. Deep-water coral mounds on the Porcupine Bank, Irish margin: preliminary results from Polarstern ARK-XIX/3a ROV cruise, in: Freiwald, A., Roberts, J.M. (Eds.), Cold-water corals and Ecosystems. Springer-Verlag, Berlin, pp. 393-402.

Wheeler, A.J., Beyer, A., Freiwald, A., de Haas, H., Huvenne, V.A.I., Kozachenko, M., Olu-Le Roy, K., Opderbecke, J., 2007a. Morphology and environment of cold-water coral carbonate mounds on the NW European margin. International Journal of Earth Sciences 96, 37-56.

Wheeler, A.J., Capocci, R., Crippa, L., Connolly, N., Hogan, R., Lim, A., McCarthy, E., McGonigle, C., O' Donnell, E., O' Sullivan, K., Power, K., Ryan, G., Vertino, A., Holland 1 ROV Technical Team, Officers and Crew of the RV Celtic Explorer, 2015. Cruise Report: Quantifying Environmental Controls on Cold-Water coral Reef Growth (QuERCi). University College Cork, Ireland.

Wheeler, A.J., Kozachenko, M., Henry, L.A., Foubert, A., de Haas, H., Huvenne, V.A.I., Masson, D.G., Olu, K., 2011d. The Moira Mounds, small cold-water coral banks in the Porcupine Seabight, NE Atlantic: Part A—an early stage growth phase for future coral carbonate mounds? Marine Geology 282, 53-64.

Wheeler, A.J., Kozachenko, M., Masson, D.G., Huvenne, V.A.I., 2008a. Influence of benthic sediment transport on cold-water coral bank morphology and growth: the example of the Darwin Mounds, north-east Atlantic. Sedimentology 55, 1875-1887.

White, M., 2007. Benthic dynamics at the carbonate mound regions of the Porcupine Sea Bight continental margin. International Journal of Earth Sciences 96, 1-9.

White, M., Dorschel, B., 2010a. The importance of the permanent thermocline to the cold water coral carbonate mound distribution in the NE Atlantic. Earth and Planetary Science Letters 296, 395-402.

White, M., Mohn, C., de Stigter, H.C., Mottram, G., 2005. Deep-water coral development as a function of hydrodynamics and surface productivity around the submarine banks of the Rockall Trough, NE Atlantic, in: Freiwald, A., Roberts, J.M. (Eds.), Cold-water Corals and Ecosystems. Springer, Berlin, Heidelberg, New York, pp. 503-514.

Wienberg, C., Hebbeln, D., Fink, H.G., Mienis, F., Dorschel, B., Vertino, A., López Correa, M., Freiwald, A., 2009. Scleractinian cold-water corals in the Gulf of Cádiz-first clues about their spatial and temporal distribution. Deep Sea Res. Part I 56, 1873-1893.

Wilson, J.B., 1979a. "Patch" development of the deep-water coral *Lophelia pertusa* (L.) on the Rockall bank. Journal of the Marine Biological Association of the United Kingdom 59, 165-177.

Wilson, J.L., 1975. Carbonate Facies in Geologic History. Springer, New York.

Wood, R.A., 1999. Reef Evolution. Oxford Univ. Press, Oxford.

Zibrowius, H., 1980. Les Scléractiniaires de la Méditerranée et de l'Atlantique nord-oriental. Mémoires de l'Institut océanographique, Monaco.

5 Conclusion

The work presented here provides a detailed multidisciplinary investigation of the hydrodynamics, sedimentology, environmental influences and habitat variability of the downslope Moira Mounds, and, in particular, the Piddington Mound. Occurring along an environmental gradient, analyses of box cores, bathymetry, backscatter, video and CTD's reveal a how sensitive these cold-water coral reefs are to their environment. On a reef-chain-scale, the downslope Moira Mounds occur at different stages of development, apparently driven by both substratum and current speed. On the individual reef-scale, reefs develop in a ring-like pattern. This pattern is related to either dominant processes found on the reef or external and changing environmental drivers. High-resolution mapping techniques (ROV-borne multibeam and video mosaicking) reveal that the surface of these mounds change at an incredible rate (~20% per 4 years), proving to be more dynamic than previously thought. Downward-facing, ROV-mounted, horizontally-gridded, video-imaging surveys are recommended to survey these dynamic environments to achieve most representative results while considering the pressures of ship time.

A number of specific research questions have been identified (outlined in the introduction) and clearly answered by this body of work. These are summarised below.

What is the nature of the current affecting the downslope Moira Mounds?

The current affecting the Moira Mounds comes from the south, flowing to the north through the downslope area. This current can be characterised by a temperature of ~8.6°C, a salinity of 35.5 kg/g and a O_2 saturation of 6.5 ml/l. The predominantly northerly-flowing current varies from the south to the north of the downslope area in velocity. In the south the current is ~37 cm s^{-1}, in the centre the current is ~30 cm s^{-1} and in the north the current is 39 – 41 cm s^{-1}. These changes in current velocity appear to be related to changes in slope angle which are in turn marked by the deposition of sands in the centre of the study site. This deposition of sand is marked by thickened sediment packages outlined in Huvenne et al. (2009) using a seismic line over the same area.

What is the effect of hydrodynamics on reef development?

Across the aforementioned current velocity gradient, mounds exhibit various differing characters. As the only variables are currents velocity and substrate type, other allogenic controls such as temperature, salinity and dissolved oxygen can therefore be elucidated. In the south, where dropstones are common and current speeds are low, mound spacing is relatively dense while the mounds themselves are small, dominated by dead coral framework and muddy sediments. In contrast, in the north, the mounds are spaced further apart while the mound surfaces are dominated by live coral frameworks and sandy sediments. Isolated, off-mound coral colonies are frequent in the south but rare in the north. In the centre of the downslope area, thickets are most common. This is related to the lack of available substrates (dropstones) restricting their lateral development to the thicket stage of development.

In light of this research, how do the downslope Moira Mounds compare with other reef habitats?

The Moira Mounds habitat show similarities to a wide range of other cold water coral habitats in terms of temperature, salinity, dissolved oxygen, current velocity, geomorphology, stage of development and depth range. However, no other cold water coral habitat has reefs as small as the Moira Mounds nor the exact same set of environmental parameters. Thus, the Moira Mounds are a unique cold water coral habitat globally.

Does the Piddington Mound exhibit a spatial organisation?

At first glance, the Piddington Mound surface facies are heterogeneous. However, using detailed spatial observations and subsequent analyses, the facies on the Piddington Mound show a significant clustering pattern across the mound surface at a 25 cm resolution. These facies occur in distinct rings, concentrically distributed around the mound summit.

What are the influences on this organisation?

Different facies form from differing processes. The facies surrounding the mound (sediment and dropstones) is typical of the off-mound Moira Mounds area and it is thought that this is the substrate that the Moira Mounds settled upon. The rarest facies is the "sorted sediment" facies which occurs around the mound base where a change in rugosity may slow the current and deposit some sand load. It also occurs behind coral frameworks where it may have been deposited during a lower energy hydrodynamic regime and is now protected from erosion by the coral framework. Two scenarios are put forward to describe how the potential processes that lead to this ring-like organisation of the mound-typical facies. The first scenario is based along traditional Growth-Death-Decay of cold water corals drawing parallels to the processes identified in the Wilsons Ring Model. The latter scenario is relating to the environmental settings and environmental change whereby the coral framework facies (dead or live) form on the mound flanks where they are higher up in the water column than the surrounding seabed. The biogenic material is formed through the degradation/bioerosion of the coral framework facies and is deposited on the flatter parts of the mound (the summit/lower flanks). Further, the live coral framework is found predominantly on the lee of the mound, where it may potentially be sheltered from the strong currents and therefore capture food more effectively in the lower flow velocity.

How representative is the Piddington Mound?

The surface facies of the Piddington Mound and another Moira Mound are compared. These show that facies occur in distinct, ring-like areas across the surface of both mounds and the geomorphology is similar in both settings. However, the other Moira Mound shows more pronounced scouring which may be related to the increase in current velocity throughout the area. Thus, the facies pattern seen at the Piddington Mound may be typical of other Moira Mounds.

What is the minimum amount of seabed imagery needed to accurately characterise the Piddington Mound?

A robust sample size estimation statistic was applied to the known quantity of facies at 25 cm^2 resolution across the surface of the Piddington Mound. This determines that a minimum of 510 images were needed to accurately (within 5 %) characterise the proportions of facies across the mound surface.

What is the most representative way by which to collect this seabed imagery?

This minimum number of images required (501) was applied to a series survey designs typical in cold water coral reef habitats. This showed that, the commonly used single-pass survey lines produce the least representative results while the least commonly used survey design (gridded line survey) produced the most representative results. The gridded line survey produced results comparable to surveying the entire reef surface while taking 1/16 of the time to acquire this data.

What is the temporal variability of the Piddington Mound over 4 years?

In applying the minimum number of samples required to accurately characterise the Piddington Mound surface via the most representative survey design (gridded line survey) to a video data set of the Piddington Mound surface 4 years later, mound surface change is compared at a 4-year resolution. This showed that in 4 years, ~19% of the mound surface facies proportion has changed suggesting that with a constant change, in 20 years the mound surface may entirely change (~100%). The facies that changed the most are "Dead coral framework" and "Biogenic hash". This is most likely due to re-exposure of buried substrates on the mound. The lowest facies proportion change observed is in the "Live coral framework" facies which is expected given the low growth rate of coral.

What are the implications for temporally and spatially separated samples?

Given the heterogeneous nature of the mound surface, the results show that 1 samples (e.g. core, box core, image) is unrepresentative of an entire mound surface and therefore insufficient for accurate analyses. Further, given the rate of change (19% mound surface change over 4 years), samples collected several years apart and subsequently utilised to study the mound in the contemporary environment are potentially inconsistent.

Based on the research presented and discussed, and in line with the aims of the study (section 1.3, page 21), following specific conclusions and key findings can be highlighted:

- Δ The downslope Moira Mounds occur along a 10 km hydrodynamic gradient where the current predominantly flowed from south to north during the sampling period. This current changes from ~30 cm s^{-1} in the south to ~40 cm s^{-1} in the north of the study area.

- Δ The downslope Moira Mounds appear to preferentially develop into reefs on dropstone-dominant substrates. In areas that lack dropstones, their diameters are restricted by the availablity of mound-derived substrates (e.g. bioclasts, coral rubble) that provide new substrate for corals to settle on facilitating the spreading of the reef.

- Δ Temperature and salinity did not appear to have an influence on mound development at the reef-chain-scale.

- Δ Comparison with other cold-water coral reef habitats globally show that they all vary in some way (e.g. temperature, salinity, current speed, sediment-type, coral status), making it difficult to directly compare them.

- Δ The first cold-water coral reef-scale video mosaic shows a ring-like facies organisation across the surface of the mound despite significant heterogeneity, typical of cold-water coral reefs.

- Δ This ring-like organisation may be influenced by *in situ* reef development processes (e.g. coral growth and decay) or by reef-external and ever-changing environmental conditions (e.g. currents and bathymetry).

- Δ The ring-like development exhibited by the Piddington Mound appears to be typical of other Moira Mounds.

- Δ The minimum number of images needed to accurately characterise the proportion of surface facies on the Piddington Mound is 510, using a downward-facing camera with a field of view of at least 0.25 cm^2.

- Δ The best survey design for downward-facing imagery is a horizontal grid. Although common, single-pass video transects yield the least representative results. Full-reef video-mosaicking achieves detailed results and imaging of the reef, but takes significantly more time (x16).

- Δ Over 4 years, the Piddington Mound changed by 19%. Similar to other studies and as expected, the proportion of live coral on the mound did not vary. By contrast, areas of biogenic hash and dead coral varied the most.

- Δ Although downward-facing camera restricts observations on the 3D microhabitat created by coral frameworks, it has many advantages over the more common obliquely-angled ROV video observations (e.g. positioning accuracy and inconsistency).

Appendix I

Additional data acquired and processed during the project

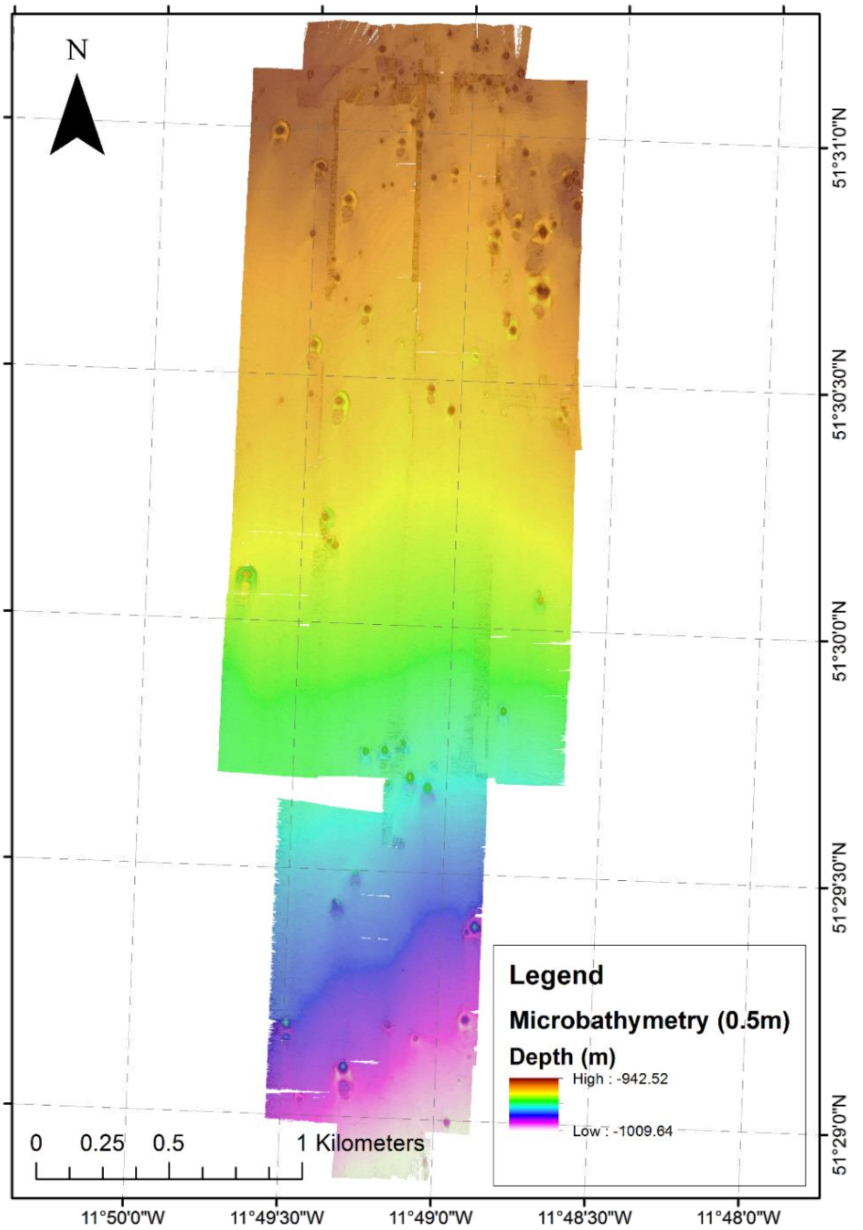

Figure 26 Bathymetry

ROV-mounted EM2040 multibeam bathymetric coverage over the northern downslope area (QuERCi 1, 2015).

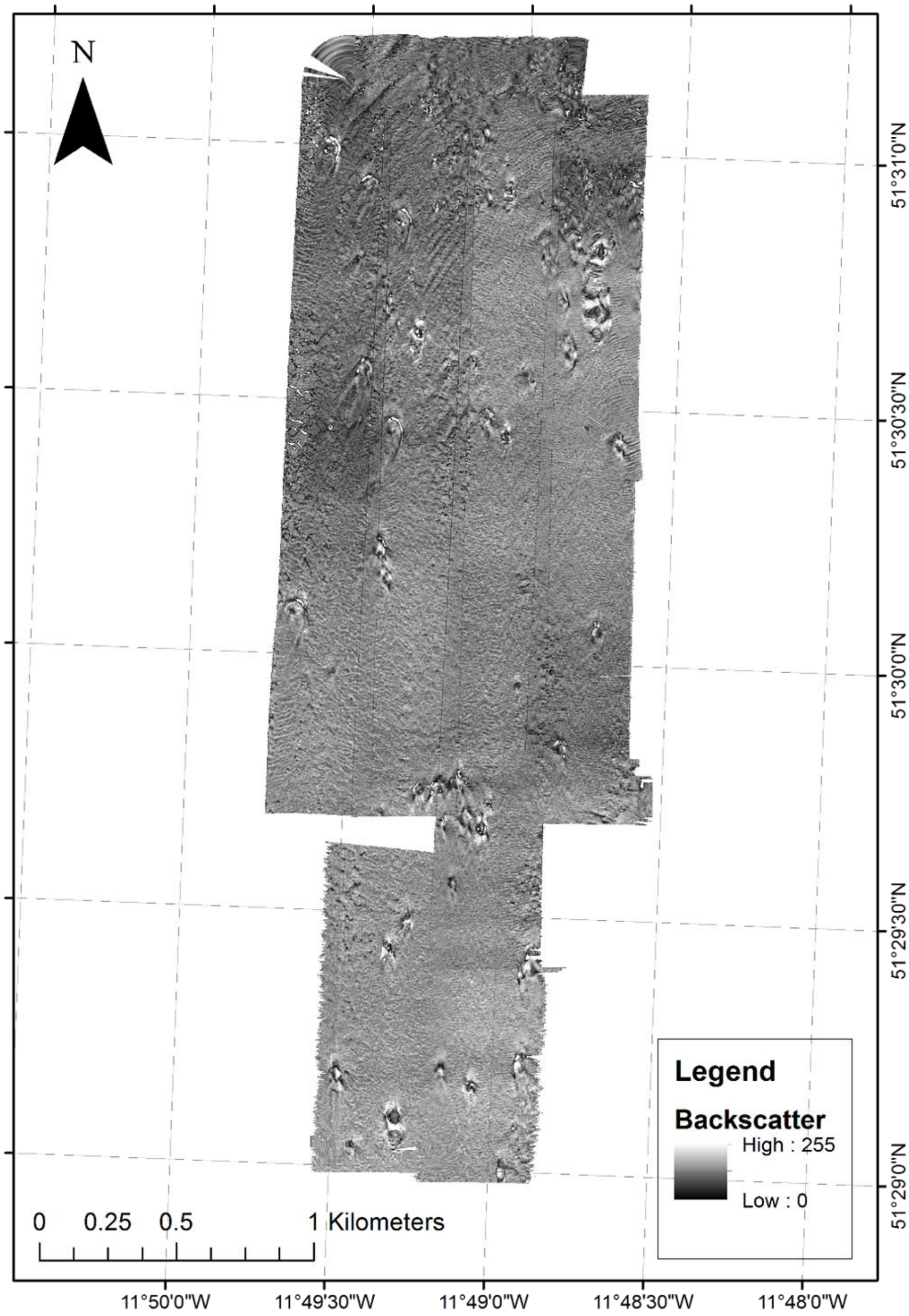

Figure 27 Backscatter

ROV-mounted EM2040 multibeam backscatter coverage over the northern downslope area (QuERCi 1, 2015).

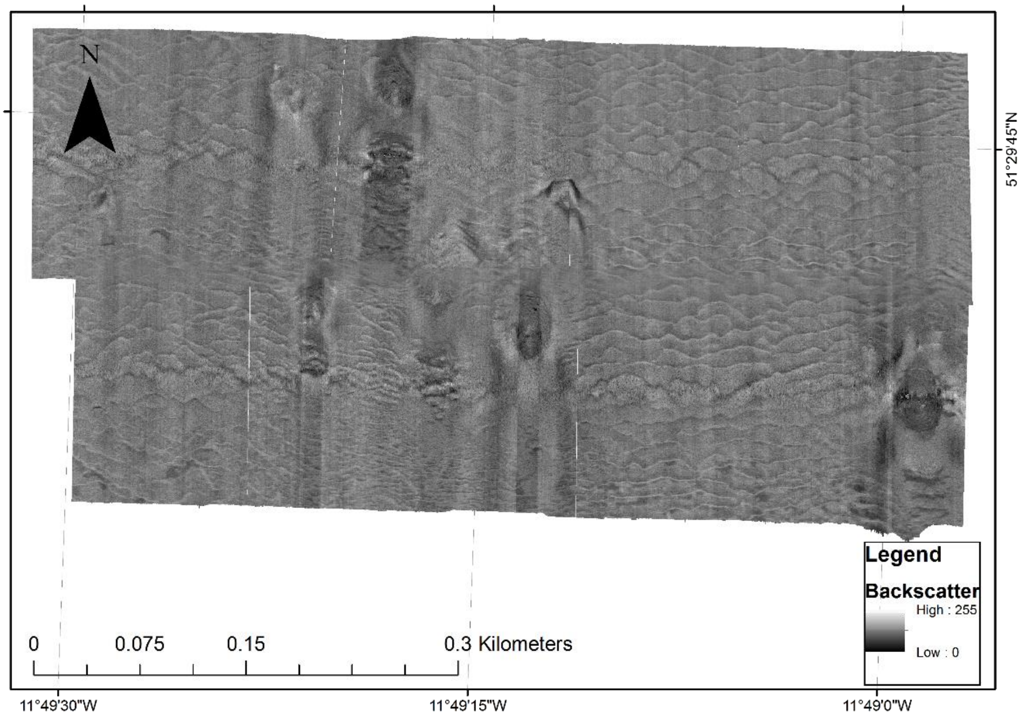

Figure 28 Piddington Mound backscatter

ROV-mounted multibeam backscatter over the Piddington Mound area (QuERCi 1, 2015).

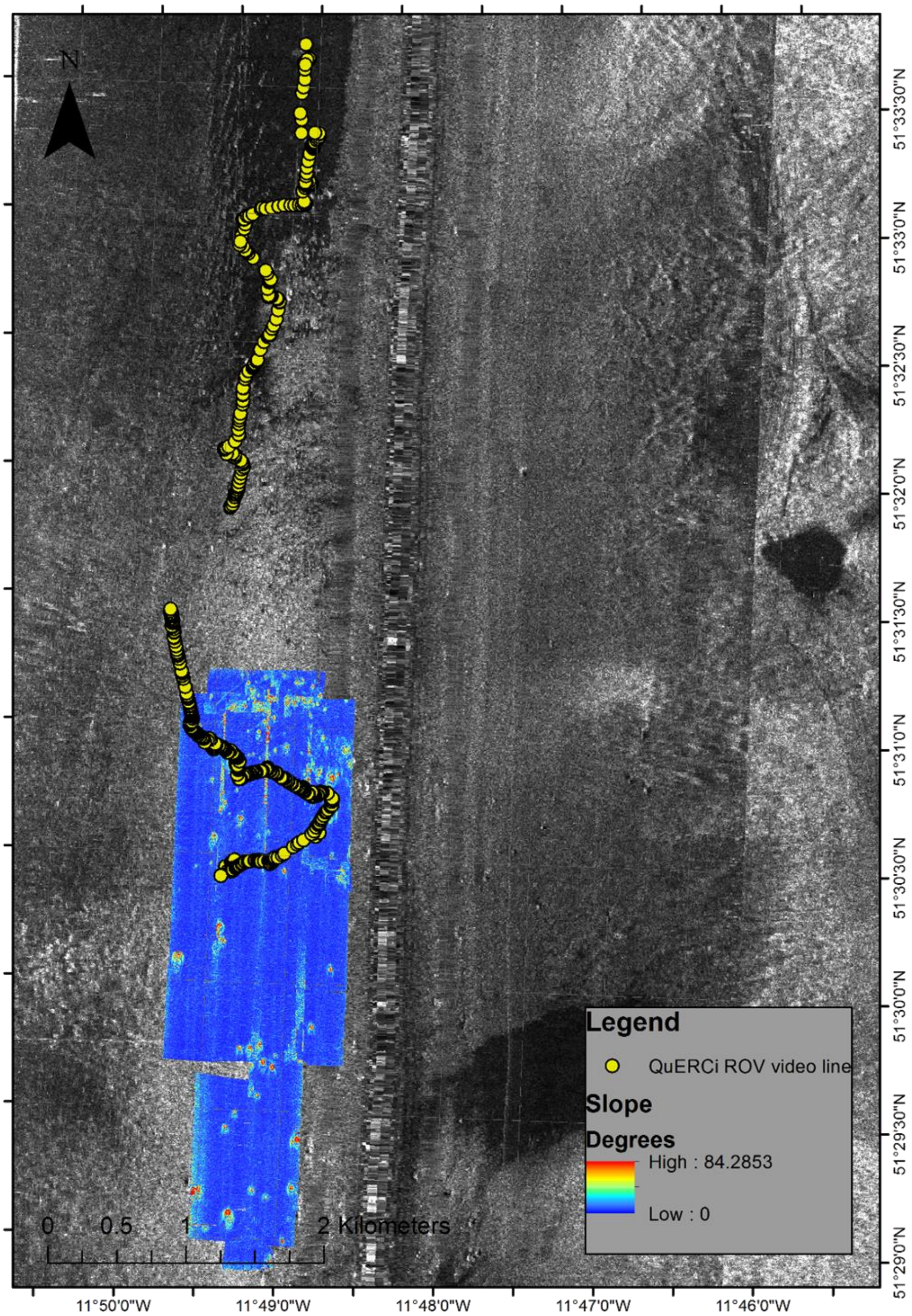

Figure 29 QuERCi 1 ROV footage

ROV-video footage (yellow dotted trail) collected during the QuERCi 1 survey with ROV-mounted multibeam-derived slope overlaid on TOBI side scan sonar.

Figure 30 WICPro gravity cores

Gravity cores collected in the downslope Moira Mounds area during the WICPro survey, 2014.

Table 11 Down core grain size and composition data for the Eurofleets (2012) Moira Mound cruise box cores.

Box Core	Sample (cm)	Depth in core (cm)	Dry Weight (g)	Treated Dry Weight (g)	% SiO2	% CaCO3 + Organic	Mean	Sort - ing	Mean	Sorting	Skewness	Kurtosity	Mode 1 (mm):	% Sand:	% Mud:
1	0-1	0.5	3.4	2.6	76.8	23.2	65.9	5.1	V F Sand	V P Sorted	V F Skewed	Platykurtic	238.1	56.4	43.6
1	1-2	1.5	3.3	2.5	76.2	23.8	37.5	5.7	V C Silt	V P Sorted	Symmetrical	V Platykurtic	238.1	44.3	55.7
1	2-5	3.5	3.6	2.6	74.2	25.8	19.8	5.1	C Silt	V P Sorted	V C Skewed	Mesokurtic	7.5	20.8	79.2
1	5-10	7.5	3.5	2.5	71.8	28.2	12.8	3.3	M Silt	Poorly Sorted	C Skewed	Mesokurtic	8.4	10.4	89.6
1	10-15	12.5	2.4	1.7	71.8	28.2	12.3	3.7	M Silt	Poorly Sorted	C Skewed	Mesokurtic	6.7	13.2	86.8
1	15-20	17.5	2.7	1.9	71.9	28.1	13.6	3.9	M Silt	Poorly Sorted	C Skewed	Mesokurtic	6.7	15.1	84.9
1	20-30	25	3.2	2.3	73.2	26.8								0.0	0.0
1	30-38	34	2.6	2.0	75.4	24.6								0.0	0.0
3	0-1	0.5	3.1	2.3	75.3	24.7	13.6	5.4	M Silt	V P Sorted	V C Skewed	Leptokurtic	5.3	17.8	82.2
3	1-2	1.5	2.9	2.2	75.7	24.3	9.9	4.3	M Silt	V P Sorted	V C Skewed	Leptokurtic	5.3	14.3	85.7
3	2-5	3.5	3.5	2.4	68.5	31.5	7.0	2.7	F Silt	Poorly Sorted	C Skewed	Mesokurtic	5.3	4.5	95.5
3	5-10	7.5	3.1	2.0	64.8	35.2	7.3	2.7	F Silt	Poorly Sorted	C Skewed	Mesokurtic	6.0	4.0	96.0
3	10-15	12.5	4.7	2.5	53.8	46.2	6.8	2.8	F Silt	Poorly Sorted	C Skewed	Leptokurtic	5.3	4.8	95.2
3	15-20	17.5	5.0	2.9	57.7	42.3	6.0	2.4	F Silt	Poorly Sorted	C Skewed	Mesokurtic	5.3	2.6	97.4
3	20-25	22.5	4.9	3.4	69.9	30.1	8.1	3.6	M Silt	Poorly Sorted	V C Skewed	Leptokurtic	5.3	10.8	89.2
3	25-28	26.5	3.5	1.7	48.9	51.1								0.0	0.0
5	0-1	0.5	2.0	1.5	78.2	21.8	53.4	5.4	V Coarse Silt	V P Sorted	V F Skewed	Platykurtic	189.1	60.1	39.9
5	1-2	1.5	2.5	1.9	76.6	23.4	32.8	5.6	V Coarse Silt	V P Sorted	Symmetrical	V Platykurtic	189.1	45.5	54.5
5	2-5	3.5	2.6	2.0	78.4	21.6	9.8	3.7	M Silt	Poorly Sorted	C Skewed	Mesokurtic	5.3	11.1	88.9
5	5-10	7.5	3.2	2.4	76.8	23.2								0.0	0.0

Table 11 Down core grain size and composition data for the Eurofleets (2012) Moira Mound cruise box cores.

Box Core	Sample (cm)	Depth in core (cm)	Dry Weight (g)	Treated Dry Weight (g)	% SiO2	% CaCO3 + Organic	Mean	Sort - ing	Mean	Sorting	Skewness	Kurtosity	Mode 1 (mm):	% Sand:	% Mud:
5	10-15	12.5	3.1	2.3	75.1	24.9								0.0	0.0
5	15-20	17.5	2.5	1.8	73.7	26.3	10.9	3.8	M Silt	Poorly Sorted	C Skewed	Mesokurtic	6.0	12.1	87.9
5	20-27	23.5	3.7	2.9	78.9	21.1	19.1	5.3	C Silt	V P Sorted	C Skewed	Platykurtic	5.3	28.5	71.5
10	0-1	0.5	3.3	2.8	84.5	15.5								0.0	0.0
10	2	2	2.0	1.4	69.6	30.4	13.7	4.1	M Silt	V P Sorted	C Skewed	Mesokurtic	7.5	14.8	85.2
10	5	5	2.9	2.1	72.6	27.4	10.9	3.2	M Silt	Poorly Sorted	C Skewed	Mesokurtic	7.5	8.2	91.8
10	10	10	2.7	2.0	73.0	27.0	10.7	3.3	M Silt	Poorly Sorted	C Skewed	Mesokurtic	6.7	8.1	91.9
10	15	15	3.1	2.3	72.9	27.1	8.2	2.6	M Silt	Poorly Sorted	Symmetrical	Mesokurtic	6.7	1.9	98.1
10	20	20	2.0	1.4	71.2	28.8	12.6	3.8	M Silt	Poorly Sorted	C Skewed	Mesokurtic	6.7	13.4	86.6
10	30	30	2.8	2.0	71.9	28.1	11.1	3.7	M Silt	Poorly Sorted	C Skewed	Mesokurtic	6.0	11.1	88.9
10	35	35	2.6	1.9	72.8	27.2	18.3	5.1	C Silt	V P Sorted	C Skewed	Platykurtic	6.0	24.7	75.3
12	0-1	0.5	3.8	2.9	77.1	22.9	19.7	4.8	C Silt	V P Sorted	C Skewed	Platykurtic	7.5	25.0	75.0
12	2	2	1.3	0.9	70.7	29.3	13.5	3.9	M Silt	Poorly Sorted	C Skewed	Mesokurtic	8.4	15.2	84.8
12	5	5	1.4	1.0	71.2	28.8	15.3	4.2	M Silt	V P Sorted	C Skewed	Mesokurtic	7.5	18.6	81.4
12	10	10	1.8	1.3	73.0	27.0									
12	15	15	2.1	1.6	77.6	22.4									
12	20	20	2.2	1.6	73.0	27.0	12.9	3.5	M Silt	Poorly Sorted	C Skewed	Mesokurtic	8.4	12.5	87.5
12	21-24	22.5	3.5	2.5	72.8	27.2	23.8	5.6	C Silt	V P Sorted	C Skewed	Platykurtic	7.5	28.4	71.6
12	30	30	2.2	1.5	70.0	30.0	15.5	4.4	M Silt	V P Sorted	C Skewed	Platykurtic	6.7	19.9	80.1
12	36	36	2.4	1.6	68.5	31.5	10.1	2.9	M Silt	Poorly Sorted	C Skewed	Mesokurtic	8.4	7.6	92.4
13	0-1	0.5	6.6	5.8	87.9	12.1									

Table 11 Down core grain size and composition data for the Eurofleets (2012) Moira Mound cruise box cores.

Box Core	Sample (cm)	Depth in core (cm)	Dry Weight (g)	Treated Dry Weight (g)	% SiO2	% CaCO3 + Organic	Mean	Sort - ing	Mean	Sorting	Skewness	Kurtosity	Mode 1 (mm):	% Sand:	% Mud:
13	2	2	8.2	7.3	89.1	10.9									
13	5	5	9.2	7.9	86.0	14.0									
13	10	10	8.6	7.7	89.2	10.8	268.6	1.6	M Sand	M W Sorted	Symmetrical	Mesokurtic	267.1	100.0	0.0
13	20	20	7.3	6.3	86.8	13.2	235.0	1.5	F Sand	M W Sorted	Symmetrical	Mesokurtic	238.1	100.0	0.0
15	0-1	0.5	3.7	2.8	76.6	23.4									
15	2	2	2.8	2.1	73.9	26.1	14.2	4.2	M Silt	V P Sorted	Coarse Skewed	Mesokurtic	7.5	16.6	83.4
15	5	5	3.0	2.2	72.9	27.1	10.7	3.2	M Silt	Poorly Sorted	Coarse Skewed	Mesokurtic	6.7	8.2	91.8
15	10	10	2.4	1.7	71.8	28.2	11.2	3.2	M Silt	Poorly Sorted	Coarse Skewed	Mesokurtic	7.5	8.6	91.4
15	15	15	2.2	1.6	72.0	28.0	9.7	2.9	M Silt	Poorly Sorted	Coarse Skewed	Mesokurtic	6.0	5.5	94.5
15	20	20	2.7	1.9	71.6	28.4	10.7	3.0	M Silt	Poorly Sorted	Symmetrical	Mesokurtic	7.5	5.9	94.1
15	28	28	3.1	2.3	73.9	26.1	8.7	2.5	M Silt	Poorly Sorted	Coarse Skewed	Mesokurtic	6.7	1.4	98.6
16	0-1	0.5	9.1	8.5	93.4	6.6	321.6	1.5	M Sand	M W Sorted	Symmetrical	Mesokurtic	336.3	100.0	0.0
16	2	2	5.0	4.5	89.8	10.2	286.1	1.6	M Sand	M W Sorted	Symmetrical	Mesokurtic	299.7	98.7	1.3
16	5	5	6.9	6.0	87.2	12.8									
16	10	10	4.5	3.6	81.4	18.6									
16	15	15	4.6	3.6	77.8	22.2									
16	20	20	3.5	2.7	75.9	24.1	14.0	4.0	M Silt	V P Sorted	Coarse Skewed	Platykurtic	6.7	17.3	82.7

Table 11 Down core grain size and composition data for the Eurofleets (2012) Moira Mound cruise box cores.

Box Core	Sample (cm)	Depth in core (cm)	Dry Weight (g)	Treated Dry Weight (g)	% SiO2	% CaCO3 + Organic	Mean	Sort - ing	Mean	Sorting	Skewness	Kurtosity	Mode 1 (mm):	% Sand:	% Mud:
16	23.5	23.5	7.7	6.6	86.6	13.4									
21	0-1	0.5	7.7	6.4	83.5	16.5	213.8	1.4	F Sand	Well Sorted	Symmetrical	Mesokurtic	212.2	96.4	3.6
21	2	2	4.1	3.2	78.9	21.1	132.3	2.8	F Sand	Poorly Sorted	V F Skewed	V Leptokurtic	212.2	82.3	17.7
21	5	5	2.8	2.0	72.2	27.8	14.4	4.0	M Silt	Poorly Sorted	Coarse Skewed	Mesokurtic	9.5	16.0	84.0
21	10	10	3.3	2.4	71.4	28.6	20.8	2.6	C Silt	Poorly Sorted	Fine Skewed	Leptokurtic	30.0	10.0	90.0
21	15	15	2.2	1.6	72.5	27.5	8.4	2.6	M Silt	Poorly Sorted	Coarse Skewed	Mesokurtic	6.0	3.0	97.0
21	20	20	2.3	1.6	68.3	31.7	10.9	2.8	M Silt	Poorly Sorted	Symmetrical	Mesokurtic	10.6	5.1	94.9
21	27.5	27.5	2.5	1.8	72.9	27.1	9.7	3.0	M Silt	Poorly Sorted	Coarse Skewed	Mesokurtic	6.7	6.8	93.2
23	0-3	1.5	11.5	7.0	61.2	38.8									
23	5	5	8.6	4.1	48.0	52.0									
23	10	10	10.5	8.3	78.6	21.4									
23	20	20	12.8	10.1	79.4	20.6									
23	27.5	27.5	11.5	9.6	83.2	16.8									
25	0-1	0.5	5.7	4.8	84.5	15.5	223.7	1.6	F Sand	Mod Sorted	Symmetrical	Mesokurtic	212.2	98.7	1.3
25	2	2	5.5	4.5	81.5	18.5	221.9	1.8	F Sand	Mod Sorted	Symmetrical	Mesokurtic	212.2	96.2	3.8
25	5	5	4.3	3.4	79.4	20.6									
25	10	10	2.0	1.4	72.0	28.0	8.2	2.7	M Silt	Poorly Sorted	Coarse Skewed	Leptokurtic	6.7	5.5	94.5

Table 11 Down core grain size and composition data for the Eurofleets (2012) Moira Mound cruise box cores.

Box Core	Sample (cm)	Depth in core (cm)	Dry Weight (g)	Treated Dry Weight (g)	% SiO2	% CaCO3 + Organic	Mean	Sort - ing	Mean	Sorting	Skewness	Kurtosity	Mode 1 (mm):	% Sand:	% Mud:
25	20	20	2.6	2.0	77.2	22.8	8.2	2.9	M Silt	Poorly Sorted	Coarse Skewed	Mesokurtic	6.0	5.7	94.3
25	30	30	1.9	1.5	77.2	22.8	8.3	2.4	M Silt	Poorly Sorted	Symmetrical	Mesokurtic	8.4	1.7	98.3
25	36	36	2.5	1.8	72.0	28.0	9.4	2.2	M Silt	Poorly Sorted	Symmetrical	Mesokurtic	11.9	0.0	100.0
26	0-1	0.5	6.5	4.6	71.0	29.0	173.1	1.8	F Sand	Mod Sorted	Fine Skewed	V Leptokurtic	189.1	93.8	6.2
26	2	2	8.6	6.4	75.0	25.0	148.0	2.6	F Sand	Poorly Sorted	V F Skewed	V Leptokurtic	189.1	84.6	15.4
26	5	5	6.2	4.8	78.0	22.0								0.0	0.0
26	10	10	5.3	3.9	73.5	26.5	181.0	1.9	F Sand	Mod Sorted	V F Skewed	V Leptokurtic	189.1	91.6	8.4
26	15	15													
26	18	18	4.7	3.6	76.4	23.6									
28	0-1	0.5	11.4	10.3	91.0	9.0									
28	2	2	7.9	6.7	84.7	15.3									
28	5	5	9.5	8.0	84.5	15.5									
28	10	10	8.8	7.2	81.7	18.3									
28	15	15													
28	20	20	3.7	2.7	72.8	27.2									
28	27	27	8.0												
29	0-1	0.5	3.4	2.4	72.0	28.0	17.3	4.2	C Silt	V Poorly Sorted	Coarse Skewed	Mesokurtic	11.9	18.1	81.9

Table 11 Down core grain size and composition data for the Eurofleets (2012) Moira Mound cruise box cores.

Box Core	Sample (cm)	Depth in core (cm)	Dry Weight (g)	Treated Dry Weight (g)	% SiO2	% CaCO3 + Organic	Mean	Sort - ing	Mean	Sorting	Skewness	Kurtosity	Mode 1 (mm):	% Sand:	% Mud:
29	2	2	2.3	1.7	75.6	24.4	9.7	2.9	M Silt	Poorly Sorted	Coarse Skewed	Mesokurtic	7.5	6.8	93.2
29	5	5	1.9	1.3	69.0	31.0	8.2	2.6	M Silt	Poorly Sorted	Coarse Skewed	Mesokurtic	6.7	2.8	97.2
29	10	10	3.2	2.3	72.9	27.1	7.7	2.2	F Silt	Poorly Sorted	Symmetrical	Platykurtic	7.5	0.0	100.0
29	20	20	1.8	1.3	72.3	27.7									
29	30	30	2.9	1.9	65.0	35.0									
29	36	36	3.2	2.5	77.5	22.5									
30	0-1	0.5	6.7	5.5	81.7	18.3									
30	2	2	3.0	2.1	68.6	31.4									
30	5	5	2.3	1.7	72.0	28.0									
30	6-7	6.5	2.6	1.9	73.5	26.5									
30	10	10	2.4	1.7	72.3	27.7									
30	20	20	3.4	2.3	68.5	31.5									
30	30	30	3.7	2.4	64.8	35.2									
30	36	36	3.2	2.2	67.3	32.7									
31	Bulk		9.1	6.7	73.2	26.8									
33	Bulk		9.1	7.1	78.0	22.0									
35	0-1	0.5	7.1	6.0	85.2	14.8									
35	2	2	6.7	5.5	82.2	17.8									
35	5	5	6.1	5.3	87.2	12.8									
35	10	10	3.0	2.5	81.2	18.8									

Table 11 Down core grain size and composition data for the Eurofleets (2012) Moira Mound cruise box cores.

Table 11 Down core grain size and composition data for the Eurofleets (2012) Moira Mound cruise box cores.

Appendix II

Courses completed during Ph. D.

2015: IXBLUE - Sub-bottom profiler acquisition and interpretation, RV Celtic Explorer, offshore Ireland

2015: Kongsberg Maritime - EM302, EM2040 Multibeam and SIS Operators course - Horten, Norway

2014: Irish Graduate Geoscience Program - Advanced GIS, National College of Ireland, Maynooth

2014: School of Biological, Earth and Environmental Sciences - Teaching and Learning, University College Cork

2013: School of Biological, Earth and Environmental Sciences - GIS Clinic, University College Cork

Appendix III

Research cruises undertaken as part of, and during, the PhD

May, 2016: QuERCi 2 (Quantifying Environmental Controls on Cold-Water Coral Reef Growth), RV Celtic Explorer and Holland 1 ROV, Galway to Cork.

Day shift leader; responsible for hull-mounted multibeam echosounder acquisition (EM302), Gravity coring operations, cruise GIS, ROV watches, data collation, back-up and management.

September, 2015: Irish Ground Fish Survey, RV Celtic Explorer, Galway to Galway.

Geophysist; responsible for multibeam echosounder acquisition (EM302 and EM1002) collection, on-the-fly processing and sound velocity profiles.

June, 2015: QuERCi 1 (Quantifying Environmental Controls on Cold-Water Coral Reef Growth), RV Celtic Explorer and Holland 1 ROV, Galway to Galway.

Day shift leader; responsible for ROV-mounted multibeam echosounder acquisition (EM2040) and hull-mounted multibeam echosounder acquisition (EM302), IXSEA CHIRP seismic acquisition, gravity core operations, cruise GIS, data collation, management and back-up.

February, 2015: Sea Acceptance Trials (SAT**),** RV Celtic Explorer, Galway to Galway.

Scientist: Multibeam and CHIRP watches

September, 2014: SMART Atlantic Summer School, RV Celtic Explorer, Cork to Galway.

Marine Geology Instructor: drop camera data acquisition, video classification and GIS, gravity core operations, box core operations, day grab operations.

March, 2014: WICPro (West of Ireland Coring Programme), RV Celtic Explorer, Cork to Galway.

Day shift leader; Gravity, Vibro- and Box core operations, cruise GIS, pinger and sparker seismic watches.

January, 2014: Geotechnical Survey, RV Celtic Explorer, Galway to Cork.

Scientist: CPT and sparker seismic watches.

December, 2013: CTD Survey, RV Celtic Voyager, Cork to Galway.

Chief Scientist: CTD operations, cruise report, cruise GIS.

October, 2013 to present: SMART, RV Celtic Voyager, Cork Harbour.

Marine Geoscience Demonstrator: Demonstrate multibeam and sub bottom profiler data acquisition and sediment grab acquisition and processing to BSc/MSc

Geology, Engineering and Geography students (Oct. ‘13, Nov, ‘14/‘15/‘16, Mar./Sep.’16).

February, 2013: Methane derived authogenic carbonate seeps (MDACS) and Geotechnical survey, RV Celtic Explorer, Galway to Cork.

Scientist: drop camera watches, pinger and sparker seismic watches, vibrocore operations

June, 2011: VENTuRE (Vents and reefs), RV Celtic Explorer

Student: geological sample cataloguing, ROV video watches, CTD watches, data back-up, grab sample processing.

Appendix IV

Awards and grants received during Ph.D.

July, 2015: 1st International Conference on Carbonate Mounds (Locarno, Switzerland) - European Research Network – European Science Foundation – Young researchers Award

June, 2015: Irish Research Council – Graduate of Ireland Scholarship

May, 2015: Marine Institute Research Travel Grant

November, 2014: Presidents Award – “Research into innovative forms of teaching”

August, 2014: CoCARDE (Copenhagen, Denmark) – European Research Network – European Science Foundation –Young researchers Award

May, 2014: GeoHab - Melbourne, Australia – Ron McDowell Student Award

September, 2013: CoCARDE (Sicily, Italy) – European Research Network – European Science Foundation –Young researchers Award

August, 2013: Irish Geological Association – Postgraduate Research Award

Appendix V

Conference presentations

Lim, A., Wheeler, A., Arnaubec, A., (2016) Cold water coral reef spatial zonation, organisation and environmental controls: the case of Piddington Mound. International Symposium on Deep Water Corals, Boston, Oral presentation

Lim, A., Wheeler, A., Arnaubec, A., Vertino, A., Spezzaferri, S., (2016) Piddington Mound spatial zonation, organisation and development. GeoHab, Winchester, UK, Poster presentation

Lim, A., Wheeler, Huvenne, V.A.I., A., Vertino, A., Spezzaferri, S., de Haas, H., (2016) Hydrodynamic and sedimentological influences on cold-water coral reef development: The Moira Mounds, Porcupine Seabight, Offshore Ireland. Irish Geological Research Meeting, University College Dublin, Ireland, Oral presentation

Lim, A., Wheeler, Huvenne, V.A.I., A., Vertino, A., Spezzaferri, S., de Haas, H., (2016) Hydrodynamic and sedimentological influences on cold-water coral reef development: The Moira Mounds, Porcupine Seabight, Offshore Ireland. 1st International Carbonate Mound Conference, Locarno, Switzerland, Oral presentation

Lim, A. (2015) Class size, organisation and composition in practical learning. InSPEcT (Inaugural Symposium on Teaching and Learning), University College Cork, Poster presentation

Lim, A., Wheeler, Huvenne, V.A.I., A., Vertino, A., Spezzaferri, S., de Haas, H., (2015) Hydrodynamic and sedimentological influences on cold-water coral reef development: The Moira Mounds, Porcupine Seabight, Offshore Ireland. GeoHab, Salvadore, Brazil, Oral presentation

Lim, A., Wheeler, Arnaubec, A., Vertino, A., Spezzaferri, S., (2014) Current work on the Moira Mounds, Porcupine Seabight, Offshore Ireland. CoCarDE Workshop and Field Seminar, Denmark, Oral and poster presentations

Lim, A., Wheeler, Arnaubec, A., Vertino, A., Spezzaferri, S., (2014) Spatial patterns at the Moira Mounds, Porcupine Seabight, Offshore Ireland. GeoHab, Lorne, Australia, Oral presentation

Lim, A., Wheeler, Arnaubec, A., Vertino, A., Spezzaferri, S., (2014) Spatio-temporal patterns and controls on cold-water coral reef development: The Moira Mounds, Porcupine Seabight, Offshore Ireland. Irish Geological Research Meeting, University College Dublin, Poster presentation

Lim, A., (2014) The Moira Mound cold water coral reefs and seabed mapping. School of Biological, Earth and Environmental Sciences, Research club, Oral presentation

Lim, A., Wheeler, Arnaubec, A., Vertino, A., Spezzaferri, S., (2013) Spatio-temporal patterns and controls on cold-water coral reef development: The Moira Mounds, Porcupine Seabight, Offshore Ireland. GEOScience Ireland, Dublin, Poster presentation

Lim, A., Wheeler, Arnaubec, A., Vertino, A., Spezzaferri, S., (2013) Spatio-temporal patterns and controls on cold-water coral reef development: The Moira Mounds, Porcupine Seabight, Offshore Ireland. INFOMAR Seminar series, Univeristy of Limerick, Poster presentation

Lim, A., Wheeler, Arnaubec, A., Vertino, A., Spezzaferri, S., (2013) Spatio-temporal patterns and controls on cold-water coral reef development: The Moira Mounds, Porcupine Seabight, Offshore Ireland. CoCarDE Workshop and Field Seminar, Sicily, Oral presentation and poster presentation